Signal Processing for Future MIMO-OFDM Wireless Communication Systems

Thesis submitted to Cardiff University in candidature for the degree of Doctor of Philosophy.

Li Zhang

Centre of Digital Signal Processing
Cardiff University
2008

ProQuest LLC
789 East Eisenhower Parkway
P.O. Box 1346
Ann Arbor, MI 48106-1346

ABSTRACT

The combination of multiple-input multiple-output (MIMO) technology and orthogonal frequency division multiplexing (OFDM) is likely to provide the air-interface solution for future broadband wireless systems. A major challenge for MIMO-OFDM systems is the problem of multi-access interference (MAI) induced by the presence of multiple users transmitting over the same bandwidth. Novel signal processing techniques are therefore required to mitigate MAI and thereby increase link performance.

A background review of space-time block codes (STBCs) to leverage diversity gain in MIMO systems is provided together with an introduction to OFDM. The link performance of an OFDM system is also shown to be sensitive to time-variation of the channel. Iterative minimum mean square error (MMSE) receivers are therefore proposed to overcome such time-variation.

In the context of synchronous uplink transmission, a new two-step hard- decision interference cancellation receiver for STBC MIMO-OFDM is shown to have robust performance and relatively low complexity. Further improvement is obtained through employing error control coding methods and iterative algorithms. A soft output multiuser detector based on MMSE interference suppression and error correction coding at the first stage is shown by frame error rate simulations to provide

significant performance improvement over the classical linear scheme.

Finally, building on the "turbo principle", a low-complexity iterative interference cancellation and detection scheme is designed to provide a good compromise between the exponential computational complexity of the soft interference cancellation linear MMSE algorithm and the near-capacity performance of a scheme which uses iterative turbo processing for soft interference suppression in combination with multiuser detection.

To my parents for their unconditional support

and my wife Jie Zhuang for her love and encouragement

ACKNOWLEDGEMENTS

I would like to give my great thanks to my supervisor Prof. Jonathon A. Chambers, who spent much time consulting with me. Thanks for his great enthusiasm and patience with me. Without his invaluable support and encouragement, this thesis would have not been accomplished. I feel lucky to have been inspired by his extraordinary motivation, great intuition and hard work. He is an example for my future career and has my deepest respect professionally and personally.

I would also like to thank my second supervisor in Belfast, Northern Ireland, Dr. Mathini Sellathurai, who has supervised me during my second and third year PhD study. She contributed greatly to every paper I have written, and to every progress step I have made. Dr. Saeid Sanei, Dr. Sangarapillai Lambotharan and Dr. Zhuo Zhang have given much help and many suggestions on not only my research and study, but also my life in Cardiff. I would also like to express sincere gratitude to them.

The thanks also go to my dear colleagues in the center of digital signal processing (CDSP). It has been my great honour to work with them: Andrew Aubrey, Clive Cheong Took, Yonggang Zhang, Cheng Shen, Qiang Yu, Yue Zheng, Min Jing, Lay Teen Ong and many others. Cardiff has been wonderful for me mainly because of all these friends.

My wife Jie Zhuang who accompanied me in Cardiff during the last

two years, is greatly appreciated. I would like to thank for her love and encouragement.

Finally, I would like to thank my parents for their unconditional patience and support while we have been separated for many years.

PUBLICATIONS

- L. Zhang, C. Shen, M. Sellathurai, and J. A. Chambers,"Low Complexity Sequential Iterative Cancellation Technique for Multi-user MIMO-OFDM Systems," *IEEE Signal Processing Lett.*, submitted, Sept. 2008.

- L. Zhang, M. Sellathurai, and J. A. Chambers, "A Joint Coded Two-Step Multiuser Detection Scheme for MIMO-OFDM System," *Proc. IEEE International Conference on Acoustics, Speech and Signal Processing, 2007 (ICASSP 2007)*, Vol. 3, pp. III-85 - III-88, Hawaii, USA, April 2007.

- L. Zhang, M. Sellathurai, and J. A. Chambers, "A Two-Step Multiuser Detection Scheme for Space-Time Coded MIMO-OFDM Systems," *Proc. 10th IEEE Singapore International Conference on Communication systems, 2006 (ICCS 2006)*, Singapore, Oct. 2006.

- L. Zhang, M. Sellathurai, and J. A. Chambers, "A Space-Time Coded MIMO-OFDM Multiuser Application With Iterative MMSE-Decision Feedback Algorithm," *Proc. 8th IEEE International Conference on Signal Processing (ICSP2006)*, Guilin, P.R.China, Nov. 2006.

- L. Zhang, M. Sellathurai, and J. A. Chambers, "An Iterative Multiuser Receiver for Space-Time Coded MIMO-OFDM Systems," *Proc. 7th International Conference on Mathematics in Signal Processing (IMA2006)*, pp. 182-184, Cirencester, UK, Dec. 2006.

- C. Shen, L. Zhang, and J. A. Chambers, "A Two-Step Interference Cancellation Technique for a MIMO-OFDM System with Four Transmit Antennas," *Proc. 2007 15th International Conference on Digital Signal Processing*, pp. 351-354, Cardiff, UK, July 2007.

LIST OF ACRONYMS

3GPP	3rd Generation Partnership Project
AMPS	Advanced Mobile Phone System
AWGN	Additive White Gaussian Noise
BER	Bit Error Rate
bps	Bits Per Second
CCM	Circulant Channel Matrix
CDMA	Code Division Multiple Access
CSD	Circuit Switched Data
DFT	Discrete Fourier Transform
DVB	Digital Video Broadcasting
FFT	Fast Fourier Transform
FER	Frame Error Rate
FFT	Inverse Fast Fourier Transform
GPRS	General Packet Radio Service
GSM	Global System for Mobile communications

HDTV	High Definition Television
HIPERLAN	High Performance Radio Local Access Network
HSPA	High Speed Packet Access
i.i.d.	Independent and Identically Distributed
iDEN	Integrated Digital Enhanced Network
IDFT	Inverse Discrete Fourier Transform
IMT-2000	International Mobile Telecommunications 2000 programme
IS-95	Interim Standard 95
ITU	International Telecommunication Union
ITU-R	ITU Radiocommunication Sector
JTACs	Japanese Total Access Communications
LS	Least Squares
LTE	Long Term Evolution
MIMO	Multiple-Input Multiple-Output
MLE	Maximum Likelihood Estimation
MLSE	Maximum Likelihood Sequence Estimation
MMS	Multimedia Messaging Service
MMSE	Minimum Mean Squared Error
NMT	Nordic Mobile Telephone

OFDM	Orthogonal Frequency Division Multiplexing
OFDMA	Orthogonal Frequency-Division Multiple Access
PDC	Personal Digital Cellular
pdf	Probability Density Function
PHS	Personal Handy-phone System
PSK	Phase Shift Keying
QAM	Quadrature Amplitude Modulation
QoS	Quality-of-Service
RTMI	Radio Telefono Mobile Integrato
SIMO	Single-Input Multiple-Output
SNR	Signal to Noise Ratio
TACS	Total Access Communications System
UMB	Ultra Mobile Broadband
UMTS	Universal Mobile Telecommunications System
WiBro	Wireless Broadband
WiDEN	Wideband Integrated Digital Enhanced Network
WiMax	Worldwide Interoperability for Microwave Access
WLAN	Wireless Local Access Network

MATHEMATICAL NOTATIONS

x	Scalar quantity
$\mathbf{x}$	Vector quantity
$\mathbf{X}$	Matrix quantity
$\mathbf{x}_n$, $\mathbf{x}(n)$	Value of $\mathbf{x}$ at discrete time n
$\mathbf{X}_{qj}$	The qj-th element of the matrix quantity $\mathbf{X}$
$\bar{\mathbf{x}}$	Mean vector
$\hat{\mathbf{x}}$	Estimate of original quantity $\mathbf{x}$
$\mathbf{0}$	Vector of Zeros
$\mathbf{I}$	Identity matrix
$(\cdot)^T$	Transpose operator
$(\cdot)^H$	Hermitian transpose operator
$(\cdot)^{-1}$	Matrix inverse
$(\cdot)^*$	Complex conjugate operator

$\lvert \cdot \rvert$	Absolute Magnitude Value
$\lvert\lvert \cdot \rvert\rvert$	Euclidean Norm
$det(\cdot)$	Matrix determinant
$min(a, b)$	Minimum value of a or b
$E\{\cdot\}$	Statistical expectation

CONTENTS

List of Figures

List of Tables

PREFACE

During the past decade, wireless communications have been enjoying their fastest growth in history; growing from a potential business in the early 1990s to one of the most promising markets for growth in the 21st century, which has now become the largest sector of the telecommunications industry. The most attractive feature of wireless technology is that it is a preferable solution to support user mobility, i.e. data exchange can happen at anytime and in anyplace. In history, the telecommunications industry did not even conceive the ability to provide wireless communications to an entire population until Bell Laboratories developed the cellular concept in the 1960s and 1970s [1], [2] and [3]. With the development of high reliability, miniaturization of radio frequency (RF) hardware, the wireless communications era was born. Nowadays, it is estimated that more than 158 million customers had subscribed to wireless services in the United States of America (USA) by the end of 2003 [4], and in China the number exceeds the population of the USA, which is currently the largest wireless communications market in the world. By the end of 2007, it is believed that the total number of worldwide wireless subscribers exceeded two billion, and this continues to grow.

With the development of the Internet, consumer-based electronics and multimedia data exchange, the demand for high data rate wireless

communications is growing higher and higher. Wireless systems are expected to not only offer voice communication services but also to be tied more closely to Internet access and multimedia service. Through successful research and huge investment, many worldwide mobile service providers started to collocate the third generation (3G) mobile/wireless network systems with legacy networks in the late 1990s. However, there exist different 3G standards adopted by different regions of world which are incompatible. Hence, it is difficult to build a unified global wireless network. Furthermore, 3G technology is able to provide a burst data rate up to 2Mbps, however, the average throughout per user is anticipated not to exceed 171Kbps [5] and [6] (There are enhanced 3G (3.5G) systems for improving the data rate). Although this data rate is sufficient for voice communications and basic media service, it still does not satisfy new high quality multimedia services such as telehospital and high-speed high-definition television (HDTV) with audio/video (A/V), which require bit rates in the range of 100Mbps to 1Gbps. To meet the demands of high rate wireless communications, more wireless technologies in the form of broadband wireless systems (BWSs) are required.

The orthogonal frequency division multiplexing (OFDM) technique, based on multi-carrier modulation (MCM) technology, has provided much improvement for wireless local area networks (WLANs) in the license-free band. In practice, OFDM has been standardized in IEEE 802.11 a and g for WLANs [7] and [8], and it is available to support more than 100Mbps data rates in more recent forms. For more coverage and data rate, OFDM can be used in combination with antenna arrays at the transmitter and receiver to form a multiple-input multiple-output

(MIMO) OFDM system, which can potentially provide up to 1Gbps data rate [9].

Motivated by the success of OFDM in WLAN, the research presented in this thesis investigates MIMO-OFDM technology for broadband wireless systems (BWSs). New algorithms and approaches are proposed for MIMO-OFDM systems to mitigate the problem of interference introduced by multiuser operation. These algorithms are evaluated by simulation studies conducted in a MATLAB environment on a P4 PC and their overall computational complexity is minimized.

Chapter 1

INTRODUCTION

The ability of mobile communication with people has evolved remarkably since Guglielmo Marconi implemented radio communication to provide contact with a ship sailing the English channel [1]. Since the 20th century, new wireless communication methods and services, that were initially beyond people's dreams, have been adopted throughout the world. Particularly during the past decade, motivated by the increasing demand for high-rate reliable data exchanges anytime and anywhere, broadband wireless systems (BWSs) are underpinning future mobile communication networks.

1.1 Broadband Wireless Communications

Nowadays, wireless broadband communications can provide its users with radio access to broadband services based on public wired networks, with data rates exceeding 2 Mbps [10]. However, multimedia and computer communications are playing an increasing role in today's wireless services, which are presenting new challenges to the development of wireless broadband communication systems. The next generation of broadband wireless communication systems such as 4G is therefore anticipated to provide wireless subscribers with high quality wireless services such as wireless television, high speed wireless Internet

access and mobile computing. The pressure of rapidly growing demand for these services is enormous which is driving communication technology towards higher data rates, higher mobility, and higher carrier frequencies for reliable transmissions over mobile radio channels.

Depending on the quality-of-service (QoS) requirements and different applications, many broadband wireless communication approaches have been proposed recently (see in [11], [12], [13] and [14]). Their target is to achieve the required high transmission rate while maintaining a certain QoS in macro cellular, pico-cellular, and indoor environments. Several approaches have been adopted such as the worldwide interoperability for microwave access (WiMax: IEEE 802.16e), wireless local area network (WLAN: IEEE 802.11a/b/g [7], [8] and Wi-Fi for which the various IEEE 802.11 technologies include IEEE 802.11a, b ,g and n [15]), wireless metropolitan area networks (WMANs IEEE 802.16 [16]), bluetooth wireless (IEEE 802.15.1) and wireless multimedia (WiMedia: IEEE 802.15.3) technologies. In some of these approaches, mobile units can move quickly with data rate requirement exceeding 100 Mbps. User bandwidths can be fixed or dynamically allocated; the specifications of the IEEE 802.11 standard family are summarized in Table 1.1 [7], [8] and [17], where complementary code keying (CCK) is a modulation scheme used with WLANs that employ the IEEE 802.11b specification.

Furthermore, at the physical layer of such systems, several research efforts are focusing upon developing efficient coding and modulation schemes to support wireless multimedia services, on the basis of effective signal processing algorithms to improve the quality and spectral efficiency of wireless communications.

Table 1.1. Summary of IEEE 802.11 standard specifications

Characteristics	802.11b	802.11a	802.11g
Standard approved	July 1999	July 1999	June 2003
Maximum data rate	11 Mbps	54 Mbps	54 Mbps
Modulation	CCK	OFDM	CCK&OFDM
Data rate	1, 2, 5.5, 11Mbps	6, 9, 12, 18, 24, 36, 48, 54 Mbps	CCK: 1, 2, 5.5, 11 Mbps OFDM: 6, 9, 12, 18, 24, 36, 48, 54 Mbps
Frequencies	2.4 - 2.497 GHz	5.15-5.35 GHz 5.425-5.675 GHz 5.725-5.875 GHz	2.4 - 2.497 GHz

However, these developments still have to cope with critical performance limitations caused by interference from the mobile radio channel, multiuser interference (MUI), size/power limitations of mobile units and so on. Normally, time-selective and frequency-selective fading exists in mobile radio channels because of carrier phase/frequency drifts, i.e. Doppler shifts and multipath propagation, respectively. Channel fading causes performance degradation and affects the reliability of high data rate wireless transmissions. Recently, research has shown that it is effective to exploit various diversity and multiplexing techniques to combat fading in wireless channels [18], [19] and [20]. Based on the domain where the diversity remains, it is usual to divide diversity techniques into three categories, namely, temporal, frequency and spatial diversities [21]. Another form is code diversity, but that is not a major focus in this thesis. Temporal and frequency diversity normally intro-

duce redundancy in the time and/or frequency domain, and therefore bring loss in bandwidth efficiency.

During the past ten years, some relatively efficient diversity and multiplexing techniques which exploit spatial techniques have become key physical layer research targets. Such research generally combined two key technologies: multi-input multi-output (MIMO) and orthogonal frequency division multiplexing (OFDM).

1.2 MIMO Communications

The explosion of interest in MIMO systems dates from the middle of the 1990s. The first papers by Foschini and Gans [22], Foschini [23] and Telatar [24] focus on this topic. However, what is not widely known is the fact that eight years before Telatar's work, another paper was written by Winters [25]. This research showed that with appropriate signal processing in the transmitter and the receiver, the channel capacity (a theoretical upper bound on system throughput) for a MIMO system is increased as the number of antennas is increased, proportional to the minimum number of transmit and receive antennas, which implies that the possible transmission rate increases linearly. This basic finding in information theory is what led to an explosion of research in this area [26].

Nowadays, MIMO technology has attracted the most attention in wireless communications, since it can offer significant increase in data throughput and link range without additional bandwidth or transmit power. It achieves this by higher spectral efficiency (more bits per second per Hertz of bandwidth) and link reliability through diversity gain (reduced fading). Because of these properties, MIMO is a current

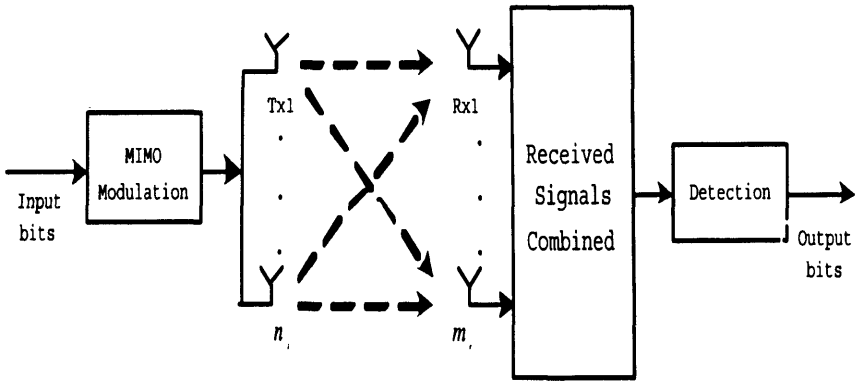

Figure 1.1. MIMO technology using multiple antennas both at a transmitter and a receiver, only baseband components shown.

key theme of international wireless research.

A baseband framework for a general MIMO system is presented in Figure 1.1 and it shows that a MIMO system consists of n_t transmit (Tx) and m_r receive (Rx) antennas, which is a so-called (n_t, m_r) MIMO system. All the Tx antennas can send their signals simultaneously in the same bandwidth of a radio channel. Each Rx antenna receives the superposition of all the transmit signals disturbed by the noise in the radio channel. If no more than $min(n_t, m_r)$ independent signals are transmitted, they can be correctly decoded at the receiver.

Several review papers have presented an overview of MIMO techniques [9] and [27]. Since different antennas are positioned at different spatial locations, MIMO systems can take advantage of spatial diversity to overcome channel fading provided the constituent paths are uncorrelated. Multiple copies of a signal are transmitted from the Tx antennas in transmit diversity and received at the Rx antennas in receive diversity. This highlights an important advantage of spatial diversity, i.e. it does not require any additional time or frequency budget to achieve diversity. In theory, it can achieve $n_t \times m_r$-th order diversity by us-

ing suitably designed transmit signals [28]. On the other hand, these additional antennas can be exploited to perform spatial multiplexing, thereby enhancing the system throughput by transmitting many parallel data streams. Since all data are transmitted both in the same frequency band and with separate spatial signatures, this technique utilizes spectrum very efficiently. From the research in [29], [23], [30] and [31], MIMO channels are shown to linearly (in $min(n_t, m_r)$) increase capacity of transmission for no additional power or bandwidth expenditure. The spatial-multiplexing gain (equivalent to the number of spatial transmitting pipes experienced within a given frequency band) can be achieved by the minimum of the number of transmit and receive antennas, assuming the receiver knows the channel state information (CSI) [32] perfectly.

Hence, since MIMO technology has been introduced in the 1990s, a significant effort has been focused upon techniques exploiting MIMO to achieve high throughput by multiplexing gain and increasing reliability by spatial diversity gain, e.g. space-time coding. An alternative practical technique is space-time block codes (STBCs), represented in [33] and [34], which act on a block of data at once (similarly to block codes) and generally provide only diversity gain, but array gain can be generated. Such space-time coding is very computational efficient and is being adapted in practical systems such as Wi-Fi. Space-time trellis codes (STTCs), on the other hand, represented in [21], distribute a trellis code over multiple antennas and multiple time-slots and provide both coding gain and diversity gain, but are much more computationally complex and hence unsuitable for many practical systems, and not pursued in this thesis.

In MIMO technology, it is assumed that different antenna signals are transmitted with different fading characteristics, which means that the antennas should be placed at appropriate distances so that the transmitting/receiving signal are uncorrelated. If the antennas are placed without appropriate spacing, then all the antenna will influence each other. So the received signals will be highly correlated. As a result, a high loss in diversity gain on transmission can result which is a potential shortcoming of this technology. Therefore, there exists a fundamental tradeoff between diversity and multiplexing gain in a MIMO system [35]. Distributed MIMO [36], not a subject of this thesis, is a potential approach to mitigate this problem.

1.3 OFDM and Multi-Carrier Communications

Multi-carrier technology potentially offers the desired high data rates for the 4G mobile environment and also has advantages for spectral efficiency and low-cost implementation [37]. The concept of multi-carrier transmission by means of frequency division multiplexing (FDM) was widely proposed in the 1960s [38], [39] and [40]. It involves using parallel data sub-streams and FDM with non-overlapping frequency domain sub-channels to avoid the use of multi-tap equalization and to combat impulsive noise and multipath distortion as well as to utilize fully the available bandwidth. The initial multi-carrier applications were realized in military communications [37]. In the telecommunication field, there are a host of terms describing multi-carrier techniques, such as discrete multi-tone (DMT), multichannel modulation, multi-carrier modulation (MCM) and the more popular OFDM, which is so-called orthogonal frequency division multiplexing, proposed in [41] and [42].

Along with OFDM, the most recent development of a multi-carrier system is multi-carrier code division multiple access (MC-CDMA). MC-CDMA was first proposed in [43], which is an alternative to the OFDM and CDMA systems, but not considered in this thesis.

OFDM is a digital multi-carrier modulation scheme, which uses a large number of closely-spaced orthogonal sub-carriers. An array of sinusoidal oscillators and coherent demodulators are required in a parallel system to generate these sub-carriers in the original scheme. This approach becomes unreasonably expensive and complex. Thus, Weinstein and Ebert applied the discrete Fourier transform (DFT) to the parallel data transmission system as part of the modulation and demodulation process [44], with quadrature amplitude modulation (QAM) constellation, where each modulated subcarrier is similar to the conventional single-carrier modulation schemes in the same bandwidth [45] and [46], at a low symbol and data rate. With the development of the fast Fourier transform (FFT) and recent advances in very large-scale integration (VLSI) technology, OFDM signals can be generated and detected by performing a large size FFT at an affordable price in practical applications, which further reduces the complexity of multi-carrier implementation.

During the past decades, OFDM has developed into a popular scheme for wideband digital communication, both for wireless and wireline applications such as copper wires. In the 1980s, OFDM applications first focused on high-speed modems, digital mobile communications and high-density recording. In the 1990s, OFDM was exploited for wideband data communication over mobile radio FM channels, high-bit-rate digital subscriber lines (HDSL, 1.6 Mbps) and very high-speed

digital subscriber lines (VHDSL, 100 Mbps). Otherwise, OFDM was widely utilized over asymmetric digital subscriber lines (ADSL, 1.536 Mbps) taking advantage of existing copper wires, following the G.DMT (ITU G.992.1) standard, and it was also introduced into digital audio broadcasting (DAB) [47] and terrestrial digital video broadcasting (DVB-T) [48].

It is obvious that the OFDM technique has induced intense attention in research and application because of its spectral efficiency and the ability to overcome difficult frequency selective and interference channel conditions without complex equalization, for example, to mitigate narrowband interference, attenuation in a long copper wire at high frequencies and frequency-selective fading due to the effect of a multipath channel [42], [49] and [45]. These features are considered as the primary advantage of OFDM over single-carrier schemes by most researchers. Channel equalization can be simply implemented because OFDM may be viewed as using many slowly-modulated narrowband signals where the provided channel remains static over the OFDM symbol. Low symbol rate makes the use of a guard interval between symbols affordable to handle time-spreading and mitigate inter-symbol interference (ISI), which is more feasible rather than one rapidly-modulated wideband signal.

In the view of diversity theory, high performance can be achieved in OFDM based system due to the advantage of multipath diversity. Some research based on spatial sampling has shown that if within an OFDM system transmit antennas are placed very closely such as 0.44 of a wavelength, performance comparable to widely spaced antennas in frequency flat channels can be achieved [50], since an OFDM sys-

tem converts multipath diversity to spatial diversity in the frequency domain. Moreover, in OFDM-based wide area broadcasting, it is very beneficial to receive signals from several spatially-dispersed transmitters simultaneously, since transmitters will only destructively interfere with each other on a limited number of sub-carriers, whereas in general they will actually reinforce coverage over a wide area.

In practical applications, OFDM may be combined in general with other forms of spatial diversity, for example antenna arrays and MIMO channels. This is exploited in the IEEE802.11n [15] standard.

1.4 MIMO-OFDM and Multiuser Detection

1.4.1 MIMO-OFDM Applications

On the one hand, OFDM has been shown to be an effective technique to combat frequency-selective fading through multipath propagation in wireless communications [45]. On the other hand, it is known that spatial multiplexing [23] and [29] with MIMO techniques can further exploit capacity of wireless communication systems [23] and [22], and improve link reliability through diversity gain [26]. However, most MIMO schemes, in fact, realize both spatial-multiplexing and diversity gain in some form of trade-off [35]. Hence, by combining two techniques, OFDM can be adopted to reinforce a multi-antenna scheme by transferring a frequency-selective MIMO channel into a set of parallel frequency-flat MIMO channels. As a result, receiver complexity decreases and the advantages of each technique are still retained. Compared with the analyses in [29] and [23] experienced on flat fading MIMO channels, the OFDM-based multi-antenna

scheme is robust with respect to multipath induced frequency-selective fading [51] [31]. Moreover, under real-world propagation conditions, multipath propagation which results in frequency-selective fading can be further beneficial for these OFDM-based MIMO solutions in terms of spatial-multiplexing gain [31]. These features, without doubt, make MIMO-OFDM very attractive for the 4th-generation (4G) wireless communication systems [18].

In frequency-selective fading MIMO channels, two sources of diversity are available: spatial diversity and frequency diversity. On the one hand, with the aim at improving spectral efficiency within MIMO utilizations, the basic idea of space-time coding [21] is adopted frequently, without the need of knowledge of CSI at the transmitter, to realize spatial diversity gain by introducing redundancy across space and time. On the other hand, in single-antenna OFDM systems, full frequency diversity can be achieved by appropriate coding and interleaving across tones at the transmitter. It is therefore easy to find out that there exists a straightforward way to exploit these two sources of diversity concurrently, which is to combine space-time coding with forward-error-correction coding ([52], [53] and [54]) and interleaving across tones. In most practical applications, bit-interleaved coded modulation has been adopted [55]. On the other hand, another systematic approach, named space-frequency codes [56], has been proposed and is becoming more and more popular due to less severe assumptions on CSI, in which the algorithm essentially spreads the transmitting symbols across each antenna (space-domain) and tones (frequency-domain), i.e. the transmitting system performs a coding process in terms of each OFDM tone and not across OFDM symbols. The framework of this coding tech-

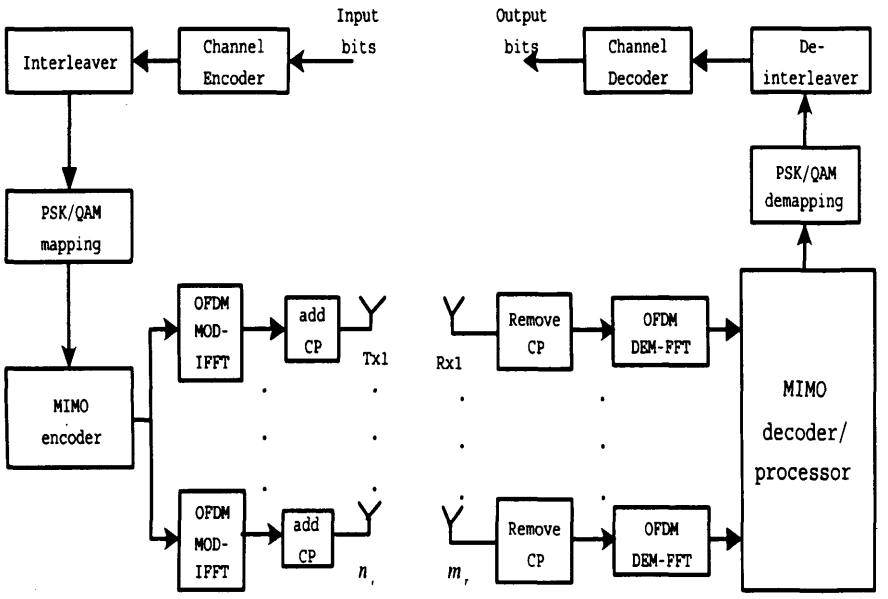

Figure 1.2. The block diagram of general baseband MIMO-OFDM system.

niques was proposed in [57], which shows that good code design has the ability to achieve full rate and full diversity in frequency-selective fading MIMO channels. The space-frequency code design in [58] also represents the ability to implicitly "learn" the channels and obtain full diversity in space and frequency.

Figure 1.2 represents a block diagram of a general baseband MIMO-OFDM system. Overviews of this attractive solution for 4G wireless communications are in [20] and [19]. This topic will be discussed in detail in the following chapters.

Although the utilization of OFDM combats ISI, there may still be high computational complexity for receivers based on the MIMO-OFDM techniques. This is because, in an OFDM-based MIMO system, spatial multiplexing is implemented by splitting transmit power uniformly though independent data streams and antennas on a tone-

by-tone basis. In general, the number of data-carrying tones typically ranges between 48 (standardized in IEEE 802.11a/g) and 1728 (standardized in IEEE 802.16e) and it may be a high cost for spatial separation to be performed on each tone.

Recently, some new algorithms [59] and [60] mitigate this problem, which result in computational complexity reductions by performing channel inversion in the case of a minimum mean-squared error (MMSE) receiver [61]. The basic idea of these algorithms is based on the fact that the structure of the transfer matrix in a MIMO-multipath channel is comparatively simple across OFDM tones due to limited length of the delay spread in the channel and this property is exploited in this thesis.

1.4.2 Multiuser Detection

During the last ten years, multiuser detection (MUD), jointly detecting the signals from different users, has been a subject of intense research as a potential method to cope with the high user demand for MIMO-OFDM applications. A multiuser MIMO-OFDM system allows multiple users to exploit the spatial resources at the cost of advanced transmit or receiver processing. Hence such OFDM-based multiuser structures are developed when the number of users is more than one. At the receive stage, multiuser receivers can exploit the structure of the multiuser signal and detect all users' data simultaneously. Since multiuser receivers can effectively suppress or cancel the multiuser interference (MUI), they substantially outperform single-user receivers in a multiuser environment. The basic multiuser detection algorithms and their variants have been well covered in the overview book by Verdu [62],

which was originally proposed for CDMA systems [63] and [64]. Recently, various MUD schemes have been proposed for MIMO-OFDM systems. Among these MUDs, the classic linear least squares (LS) ([62] and [65]) and MMSE ([62], [65] and [66]) MUDs represent a low complexity solution at the cost of a reduced performance.

By contrast, the high-complexity optimum maximum-likelihood (ML) or maximum a posteriori probability (MAP) MUDs [62], [65], [67] and [68] have the ability to achieve the best performance because the algorithm implements an exhaustive search, which impacts the computational complexity, however, typically increasing exponentially with the number of simultaneous users within a MIMO-OFDM system. As a result, this scheme has to be limited to high-user-load scenarios.

Several other suboptimal nonlinear MUDs have also been proposed in the literature, such as for example the MUDs based on sequential interference cancellation (SIC) [62], [65] and [67] or parallel interference cancellation (PIC) [62] and [65] techniques. An MMSE-based iterative inference cancellation scheme for MUDs was first proposed in [69]. In contrast to the linear MUDs, in order to achieve more accurate detection, the output signal by the scheme of [69] obtained from the last detection iteration can be re-modulated and fed back to the input of the MUD for the next iterative detection step, which is similar to decision-feedback techniques [70] invoked in channel equalization [71] [72]. Moreover, this iterative cancellation is exploited with combination of "turbo coding" [73], [74] and [75]. These idea will be exploited in this thesis to provide new low complexity solutions to multiuser MIMO-OFDM receiver design.

1.5 Contributions

In this thesis, some new digital signal processing algorithms for implementation of the transmitters and receivers within MIMO-OFDM systems are proposed, with and without multiuser interference. As by-products of this study, further research on iterative detection and interference cancellation techniques is also performed. The main contributions of this thesis can be summarized as follows:

1. Certain physical layer processing issues relating to the implementation of both MIMO and OFDM systems have been presented in this thesis. In particular, allowing multiuser operation for certain MIMO-OFDM baseband systems has been a focus.

2. An iterative MIMO-OFDM receiver structure for a space-time block coded (STBC) MIMO-OFDM scheme has been investigated and exploited over both a classical quasi-static multipath channel and a similar slowly fading channel, exploiting Jakes' extended model [76]. Iterative detection based on a minimum mean square error update with decision feedback (MMSE-DF) is utilized. Extrinsic information is exploited to develop log-likelihood ratios (LLRs) for the updates. Simulation results indicate that the scheme is suitable for the considered scenario and outperforms a classical linear MMSE estimator.

3. The idea of two-step interference cancellation was first introduced in [77]. In this thesis, a two-step hard-decision interference cancellation receiver is investigated for a multiuser MIMO-OFDM synchronous uplink system which employs STBC over slowly time-varying channels. The STBC has been implemented either over adjacent tones or adjacent OFDM symbols. The two-step receiver structure uses a combined interference suppression scheme based on minimum mean-squared er-

ror (MMSE) and symbol-wise likelihood detectors, which is then followed by an interference cancellation step. The receiver can suppress and cancel the interference from the co-channel users effectively without increasing the complexity significantly. Additionally, based on the prototype of the two-step MMSE multiuser receiver, a joint coded two-step multiuser detection scheme for a MIMO-OFDM system is further developed, which introduces soft-decision feedback and forward-error-correction coding for more accurate signal detection. The performance of the system is shown by simulation to be significantly improved in a low SNR environment.

4. Recent research shows that iterative turbo processing for soft interference suppression and multiuser detection also has the ability to offer near-capacity performance for multiuser MIMO-OFDM applications over classical multipath MIMO channels. Thus, a novel sequential iterative MMSE multiuser detection scheme is proposed for an OFDM-based multiuser MIMO application. Its turbo-based evolvement is presented, which exploits convolutional error correction coding-decoding techniques. The study results indicate that the proposed scheme is robust in terms of bit error performance as compared with linear algorithms. However, combining iterative MMSE processing with multiuser detection is challenging due to the exponential computational complexity of the soft interference cancellation linear MMSE (SIC-LMMSE) algorithm. A low complexity sequential iterative turbo interference cancellation and multiuser detection algorithm, is therefore further developed, which invokes a low complexity affine MMSE algorithm, followed by highly efficient MUI cancellation and recursive updating processing technique.

1.6 Thesis Outline

This thesis is divided into seven chapters:

Following the introduction chapter the fundamental theories underlying the STBC, OFDM and MIMO techniques for classical wireless channels are provided in Chapter 2. To deal with MIMO-OFDM transmission within high noise and slow fading multipath channel environments, a new framework using an iterative algorithm is proposed for MIMO-OFDM in Chapter 3. Further research on multiuser MIMO-OFDM applications is given in the remaining chapters. In Chapter 4, multiple user interference is discussed in detail and then the concept of a two-step interference cancellation (IC) based linear MMSE algorithm is described. The STBC is implemented either over adjacent tones or adjacent OFDM symbols. Research on iterative MMSE multiuser detection algorithms is then performed for two user MIMO-OFDM in Chapter 5. To improve the performance of the iterative multiuser detection scheme, the idea of soft IC is introduced into non-linear iterative receiver in Chapter 6, where a novel joint multiuser OFDM-based MIMO receiver is firstly investigated combining the IC algorithms with soft error correction techniques, and then, a highly efficient iterative turbo two-step multiuser receiver is proposed with low computational complexity. Chapter 7 provides the summary of this thesis and gives suggestions for future work.

Additionally, in this thesis, both BPSK and QPSK constellation are used in the simulations of the later contribution chapters for average bit error rate (BER). In terms of SNR for BPSK, this is identical to E_b/N_0 whereas for QPSK it is $2E_b/N_0$. The choice of BPSK rather than QPSK corresponds to the way in which the work evolved over time, but for

relative comparisons of the proposed schemes, the relative ordering will be the same whether BPSK or QPSK is used, and therefore performance assessment is possible.

Chapter 2

BACKGROUND REVIEW

2.1 Introduction

The challenge for broadband wireless communications is to provide a high quality-of-service (QoS) at a similar cost to wireline-based technologies. In order to achieve this goal in emerging 4G broadband wireless, multiple antennas are likely to be installed at both the base station and subscriber ends. These technologies endow such systems with the potential ability to achieve high capacities for mobile-access Internet and multimedia services, and thereby dramatically increase coverage and reliability of wireless communications. Orthogonal frequency division multiplexing (OFDM) technology also has advantages for spectrum efficiency and low-cost implementation. Therefore, combination of both powerful technologies is likely to enable the objectives of 4G design, including good coverage, reliable transmission, high peak data rates and high spectrum efficiency [18].

In this chapter, some preliminary research in the fields of MIMO and OFDM technologies is introduced, including the basic MIMO system model and its characteristics, space-time coding theory, OFDM fundamentals and system model, and studies of an OFDM system on both linear time-invariant (LTI) channels and doubly-selective channels.

2.2 Towards Fourth Generation Wireless Communications

During the past century, wireless communications has been enormously developed by three evolutions. In the first generation of wireless communications (1G), analog technology was generally employed motivated by transferring voice as the primary objective. Example standards for 1G included nordic mobile telephone (NMT) used in nordic countries, Switzerland, Netherlands, Eastern Europe and Russia, advanced mobile phone system (AMPS) used in the United States of America and Australia, total access communications system (TACS) in the United Kingdom, Japanese total access communications system (JTACS) in Japan, C-450 in West Germany, Radiocom 2000 in France, and radio telefono mobile integrato (RTMI) in Italy [78]. For second generation (2G), all wireless communications were standardized in terms of digital modulations based on commercial centric applications. Around 60% of the current 2G worldwide market is dominated by the European standards. The family of 2G standards includes global system for mobile communications (GSM), integrated digital enhanced network (iDEN), interim standard 95 (IS-95), personal digital cellular (PDC), circuit switched data (CSD), personal handy-phone system (PHS), general packet radio service (GPRS) and wideband integrated digital enhanced network (WiDEN) [1]. In order to cope with the growing demands for network capacity, required rates towards Mbps level for high speed data transfer and multimedia applications, third generation (3G) type standards started evolving after 2G. They were generally based on the international telecommunication union (ITU) family of standards under the international mobile telecommunications 2000 programme (IMT-2000). The systems in this standard are essentially a linear en-

hancement of 2G systems, supporting data rates up 5-10 Mbps. Currently, there are numerous technologies standardized for 3G, including wideband code division multiple access (W-CDMA), CDMA2000, time division (synchronous) code division multiple access (TD-CDMA/TD-SCDMA), universal mobile telecommunications system (UMTS) sometimes marketed as 3GSM and high speed packet access (HSPA) [79].

While the roll-out of 3G systems is under progress, research activities on fourth generation (4G) systems, a term used to describe the next step in wireless communications, have already started. In particular, 4G is targeting the QoS and rate requirements by forthcoming applications such as wireless broadband access, multimedia messaging service (MMS), video chatting, mobile TV, high definition TV content (HDTV), digital video broadcasting (DVB) and other streaming services for anytime and anywhere communications [80].

Currently, there is no formal definition for 4G, however, there are certain objectives that are projected for 4G, including higher spectrally efficient systems (increased bits/s/Hz and bits/s/Hz/site) [80], higher network capacity (more simultaneous users per cell) [81], a further increase in data rates towards 100 Mbps for physically mobile clients and 1 Gbps for relatively immobile clients (as defined by the ITU Radiocommunication Sector (ITU-R)) [82], and high reliability (quality) of service for next generation multimedia support [83]. For local coverage, WLANs standards can already provide data rates up to 54 Mbit/s (example WLAN standards are: IEEE 802.11a/b/g in the USA and high performance radio LAN V.2 (HIPERLAN/2) in Europe). On the other hand, some pre-4G technologies have already been exploited in practical applications such as worldwide interoperability for microwave access

(WiMax), wireless broadband (WiBro), the 3rd generation partnership project (3GPP) long term evolution (LTE) and 3GPP2 ultra mobile broadband (UMB) [80]. In these contexts, it is widely acknowledged that key physical layer techniques are expected to be utilized in future 4G systems, including MIMO (to attain high coverage and capacity), OFDM (to mitigate the frequency selective channel property and obtain high spectral efficiency), and the turbo principle (to minimize the required SNR for high reliability transmission).

2.3 Basic MIMO Model

Recently, research on 4G wireless communications at the physical layer has focused on exploiting multiple-input, multiple-output (MIMO) technology. In theory, the utilization of multiple antenna arrays at both ends of the link can linearly enhance the system capacity at a level equal to the minimum number of transmit and receive antennas [22], provided the link are statistically uncorrelated, which will be assumed to be true throughout this thesis.

2.3.1 Basic MIMO Model Over Rayleigh Flat Fading Channels

Here, a basic baseband MIMO system model with n_t transmit antennas and m_r receive antennas is represented over a MIMO fading noise free channel as in Figure 2.1.

At the first stage of this system, the MIMO transmitter demultiplexes the transmitting signal stream denoted by $\mathbf{b}(n)$, where n denotes the discrete time index, onto the multiple antennas by a modulation algorithm; then sends each substream through the transmit antennas in parallel. At the receiver stage, demodulation and detection algorithms

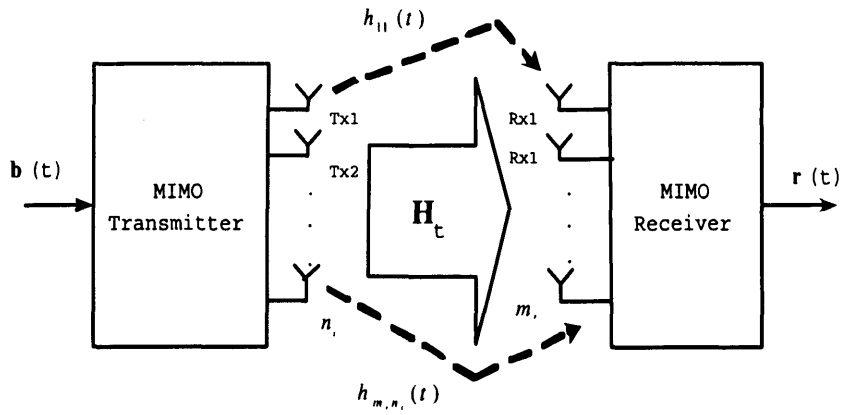

Figure 2.1. Basic baseband MIMO system model over MIMO fading channels

are invoked, and once ready the receive signal terms are multiplexed into the received observations so that the original data stream can be received.

The basic MIMO signal model with n_t transmit antennas and m_r receive antennas respectively together with channel noise can be expressed for Rayleigh frequency flat fading channels as:

$$\mathbf{r}(n) = \mathbf{H}_n(n)\mathbf{b}(n) + \mathbf{v}(n) \tag{2.3.1}$$

where

$$\mathbf{b}(n) = [b_1(n), b_2(n), \cdots, b_{n_t'}(n), \cdots, b_{n_t}(n)]^T$$

and

$$\mathbf{r}(n) = [r_1(n), r_2(n), \cdots, r_{m_r'}(n), \cdots, r_{m_r}(n)]^T$$

which denote the transmit and the receive signal vectors respectively. Note that $b_{n_t'}(n)$ represents the transmitted symbol at the time n, which is generally a QAM/PSK symbol transmitted from the n_t'th

transmit antenna, where $n_t' = 1, 2, \cdots, n_t$. Similarly, $r_{m_r'}(n)$ denotes the received symbol at index n at the m_r'th receive antenna, where $m_r' = 1, 2, \cdots, m_r$. The noise vector is described as

$$\mathbf{v}(n) = [v_1(n), v_2(n), \cdots, v_{m_r'}(n), \cdots, v_{m_r}(n)]^T$$

and each element is complex zero-mean circular Gaussian noise vector with variance σ_v^2, i.e. $\mathbf{v} \sim N(\mathbf{0}, \sigma_v^2 \mathbf{I})$ and $\mathbf{H}_n$ is defined as the discrete time-domain channel matrix for a MIMO channel as

$$\mathbf{H}_n = \begin{pmatrix} h_{11} & h_{12} & \cdots & h_{1n_t'} & \cdots & h_{1n_t} \\ h_{21} & h_{22} & \cdots & h_{2n_t'} & \cdots & h_{2n_t} \\ \vdots & \vdots & \ddots & \vdots & \ddots & \vdots \\ h_{m_r'1} & h_{m_r'2} & \cdots & h_{m_r'n_t'} & \cdots & h_{m_r'n_t} \\ \vdots & \vdots & \ddots & \vdots & \ddots & \vdots \cdots \\ h_{m_r1} & h_{m_r2} & \cdots & h_{m_rn_t'} & \cdots & h_{m_rn_t} \end{pmatrix} \tag{2.3.2}$$

where $h_{m_r'n_t'}$, with $1 \leq m_r' \leq m_r$ and $1 \leq n_t' \leq n_t$, is the complex channel fading coefficient, drawn from an independent complex zero-mean circular Gaussian pdf, from the n_t'th transmit antenna to the m_r'th receive antenna. In MIMO transmission, several detection and equalization techniques can be utilized to realize full capacity and recover data symbols at the receive end, such as minimum mean squared error (MMSE) and interference cancellation (IC) approaches [84], [85] and [86] and the iterative detection schemes [87], [88] and [89].

2.3.2 Signal Model over MIMO-Multipath Fading Channels

In this model $h_{m_r' n_t'}(l)$ is defined as the lth multipath complex fading coefficient of the MIMO-multipath channel forming the transmission pipe from the n_t'th transmit antenna to the m_r'th receive antenna. It is assumed all impulse responses of all channels are finite duration with the same length denoted as L. Therefore, we define $[\mathbf{H}_n(l)]_{m_r' n_t'} = h_{m_r' n_t'}(l)$, so that

$$\mathbf{H}_n(l)= \begin{pmatrix} h_{11}(l) & h_{12}(l) & \cdots & h_{1n_t'}(l) & \cdots & h_{1n_t}(l) \\ h_{21}(l) & h_{22}(l) & \cdots & h_{2n_t'}(l) & \cdots & h_{2n_t}(l) \\ \vdots & \vdots & \ddots & \vdots & \ddots & \vdots \\ h_{m_r'1}(l) & h_{m_r'2}(l) & \cdots & h_{m_r' n_t'}(l) & \cdots & h_{m_r' n_t}(l) \\ \vdots & \vdots & \ddots & \vdots & \ddots & \vdots \cdots \\ h_{m_r 1}(l) & h_{m_r 2}(l) & \cdots & h_{m_r n_t'}(l) & \cdots & h_{m_r n_t}(l) \end{pmatrix} \tag{2.3.3}$$

The received baseband signal model, therefore, can be described for a MIMO-multipath channel as

$$\mathbf{r}(n)=\sum_{l=0}^{L-1} \mathbf{H}_n \mathbf{b}(n-l)+\mathbf{v}(n) \tag{2.3.4}$$

From Eq.2.3.4, the channel matrix in Eq.2.3.3 is convolved with the transmitted signal vector to obtain the received signal $\mathbf{r}(n)$. Thus the MIMO system over multipath channels suffers from inter-symbol interference (ISI). Perfect synchronization between the transmitter and receiver is assumed throughout this thesis. OFDM techniques are robust for mitigating ISI and hence achieving the potential capacity of the MIMO channels as will be explained in Section 2.6.

2.4 Further MIMO Preliminaries

2.4.1 Multi-Antenna Systems

There exist different antenna configurations in practical MIMO applications as shown in Figure 2.2. As expressed in Eq. (2.3.2), for $n_t = 1$

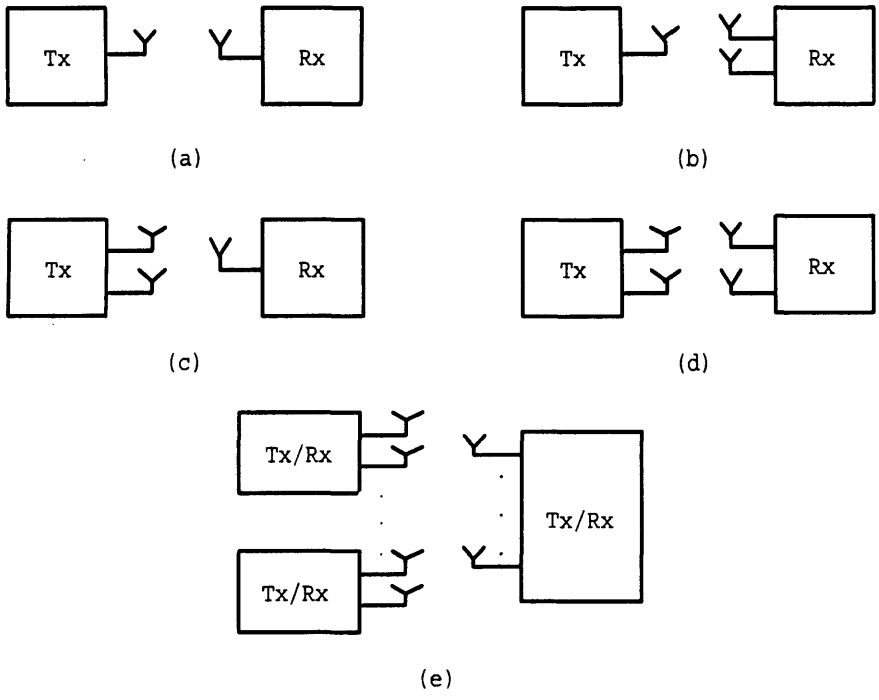

Figure 2.2. Different multi-antenna system models: (a) SISO model; (b) SIMO model; (c) MISO model; (d) MIMO model; (e) Multiuser MIMO model (MU-MIMO).

the MIMO system transforms to a single-input multiple-output (SIMO) wireless communication system, for which it is well-known that only the receiver end is equipped with multiple (m_r) receive antennas but a single transmit antenna is used (as in Figure 2.2b). Similarly, the MIMO configuration can also be simplified to a multiple-input single-output (MISO) deployment when $m_r = 1$, i.e. only multiple (n_t) transmit antennas at the transmitter end are utilized but with a single receive

antenna (see in Figure 2.2c). A simple scalar MIMO scheme, therefore, can be defined when both $n_t = m_r = 1$, which is a so-called single-input single-output (SISO) configuration (see in Figure 2.2a). Otherwise, multiuser-MIMO applications (MU-MIMO) exploit a configuration where the base station consists of multiple antennas, and one or more transmit/receive antennas are positioned on each terminal (see Figure 2.2e).

It is traditionally well-known that it is effective to take advantage of multiple antennas at one side of a wireless transmission system to implement IC and realize diversity and array gain through the coherent combining effect of multiple antennas. Moreover, another fundamental gain - spatial multiplexing can be achieved through utilization of multiple antennas at both sides of a wireless transmission (MIMO), which induces increased spectral efficiency.

2.4.2 Array Gain

In MIMO communication systems, array gain means the power gain of the transmitted signals that is achieved through employing multiple-antennas at the transmitter and/or receiver. It therefore can be simply called power gain, which depends on the number of transmit and receive antennas. Array gain can be realized both at the transmitter and the receiver and induces an increase in average receive signal-to-noise ratio (SNR), which arises from the coherent combining effect of multiple antennas at the receiver/transmitter or both, and hence improved coverage. Channel knowledge is required to achieve array gain at the transmitter and receiver end, respectively. When assuming perfect knowledge of the channel at the transmitting end, the transmitter

obtains the ability to enhance the transmitting propagation through processing of the signals transmitted by the multiple antennas by complex weights, depending on the channel coefficients, i.e. beamforming. Each single receive antenna combines the signal from all transmit antennas, to achieve so-called transmitter array gain (i.e. the MISO case in Figure 2.2c). Similarly, assuming a single antenna is employed at the transmitter without knowledge of the channel, a multiple antenna receiver with perfect knowledge of channel state information (CSI) will implement coherent combination of the incoming signals at multiple receive antennas, through performing additional processing, and thereby enhance the signal, which is so-called receiver array gain (i.e. the SIMO case in Figure 2.2b). Basically, CSI is available at the receiver through some channel estimation algorithm, however this is more difficult to maintain at the transmitter, and depends upon whether time division duplex (TDD) or frequency division duplex (FDD) is assumed. In TDD the up and down links can be assumed to be symmetric, thereby reducing any feedback overhead, whereas this does not apply for FDD so feed back would be necessary. Therefore, the receiver array gain is easier to exploit but limited feedback is possible in real systems.

2.4.3 Diversity Gain

Due to the effect of channel fading, the transmitted signal suffers random fluctuation in its strength over a wireless channel. When the received signal power drops significantly, the channel is said to be in a fade, which gives rise to high bit error rate (BER) which affects the reliability of the link. Diversity is a powerful technique to improve link reliability by mitigating fading in wireless channels and increasing

the robustness to co-channel interference. Diversity gain is obtained by providing replicas of the transmitted signal over multiple (ideally) independently fading dimensions (in time/frequency/space) and implementing a proper combining scheme at the receiver end.

Time diversity, frequency diversity or spatial diversity techniques are often used to greatly reduce the chance of a deep fade. However, spatial diversity is more attractive and applicable compared with time or frequency diversity, because it presents no increased cost in transmission time or bandwidth, respectively. In general, time diversity is obtained by retransmitting data at least after a delay of the channel coherence time. However, it requires that the channel must provide sufficient variations in time, which reduces the data rate, when replicas of the data are sent. Alternatively, a redundant forward error correction code is added and the message is spread in time by means of bit-interleaving before it is transmitted. However, redundancies are introduced into transmitting signals which decreases the transmission efficiency. Frequency diversity can be extracted by transmitting replicas of the original data simultaneously at different frequency bands which are separated greater than the coherence bandwidth of the channel. However, this is often unapplicable as it induces an expenditure in valuable bandwidth, unless as in OFDM techniques, sub-carriers are selected to achieve frequency diversity. Spatial diversity can be obtained by exploiting multiple antennas at the transmitter (MISO), receiver (SIMO) or both (MIMO), which does not require extra transmission time or bandwidth, but renders addition in complexity and cost to the base station, mobile or both. However, it is often preferable due to the reduction of the cost of base station hardware that has been experienced

over the last decade [90]. Assuming uncorrelated channel fading and a properly constructed transmitted signal in an (n_t, m_r) MIMO link, as compared with a SISO link, the arriving diversified waveform at the receiver can be combined to obtain a receive signal which achieves a considerable ability to combat the effect of signal amplitude fluctuation, i.e. fading, and obtains $n_t \times m_r$th-order diversity.

Such spatial diversity can also be further categorized as transmit diversity or receive diversity. The transmit diversity (i.e. extracting the spatial diversity through the transmitter) can be realized applicably by introducing controlled redundancies in the transmitting processing stage in the absence of channel knowledge at the transmitter. The corresponding technique is known as space-time coding [33] and [21]. The receive diversity is frequently leveraged by a maximum-ratio-combining (MRC) algorithm that coherently combines signals at multiple receivers to maximize signal to noise ratio (SNR) and thereby improve signal quality. However, there exists a trade-off between complexity, cost and performance [90] when performing MRC which limits its deployment in cell phones. Transmit diversity is thereby becoming popular since it is easier to implement at the base station.

In the case where there is full correlation between the data streams carried by the multiple data pipes of a MIMO link, no throughput (bits/second) advantage is obtained, however, it achieves full diversity advantage. On the other hand, in the case assuming no correlation between all transmission links, i.e. the data streams are absolutely independent, no diversity is present but higher throughput is available compared to the former case, i.e. rise in capacity is induced. Thus the MIMO system can not provide full diversity and capacity at the same

time [91] and [35]. Therefore, there exists a trade-off between diversity and capacity. This problem can be further optimized by spatial multiplexing (SM).

2.4.4 Spatial Multiplexing for Capacity

There is a huge gap between the throughput in cable, wireline and wireless communications. In high data rate wireless communications, high throughput is expected. However, currently due to legislative reasons, wireless transmission can not be performed over the whole radio frequency bandwidth because of interference from other radio transmissions. Thus the amount of bandwidth assigned to the particular wireless network is crucial. In order to extend the throughput, performing spatial multiplexing in MIMO systems is considered as an effective solution to increase the spectral efficiency and yield a linear (i.e. $min(n_t, m_r)$) capacity (or transmission rate) increase, compared to a SISO system, with no additional power and keeping the same bandwidth and SNR [26], [23], [30] and [31].

2.4.4.1 Capacity for SISO and MIMO Models

The channel throughput was expressed by C. Shannon in 1948 [92] as the limit to reliable transmission over a noisy channel. The capacity is commonly considered as the potential of the channel to transmit data. That means the possible maximum transmission rate in a unit bandwidth with arbitrarily low bit error rate. Hence, the capacity is the upper bound of the spectral efficiency achievable in the specific radio channel. Shannon showed that the upper bound limit on the capacity C of the channel with additive white Gaussian noise is given by the

following equation:

$$C = \log_2(1 + SNR) \tag{2.4.1}$$

or, when including a SISO channel coefficient h, it can be expressed as:

$$C = \log_2(1 + SNR \cdot |h|^2) \tag{2.4.2}$$

where SNR is the unfaded signal to noise ratio at the receive antenna and h is considered as a normalized channel power complex scalar ($E\{|h|^2\} = 1$, where $E\{\cdot\}$ denotes the statistical expectation operation and $|\cdot|$ denotes absolute value). The capacity unit is bps/Hz. In this case, 3dB more SNR induces one more bps/Hz capacity.

In a receive diversity SIMO case with a single transmit antenna and m_r receive antennas, when the receiver uses optimum combining (maximum ratio combining), the capacity can be given by [22]:

$$C = \log_2\left(1 + SNR\sum_{i=1}^{m_r}|h_i|^2\right) \tag{2.4.3}$$

For a transmit diversity MISO system with n_t transmit antennas and a single receive antenna, assuming the total transmit power across all antennas is constant, then the capacity can be expressed as:

$$C = \log_2\left(1 + \frac{SNR}{n_t}\sum_{i=1}^{n_t}|h_i|^2\right) \tag{2.4.4}$$

In 1987, Winters published the concept of a new technique using multiple antennas at both the transmitter and receiver [25], now known as MIMO. In 1995, Teletar published derivations of capacities in Gaussian and fading channels for MIMO systems [24]. In 1996, Foschini

presented his derivation for the upper bound capacity for the (n_t, m_r) MIMO model [23], with n_t transmit antennas and m_r receive antennas as:

$$C = \log_2 \det \left[\mathbf{I}_{m_r} + \left(\frac{SNR}{n_t} \right) \mathbf{H}\mathbf{H}^H \right] \tag{2.4.5}$$

where $\det(\cdot)$ is the matrix determinant operation, $\mathbf{I}_{m_r}$ is the $m_r \times m_r$ identity matrix. $\mathbf{H}$ is the channel matrix with $m_r \times n_t$ dimension and $(\cdot)^H$ is the complex conjugate transpose or Hermitian transpose operation. Here SNR is considered as the ratio of the total transmit power to the noise power at the receive antenna. The transmitted signals over the models are assumed independent. The capacity from Eq.(2.4.5) can be calculated as [24]:

$$C = \sum_{i=1}^{G} \log_2 \left(1 + \frac{SNR}{n_t} \lambda_i^2 \right) \tag{2.4.6}$$

where G is defined as the rank of the matrix $\mathbf{H}$, and $\lambda_1, \lambda_2, \ldots, \lambda_G$ are defined as the non-negative square roots of the eigenvalues of the matrix $\mathbf{H}\mathbf{H}^H$, which are the so-called singular values of $\mathbf{H}$ [93]. In the case when the transfer functions of the MIMO subchannels are not correlated, e.g. in a richly scattered environment, G therefore is maximal and is equal to $min(n_t, m_r)$. Note that average receive signal-to-noise ratio can be calculated as:

$$SNR_{average} = \frac{SNR \sum_{m_r'=1}^{m_r} \sum_{n_t'=1}^{n_t} \left| h_{m_r' n_t'} \right|^2}{n_t \cdot m_r} \tag{2.4.7}$$

In Eq.(2.4.5) and Eq.(2.4.6), it is assumed that the receiver, but not the transmitter, has the knowledge of CSI and complex flat fading channels are assumed over the signal bandwidth. From this case, it is therefore shown that the capacity of a MIMO channel increases

proportionally to $G = min(n_t, m_r)$, compared to SISO model.

2.4.4.2 Spatial Multiplexing Gain

In the case of an (n_t, m_r) MIMO system, assuming the propagation channel exhibits rich scattering, the spatial multiplexing gain is essentially realized by multiplexing a high-rate signal into a set ($G = min(n_t, m_r)$) of lower-rate independent sub-streams, each of which is encoded, modulated, and transmitted over individual data pipes simultaneously at the same frequency slot. Then at the receive end, with full knowledge of CSI, the receiver recovers these individual streams with appropriate detection techniques and combines them into an original signal. Thus spatial multiplexing increases the capacity proportionally with the minimum number of transmit-receive antenna pairs ($G = min(n_t, m_r)$), i.e. the spectral efficiency grows G times and the spatial multiplexing gain is equal to G.

This processing can be also extended to multiuser MIMO (MU-MIMO) case. In such a case, similarly, assuming the data streams are simultaneously transmitted from K user terminals to the base station equipped with m_r antennas, the base station can likewise separate and detect these signals for each user. This allows capacity to increase proportionally to the number of antennas of the base station and user pairs.

2.5 Space-Time Block Codes

2.5.1 Review of Space-Time Codes

In many mobile applications, CSI may not be available at the transmitter, hence it is a challenge to extract the spatial diversity at the transmitter without knowledge of CSI. However, the transmit diversity can still be realized by introducing controlled redundancies into the transmitting processing stage without CSI. One of the corresponding techniques is known as space-time coding (STC) which introduces a coding jointly with the time dimension at the transmitter [21], [28] and [33]. There are two major categories of space-time codes: space-time trellis codes (STTC) and space-time block codes (STBC).

Within an STTC scheme, the coding processing is based on a trellis rule for the transmitted symbols over multiple antennas and multiple time-slots, and both full diversity gain and coding gain can be achieved by a maximum likelihood (ML) receiver [21].

Within an STBC scheme, a block of data is formed at once in terms of a transmission matrix (similarly to block codes [52]), then these multiple copies of symbols are transmitted across multiple antennas, e.g. in the case of the transmission with n_t transmit antennas, the symbols are transmitted from the other antennas as essentially conjugated versions of the symbols transmitted from the first Tx antenna. So, additional Tx antennas do not transmit additional data symbols but only copies of the transmitting symbols from the first antenna. After traversing channels, some of these received copies of the data may have the ability to overcome the potentially difficult environment of channels and to improve the reliability of data-transfer [94]. It is the fact that STBC

combines all the copies of the received signal in some optimal algorithm to extract as much correct information as possible that underpins its advantage, and a higher chance to decode correctly the received signal results.

Although in (n_t, m_r) frequency flat MIMO applications, STBC only provides possible full diversity of $n_t \times m_r$th-order without improvement in terms of spectral efficiency, it takes much less computational complexity for implementation compared to STTC [33], [34] and [94] and therefore is exploited in this thesis.

There are several categories of STBC including orthogonal STBCs (O-STBCs) [34] and [33], quasi-orthogonal STBCs (QO-STBCs) [95], differential STBCs [96] and [97] and unitary space-time modulation [98].

2.5.2 Alamouti's STBC

The simplest scheme for STBCs was invented for two Tx antennas and arbitrary number of Rx antennas by Alamouti in 1998 [33]. His STBC scheme is the only example of an O-STBC, which has the ability to achieve both full diversity and full code rate, i.e., it is a rate-1 code because it takes two time-slots to transmit two complex constellated symbols. Due to its simplicity of decoding, Alamouti's STBC has been widely utilized in practical applications such as 3G systems [79]. For a two transmit, one receive antenna scheme with a flat-fading channel, the encoding scheme can be described as follows.

$$\mathbf{X}_{coded} = \begin{bmatrix} x_1 & x_2 \\ -x_2^* & x_1^* \end{bmatrix} \tag{2.5.1}$$

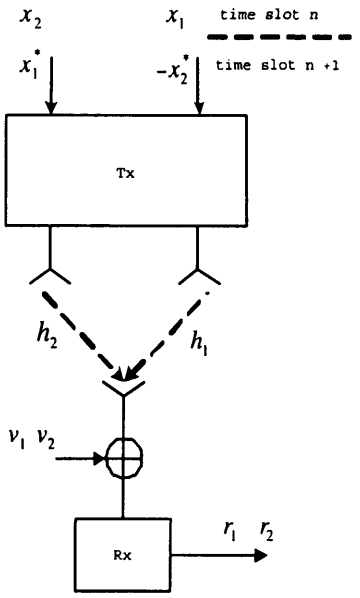

Figure 2.3. Alamouti's STBC scheme with two transmit antennas and a single receive antenna, representing two consecutive time slots.

From Eq.(2.5.1), at time slot n, the two symbols x_1 and x_2 are transmitted simultaneously from the first and second transmit antennas respectively. Then, at the next time slot $n+1$, the two symbols $-x_2^*$ and x_1^* are transmitted from the transmit antennas in the same order. The symbols are coded in the space domain (two Tx antennas) and in the time domain (two time slots required for the transmission). The transmitted symbols are assumed as zero-mean with unity variance. In this case, four transmitted symbols during two time slots form the block of data, but two of them are repeated. There are two orthogonal transmit vectors: $\alpha_1 = [x_1, x_2]$ and $\alpha_2 = [-x_2^*, -x_1^*]$ in this coding matrix. Therefore, the transmit vectors in STBC are always orthogonal, which induces [34]:

$$\mathbf{X}_{coded}^{H}\mathbf{X}_{coded} = (|x_1|^2 + |x_2|^2)\mathbf{I} \qquad (2.5.2)$$

Considering the case with a single receive antenna, as shown in Figure 2.3, the receive signals at time slots n and $n+1$ can be piled up in the elements of a vector as

$$\begin{bmatrix} r_1 \\ r_2 \end{bmatrix} = \begin{bmatrix} x_1 & x_2 \\ -x_2^* & x_1^* \end{bmatrix} \begin{bmatrix} h_1 \\ h_2 \end{bmatrix} + \begin{bmatrix} v_1 \\ v_2 \end{bmatrix} \tag{2.5.3}$$

which can be further simplified as

$$\mathbf{r} = \mathbf{X}_{coded}\mathbf{h} + \mathbf{v} \tag{2.5.4}$$

where v_1 and v_2 are independent zero-mean complex circular additive white Gaussian noise terms. The channel coefficients h_1 and h_2 are assumed to keep static over two transmitting time slots, i.e. the channel is assumed quasi-static. For simplicity of analysis, Eq.(2.5.3) can be written equivalently as

$$\begin{bmatrix} r_1 \\ r_2^* \end{bmatrix} = \begin{bmatrix} h_1 & h_2 \\ h_2^* & -h_1^* \end{bmatrix} \begin{bmatrix} x_1 \\ x_2 \end{bmatrix} + \begin{bmatrix} v_1 \\ v_2^* \end{bmatrix} \tag{2.5.5}$$

and Eq.(2.5.5) can be also simplified as

$$\tilde{\mathbf{r}} = \tilde{\mathbf{H}}\mathbf{x} + \tilde{\mathbf{v}} \tag{2.5.6}$$

where $\mathbf{x} = [x_1, x_2]^T$ represents the original transmitting symbol vector, and $\tilde{\mathbf{r}} = [r_1, r_2^*]^T$ denotes the equivalent received signal vector at the receive antenna, and $\tilde{\mathbf{H}} = \begin{bmatrix} h_1 & h_2 \\ h_2^* & -h_1^* \end{bmatrix}$ denotes the overall equivalent channel matrix, and $\tilde{\mathbf{v}} = [v_1, v_2^*]^T$ represents the equivalent noise of the whole channel. Because there also exists the characteristic of

orthogonality for $\tilde{\mathbf{H}}$ as in $\mathbf{X}_{coded}$, therefore, it follows that

$$\tilde{\mathbf{H}}^H\tilde{\mathbf{H}} = (|h_1|^2 + |h_2|^2)\mathbf{I} \tag{2.5.7}$$

Alamouti's STBC could also be exploited with multiple receive antennas. Assuming a receiver with m_r receive antennas, the equivalent receive signal vectors at the $1, 2, \ldots, m_r$th receive antennas can be expressed respectively as

$$\begin{aligned} \tilde{\mathbf{r}}_1 &= \tilde{\mathbf{H}}_1\mathbf{x} + \tilde{\mathbf{v}}_1 \\ \tilde{\mathbf{r}}_2 &= \tilde{\mathbf{H}}_2\mathbf{x} + \tilde{\mathbf{v}}_2 \\ &\cdots \\ \tilde{\mathbf{r}}_{m_r} &= \tilde{\mathbf{H}}_{m_r}\mathbf{x} + \tilde{\mathbf{v}}_{m_r} \end{aligned} \tag{2.5.8}$$

From the set of Eqs.(2.5.8), stacking can be used to put them into an equation in terms of matrices as

$$\begin{bmatrix} \tilde{\mathbf{r}}_1 \\ \tilde{\mathbf{r}}_2 \\ \vdots \\ \tilde{\mathbf{r}}_{m_r} \end{bmatrix} = \begin{bmatrix} \tilde{\mathbf{H}}_1 \\ \tilde{\mathbf{H}}_2 \\ \vdots \\ \tilde{\mathbf{H}}_{m_r} \end{bmatrix} \begin{bmatrix} x_1 \\ x_2 \end{bmatrix} + \begin{bmatrix} \tilde{\mathbf{v}}_1 \\ \tilde{\mathbf{v}}_2 \\ \vdots \\ \tilde{\mathbf{v}}_{m_r} \end{bmatrix} \tag{2.5.9}$$

Eq.(2.5.9) can also be simplified in the same way as Eq.(2.5.6) as

$$\acute{\mathbf{r}} = \acute{\mathbf{H}}\mathbf{x} + \acute{\mathbf{v}} \tag{2.5.10}$$

One particularly attractive feature of orthogonal STBCs including Alamouti's scheme is that the transmitting data symbols can be recovered simply by maximum likelihood (ML) decoding [99] with only

linear processing at the receiver of not only a single receive antenna but also a multiple set. In the case of multiple receive antennas as shown in Eqs.(2.5.8), the ML detector estimates the data symbols by minimizing the expression $\left|\tilde{\mathbf{r}}_j - \tilde{\mathbf{H}}_j\mathbf{x}\right|^2$ for all the j ($j = 1, 2, \ldots, m_r$) receive signal vectors by invoking the possible data symbol pair $\mathbf{X} = \{x_1, x_2\}$ i.e.

$$\{\hat{x}_1, \hat{x}_2\} = \arg\min_{\forall \mathbf{X}} \sum_{j=1}^{m_r} \left\{ \left|\tilde{\mathbf{r}}_j - \tilde{\mathbf{H}}_j\mathbf{x}\right|^2 \right\} \tag{2.5.11}$$

In conclusion, Alamouti's STBC is the only scheme of O-STBC with simple linear decoding processing for complex symbols, which provides both maximal diversity order of two and full code rate up to one (one symbol coded per time slot).

2.5.3 Quasi-Orthogonal STBC

All O-STBCs have the ability to achieve full diversity, but only Alamouti's scheme can obtain full code rate whilst extracting full diversity. In the past decade, a STBC scheme called 'quasi-orthogonal STBC' (QO-STBC) was proposed that is extended from O-STBCs but can achieve a higher data rate. These codes provide partial orthogonality and provide only part of the diversity gain. An example is proposed by H. Jafarkhani [95]. It is the straightforward extension of Alamouti's STBC for four transmit antennas, which constructs the code matrix using two sets of Alamouti's codes. The encoding scheme can be described as

$$\mathbf{X}_{QO-coded}= \begin{bmatrix} x_1 & x_2 & x_3 & x_4 \\ -x_2^* & x_1^* & -x_4^* & x_3^* \\ -x_3^* & -x_4^* & x_1^* & x_2^* \\ x_4 & -x_3 & -x_2 & x_1 \end{bmatrix} \tag{2.5.12}$$

The orthogonality criterion only holds for columns (1 and 2), (1 and 3), (2 and 4) and (3 and 4). However, it clearly has the full rate code equal to unity, i.e. four data symbols are coded over four time slots. This scheme still only requires linear processing at the receiver.

Assuming the case of the system with four transmit antennas and a single receive antenna with the same channel environment as in Eq.(2.5.5), the transfer function could be expressed in terms of equivalent matrices by taking the complex conjugate in the range from the second to the third rows, as follows

$$\begin{bmatrix} r_1 \\ r_2^* \\ r_3^* \\ r_4 \end{bmatrix} = \begin{bmatrix} h_1 & h_2 & h_3 & h_4 \\ h_2^* & -h_1^* & h_4^* & -h_3^* \\ h_3^* & h_4^* & -h_1^* & -h_2^* \\ h_4 & -h_3 & -h_2 & h_1 \end{bmatrix} \begin{bmatrix} x_1 \\ x_2 \\ x_3 \\ x_4 \end{bmatrix} + \begin{bmatrix} v_1 \\ v_2^* \\ v_3^* \\ v_4 \end{bmatrix} \tag{2.5.13}$$

which simplified as

$$\tilde{\mathbf{r}}_{QO} = \tilde{\mathbf{H}}_{QO}\mathbf{x} + \tilde{\mathbf{v}}_{QO} \tag{2.5.14}$$

From Eq.(2.5.14), the transmitted signal can be estimated by performing linear processing as

$$\hat{\mathbf{x}} = \tilde{\mathbf{H}}_{QO}^{H}\tilde{\mathbf{r}}_{QO}= \mathbf{\Delta}\mathbf{x} + \tilde{\mathbf{H}}_{QO}^{H}\tilde{\mathbf{v}}_{QO} \tag{2.5.15}$$

Eq.(2.5.15) can be expressed as

$$\begin{bmatrix} \hat{x}_1 \\ \hat{x}_1 \\ \hat{x}_1 \\ \hat{x}_1 \end{bmatrix} = \begin{bmatrix} \gamma & 0 & 0 & \alpha \\ 0 & \gamma & -\alpha & 0 \\ 0 & -\alpha & \gamma & 0 \\ \alpha & 0 & 0 & \gamma \end{bmatrix} \begin{bmatrix} x_1 \\ x_2 \\ x_3 \\ x_4 \end{bmatrix} + \begin{bmatrix} \acute{v}_1 \\ \acute{v}_2 \\ \acute{v}_3 \\ \acute{v}_4 \end{bmatrix} \tag{2.5.16}$$

In Eq.(2.5.16), the term α is a form of coupling of symbols, which is caused by the interference from other symbols (e.g. the fourth symbol interferes with the first one and the second symbol suffers from the third one). These couplings of symbols induce loss of diversity gain. This problem can be further optimized by a preprocessing operation at the transmitter [100] and [101], and closed-loop operation to provide CSI.

2.6 A Brief Overview of the OFDM Technique

Digital multimedia applications create an ever increasing demand for broadband communication systems, however, the technical requirements for related products are very high so that the solution is not cheap. Whereas for the satellite channel and for the cable channel, where the cost-efficient solutions already exist, in the case of the terrestrial link (i.e. classical TV broadcasting), the requirements are so high that the 'standard' solutions are no longer feasible or lead to optimal results. An optimal solution called orthogonal frequency division multiplexing (OFDM) attracts tremendous interest currently because it allows transmission of high data rates over extremely hostile channels at a comparable low complexity. Nowadays, OFDM has been chosen as the transmission method for the European radio (DAB) and TV (DVB-T)

standards [102], [47] and [48]. Due to its numerous advantages such as low inter symbol interference, spread spectrum and low implementation cost, it is therefore under discussion for future broadband wireless applications such as WiMax and Wi-Fi [37], [39] and [103].

2.6.1 Multipath Propagation and Multi-Carrier Approach

In contrast to satellite communications where one single direct path from the transmitter to the receiver is present, in the classical terrestrial broadcasting scenario, a multi-path channel should be addressed: the transmitted signal arrives at the receiver over various paths of different lengths. Since multiple versions of the signal interfere with each other (ISI), it becomes very hard to extract the original information. The common representation of the multi-path channel is the channel impulse response (CIR) of the channel which is the signal measured at the receiver if a single pulse is transmitted.

Assuming a system transmitting discrete information in time intervals T, the critical measure concerning the multi-path channel is the delay $\tau_{\max}$ of the longest path with respect to the earliest path. A received symbol can theoretically be influenced by $\tau_{\max}/T$ previous symbols. This influence has to be estimated and compensated for in the receiver, a task which may become very challenging. In a single carrier transmission system, the transmitted symbols are pulse formed by a transmitter filter. The transmitting data rate R can be expressed in general as:

$$R = \frac{1}{T} \tag{2.6.1}$$

Hence, for the single carrier system, the ISI term can be expressed as:

$$\frac{\tau_{\max}}{T} = R \cdot \tau_{\max} \tag{2.6.2}$$

From Eq.(2.6.2), it can be seen that the ISI will be large as the transmission rate is high in single carrier systems. Hence, the complexity involved in removing this interference at the receiver is considerable for multimedia application systems because of its high transmission data rates. Hence a cost-effective implementation using such an approach can not be obtained. This is the main reason why the multi-carrier approach has become so popular. In multi-carrier transmission systems, the original data stream of rate R is multiplexed into N parallel data substreams with reduced data rate as

$$R_{mc} = \frac{1}{T_{mc}} = \frac{R}{N} \tag{2.6.3}$$

where each of the data substreams is modulated with a different frequency and the resulting signals are transmitted together in the same band. Correspondingly, the receiver consists of N parallel receiver paths. Due to the prolonged distance among transmitted symbols the ISI for each substream reduces to

$$\frac{\tau_{\max}}{T_{mc}} = \frac{\tau_{\max}}{N \cdot T} = \frac{R \cdot \tau_{\max}}{N} \tag{2.6.4}$$

Comparing Eq.(2.6.2) with Eq.(2.6.4), ISI is reduced by a factor of N as compared to a single carrier application for the same transmission data rates and the channel environment. Such a small amount of ISI can often be tolerated and no extra equalization is required. As far as the

complexity of a receiver is concerned, a system with too much parallel multiplexing is still not feasible. This demands for a slight modification of the approach which leads us to the concept of OFDM.

2.6.2 FDM & OFDM: A Common Interpretation

OFDM is a highly cost-effective example of the multi-carrier transmission technique. The idea is to make the symbol period long with respect to the channel impulse response in order to reduce ISI. This implies that the bandwidth of the sub-carriers becomes small (with respect to the channel's coherence bandwidth [54]), thus the impact of the channel is reduced to an attenuation and phase distortion of the sub-carrier symbols ("flat fading"), which can be compensated by efficient one-tap equalization, provided the channel is static during the OFDM symbol.

The principle of signal processing in OFDM technique is very similar to the technique of frequency division multiplexing (FDM). It uses the same principle as FDM to multiplex data streams into several parallel substreams in the frequency domain over a single radio channel. In conventional FDM broadcasting, each transmitting substream is modulated by a separated transmitting station on a different frequency and the separation between any two frequencies is kept high so that the carriers do not interfere with each other. Thus, synchronization is not required between the stations however, this induces comparable low spectrum efficiency.

On the other hand, in OFDM, the data of each substream are simultaneously transmitted on different densely packed orthogonal subcarriers so that high spectral efficiency can be achieved. All the subcarriers of OFDM signal are required to be synchronized to each other in time

and frequency, which makes sure interference between the subcarriers is ideally equal to zero due to the nature of orthogonality. Hence, it provides an ability to avoid inter-carrier-interference (ICI), although the spectra of the sub-carriers actually overlap. Figure 2.4 shows the nature of orthogonality within the overlapping spectra (sinc-functions) of four adjacent OFDM sub-carriers. In general, the subcarrier pulse forming and modulation in OFDM techniques can be simply performed by an inverse discrete Fourier transform (IDFT). Currently, the processing can be implemented very efficiently in the terms of an inverse fast Fourier transform (IFFT). Accordingly, only an FFT is needed to reverse this operation at the receiver.

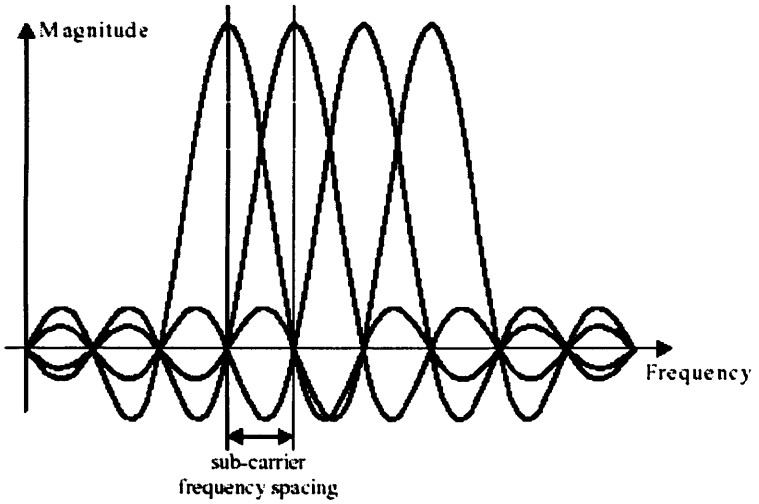

Figure 2.4. The overlapping spectra (sinc-functions) of four adjacent OFDM sub-carriers. At one sub-carrier center frequency, all other spectra are zero, demonstrating the sub-carrier orthogonality.

2.6.3 OFDM System Model

A basic baseband model of the OFDM system is shown in Figure 2.5. First of all, the source data bits are re-structured by a serial to parallel

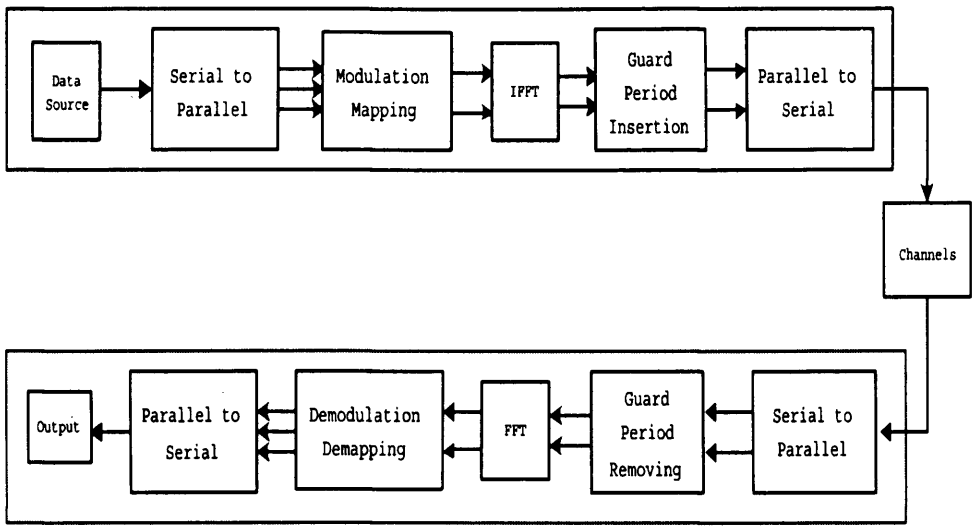

Figure 2.5. OFDM transceiver diagram consist of the transmitter, channel and receiver.

(S/P) converter, and then are modulated as a data block of N mapped symbols generally using a phase shift keying (PSK) or quadrature amplitude modulation (QAM) constellation. These mapped symbols are then converted into the time domain by applying an IFFT operation. After that, a cyclic prefix (CP) of length P is inserted at the head of the time interleaved samples; the CP length P should not be less than channel length L ($P \geq L$) to guarantee that the ISI is completely removed.

Here the whole block of data is considered as a random-OFDM symbol. When the signal is propagating through the radio channel, the channel matrix can be represented as a circulant matrix $\mathbf{H}$ due to CP insertion [93], the columns of which are composed in the terms of cyclically shifted versions of a zero padded channel vector, i.e. the channel matrix is performed as a circular convolution matrix by introducing a CP in the time domain. An attractive property of a circulant

matrix is that it can be exactly diagonalized by performing a DFT operation. The DFT is often simplified by using an FFT at the receiver with concomitant low computational complexity. The same process as the transmitting stage is inversely performed at the receiving end, with CP removal, FFT, demapping and parallel to serial converting.

As a result from the nature of circulant matrix, it thus only simply requires one-tap channel equalization performed on frequency domain for signal estimation, with a static channel.

2.6.4 Signal Processing of OFDM Model in a Static Channel

As shown in Figure 2.5, assuming the transmitting signals are independent and identically distributed (i.i.d.), and that the mapped symbols set can be expressed as $\{s_k\}$, and the $\{x_n\}$ are the time samples after the IFFT operation, which can be described by the following N-point IDFT operation as,

$$x_n = \frac{1}{\sqrt{N}} \sum_{k=0}^{N-1} s_k e^{j\frac{2\pi}{N}kn} \tag{2.6.5}$$

where $n = 0, 1, 2, \ldots, N-1$ for x_n and the component of $\frac{1}{\sqrt{N}}$ represents the normalization of the FFT or IFFT operations. The vector form of the sequence $\{x_n\}$ can be written as

$$\mathbf{x} = \mathbf{F}^H \mathbf{s} \tag{2.6.6}$$

where $\mathbf{F}$ is the DFT matrix of size $N \times N$ and $\mathbf{s}$ is the transmitting mapped symbol vector in the frequency domain. After the insertion of a CP of length P, the transmitting guarded-OFDM symbol sequence

$\{\tilde{x}_p\}$ can be defined as

$$\tilde{x}_p \in \{\tilde{x}_{N-P}, \tilde{x}_{N-P+1}, \ldots, \tilde{x}_{N-1}, \tilde{x}_0, \tilde{x}_1, \ldots, \tilde{x}_{N-1}\} \tag{2.6.7}$$

where $-P \leq p \leq N-1$ for $\tilde{x}_p$. As the signal is traversing an L path static channel where $L \leq P$, the received baseband signal at sample time n can be described after removing the CP as

$$r_n = \sum_{l=0}^{L-1} h(l)\tilde{x}_{n-l} + v_n \tag{2.6.8}$$

where $h(l)$ is the lth tap of the complex channel and v_n is the complex white circular zero mean Gaussian noise at sample time n for r_n and v_n. Hence, the received signal in the time domain can be written in vector form of length N as

$$\mathbf{r} = \mathbf{H}\mathbf{x} + \mathbf{v} = \mathbf{H}\mathbf{F}^H\mathbf{s} + \mathbf{v} \tag{2.6.9}$$

Performing the FFT on Eq.(2.6.9), the receive sample vector in the frequency domain becomes

$$\begin{aligned} \mathbf{F}\mathbf{r} &= \mathbf{F}\mathbf{H}\mathbf{x} + \mathbf{F}\mathbf{v} \\ &= \mathbf{F}\mathbf{H}\mathbf{F}^H\mathbf{s} + \mathbf{F}\mathbf{v} \\ &= \mathbf{H}_{df}\mathbf{s} + \mathbf{F}\mathbf{v} \end{aligned} \tag{2.6.10}$$

where $\mathbf{H}_{df} = \mathbf{F}\mathbf{H}\mathbf{F}^H$ is the inter-carrier interference (ICI) matrix, i.e. the "subcarrier coupling matrix", which is diagonal when the channel is static. Herein the signal and noise are assumed zero mean and mutually uncorrelated, thus,

$$E\{\mathbf{s}\} = E\{\mathbf{v}\} = 0$$

$$E\left\{\mathbf{s}\mathbf{s}^H\right\} = \mathbf{I}$$

$$E\left\{\mathbf{s}\mathbf{v}^H\right\} = \mathbf{0}$$

$$E\left\{\mathbf{v}\mathbf{v}^H\right\} = \sigma^2\mathbf{I}$$

where σ^2 denotes noise variance. Hence, it only needs a one-step lin-

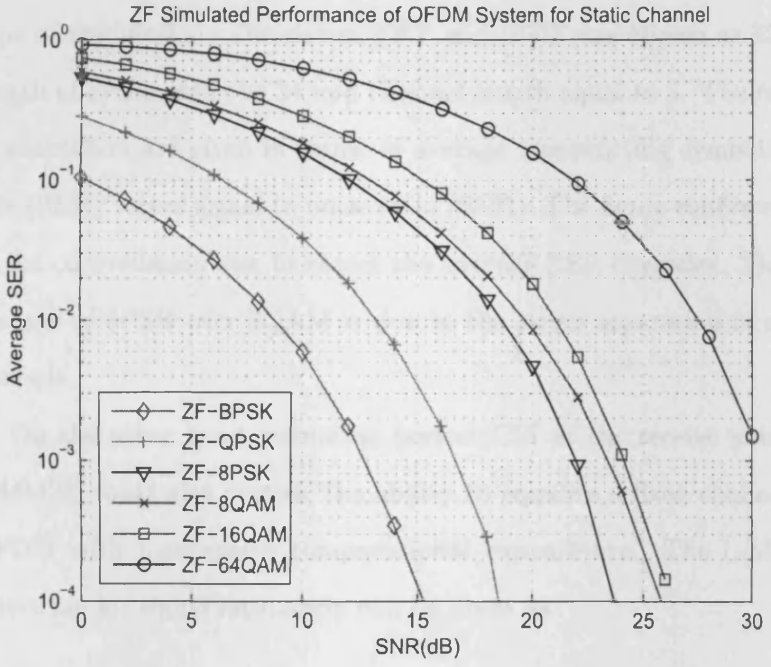

Figure 2.6. The average SER vs. SNR performance for an OFDM system: the simulation is implemented over a static channel and performs ZF channel equalization.

ear equalization algorithm for frequency domain operation with low computational complexity, such as zero-forcing (ZF) equalization and linear minimum mean square error (L-MMSE) equalization. The ZF equalization algorithm is given as

$$\hat{\mathbf{s}}_{ZF} = (\mathbf{H}_{df})^{+} \cdot \mathbf{Fr} \tag{2.6.11}$$

where $(\cdot)^{+}$ denotes the Moore-Penrose pseudo-inverse [104] and [105]. Figure 2.6 shows the performance of an OFDM system employing different types of QAM and PSK modulation, where the ZF algorithm is used for channel equalization. The OFDM system was simulated under static multipath channel conditions. The simulations were of length 200,000 symbols and were taken from $0dB < SNR < 30dB$ for each type of modulation. The size of FFT and IFFT was chosen as 32, the length of cyclic prefix as 24 and channel length equal to 3. The results of simulation are given in terms of average transmitting symbol error rate (SER) versus signal to noise ratio (SNR). The figure confirms that as the constellation size increases the average SER degrades. The advantage of 8PSK over 8QAM is due to the larger separation of all its symbols.

On the other hand, assuming perfect CSI at the receive antenna, L-MMSE could also provide the ability to equalize a fixed channel for OFDM with inexpensive computational expenditure. The L-MMSE algorithm for signal estimation can be given as

$$\hat{\mathbf{s}}_{MMSE} = \left(\mathbf{H}_{df}^{H}\mathbf{H}_{df} + \sigma^{2}\mathbf{I}\right)^{-1}\mathbf{H}_{df}^{H} \cdot \mathbf{Fr} \tag{2.6.12}$$

where $(\cdot)^{-1}$ denotes the matrix inversion operation. For static channel conditions, both the ZF and L-MMSE equalization algorithm only require $\mathcal{O}(N)$ (the order of N) operations. Hence, they represent the classical motivation for the use of OFDM for multipath static channels. Figure 2.7 the average SER performance of an OFDM system perform-

ing L-MMSE algorithm for channel equalization for various symbol constellations is shown. The simulation of Figure 2.7 has been initialized to be the same as the simulation of Figure 2.6. It clearly shows that for simple multipath static channels the L-MMSE and ZF can achieve essentially identically robust performance within the use of an OFDM system.

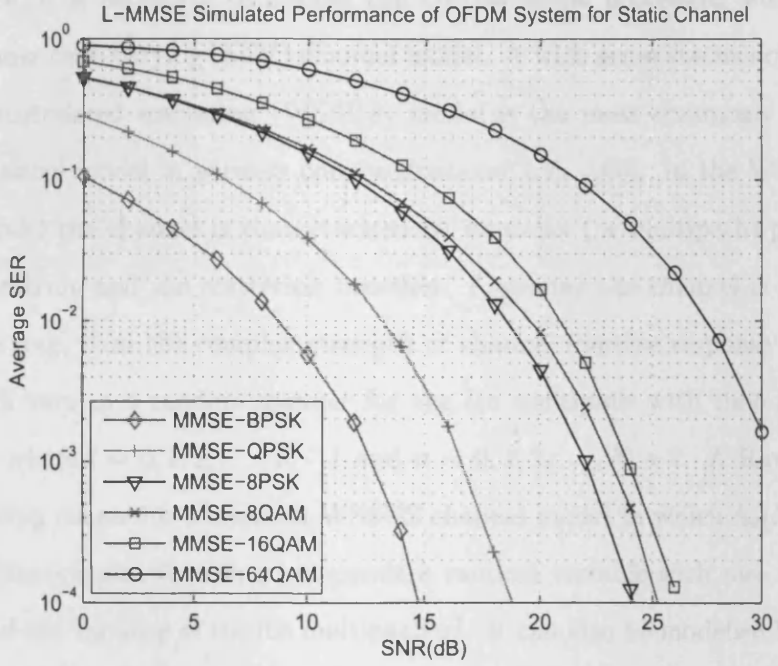

Figure 2.7. The average SER vs. SNR performance for an OFDM system: the simulation is implemented over static channels and performs L-MMSE channel equalization.

2.6.5 Signal Processing of OFDM Model in LTV Channel

Due to the mobility nature of wireless communications, the channel is not stationary at all times, hence the channel coefficients may vary with respect to time.

In OFDM-based communications, the strategy of data transmission is often based on transmitting information bits in terms of frames (OFDM symbols) and it is assumed that the channel is static during one frame at least [54], which is so-called quasi-static. However, sometimes the channel does not remain constant even in one OFDM symbol, e.g. results from high speed mobility which induces Doppler shift. Therefore, it is necessary to discuss the OFDM signal processing within a linear time-varying (LTV) channel model. A wide sense stationary and uncorrelated scattering (WSSUS) model is the most commonly used channel model in wireless communications [54], [106]. In the WSSUS model the channel is characterized by its delay (or multipath) power spectrum and the scattering function. Assuming the channel is time-varying, then the complex strength of channel impulse response $h_n(l)$ will vary in a random manner for the lth multipath with time index n, where $l = 0, 1, 2, \ldots, L-1$ and $n = 0, 1, 2, \ldots, N-1$. A Rayleigh fading channel is a classical WSSUS channel model in which $h_n(l)$ is a white complex Gaussian independent random variable with zero mean and the variance of the lth multipath σ_l^2. It can also be modelled based on the classic Jakes' model [76] which induces correlation in the time variation of the channel coefficient as a function of the mobile velocity. Similarly, as for the OFDM signal modelling in a static channel as in Eq.(2.6.8), the received OFDM baseband signal of sample time n can be described after removing the CP as

$$r_n = \sum_{l=0}^{L-1} h_n(l)\tilde{x}_{n-l} + v_n \tag{2.6.13}$$

where $h_n(l)$ is the lth tap of the complex channel, which varies in a

Gaussian random manner. The time domain transmitting vector without CP can be defined as $\mathbf{x} = [x_0, x_1, \ldots, x_{N-1}]^T$. Choi describes the estimation of the time-variant channel parameters in [107]. Herein, it is assumed that perfect knowledge of the channel is available. Thus, similarly to Eq.(2.6.9), the received signal can be written in terms of a vector yielding

$$\mathbf{r} = \mathbf{H}_c\mathbf{x} + \mathbf{v} = \mathbf{H}_c\mathbf{F}^H\mathbf{s} + \mathbf{v} \tag{2.6.14}$$

where $\mathbf{H}_c$ is a circulant channel matrix of size $N \times N$, note that the subscript n on $\mathbf{H}_c$ is dropped here for clarity, the channel coefficients of which will vary with respect to the time index in each transmitting frame period. $\mathbf{H}_c$ is described in Eq.(2.6.15) and in [108],

$$[\mathbf{H}_c]_{N\times N} = \begin{bmatrix}
h_0(0) & 0 & \cdots & h_0(L-1) & h_0(L-2) & \cdots & h_0(1) \\
h_1(1) & h_1(0) & 0 & \cdots & h_1(L-1) & \cdots & h_1(2) \\
\vdots & & \ddots & & \ddots & & \vdots \\
h_{L-2}(L-2) & \cdots & h_{L-2}(0) & 0 & \cdots & 0 & h_{L-2}(L-1) \\
h_{L-1}(L-1) & h_{L-1}(L-2) & \cdots & h_{L-1}(0) & 0 & \cdots & 0 \\
0 & h_L(L-1) & h_L(L-2) & \cdots & h_L(0) & 0 & \cdots \\
\vdots & & \ddots & & & \ddots & \vdots \\
0 & \cdots & h_{N-2}(L-1) & h_{N-2}(L-2) & \cdots & h_{N-2}(0) & 0 \\
0 & 0 & \cdots & h_{N-1}(L-1) & h_{N-1}(L-2) & \cdots & h_{N-1}(0)
\end{bmatrix} \tag{2.6.15}$$

and the OFDM symbol transmission can also be expressed in the same

signal processing model of the frequency domain, as for Eq.(2.6.10) as

$$\begin{aligned}\mathbf{R} &= \mathbf{F}\mathbf{H}_c\mathbf{F}^H\mathbf{s} + \mathbf{F}\mathbf{v} \\ &= \mathbf{H}_{df}\mathbf{s} + \mathbf{F}\mathbf{v}\end{aligned} \tag{2.6.16}$$

where $\mathbf{R} = \mathbf{F}\mathbf{r}$ denotes the frequency domain received signal. Note that the ICI matrix $\mathbf{H}_{df}$ is not diagonal due to the time-variant channel parameters, hence ICI is introduced into the transmission processing in the case of the LTV channel environment. In order to mitigate the effect of fading and interference from LTV channels, the equalization processing is still required at the receiving stage. However, both simple ZF and L-MMSE are not feasible for LTV channel equalization because only poor BER performance can be achieved by both schemes [107]. See also in Figure 2.8, the simulation shows the BPSK and QPSK average symbol error rate (SER) performance for an OFDM system, which performs L-MMSE equalization over LTI and LTV channels respectively, assuming normalized Doppler spread (DS) equal to 0.05. This figure confirms that with time-variation in the channel there is a clear SER floor for both BPSK and QPSK, hence average SER below 10^{-2} is impossible without further processing. The focus of this thesis is to overcome this limitation, in particular when multiuser interference is also present. The inversion of an Hermitian matrix obtained by $\mathbf{H}_{df(N\times N)}$ for both ZF and L-MMSE algorithm require $\mathcal{O}(N^2)$ operations [108], which is high computational expenditure when the size of frame N is large. Some non-linear equalization algorithms have been developed for better performance of signal estimation during the past three decades, such as maximum likelihood detection (ML) [109], [110], decision feed-

back equalization (DFE) [111], [112], and some robust optimal iterative equalization [108], which will be discussed in the following chapters, together with methods to reduce computational complexity.

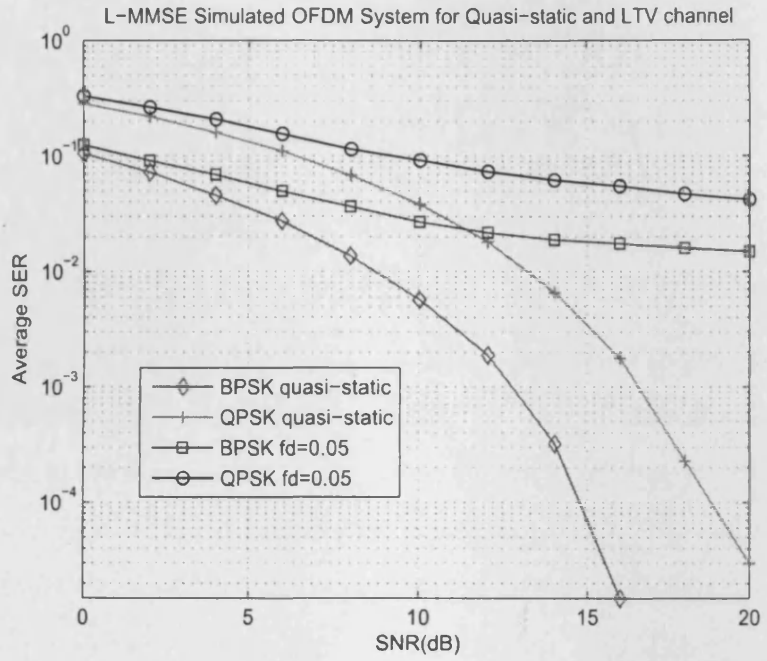

Figure 2.8. The average SER vs. SNR performance for an OFDM system: the simulation implements BPSK and QPSK over quasi-static and LTV channels and performs L-MMSE channel equalization, where the normalized Doppler spread is 0.05 for the LTV channels.

2.7 Chapter Summary

The background reviews for key physical layer technology of next generation wireless communications, including space time codes, MIMO and OFDM techniques, are provided in this chapter. The purpose was to give a broad discussion as details are available in the cited works. Those techniques will be utilized in a MIMO-OFDM system, as will be described in the following chapter. The introduction also provides a

basis for the further research on multiuser applications, which will be described in Chapter 4 and Chapter 5, and a low-complexity iterative algorithm in Chapter 6.

Chapter 3

MIMO-OFDM COMMUNICATIONS

The use of multiple antennas at both ends of a wireless link (MIMO technology) offers the potential ability to improve considerably the spectral efficiency and link reliability in future wireless communications systems [26]. In particular, combination of MIMO technology with OFDM is well known as one of the promising candidates for next-generation fixed and mobile wireless systems. This design is motivated by the growing demand for broadband wireless communications. This chapter provides an overview of the basic principles of combining space time block coding (STBC) with MIMO-OFDM techniques. The specifics of the design of STBC MIMO-OFDM systems are discussed in this chapter and the relative issue of performance analysis is provided in detail. The material describing the idea of iterative signal detection included in this chapter also provides a basis for the remaining chapters.

This chapter is organized as follows: The ISI problem caused by a frequency selective channel is discussed for the broadband MIMO communication environment in Section 3.1. Thus the MIMO-OFDM technique is introduced to deal with this problem in Section 3.2. The expressions for capacity of MIMO-OFDM systems are discussed in Section

3.3 in detail. In Section 3.4, a space-time block coded MIMO-OFDM system is described in terms of a signal processing model. A non-linear detection algorithm is introduced in Section 3.5. Based on both the principle of decision feedback (DF) and a sequential iterative detection algorithm, a novel STBC MIMO-OFDM receiver scheme using an iterative MMSE detection algorithm is designed for both a quasi-static frequency-selective wireless radio channels and a slowly fading time variant channel in Section 3.6, together with performance analysis. Section 3.7 provides the conclusions.

3.1 Broadband MIMO Communications

As explained in Chapter 2, most MIMO diversity techniques are designed for narrowband flat fading channels, such as space-time block coding, where each radio subchannel is assumed to be single path. However, when a MIMO system is considered for wideband transmission, the radio channel has a frequency-selective nature which is caused by the phenomenon of multipath propagation. The problems also exists for SISO systems wherein the main challenge is again to mitigate the inter-symbol interference (ISI) occurring due to the channel delay spread. As explained in Section 2.3.2, the lth MIMO-multipath fading channel for

an (n_t, m_r) multi-antenna transmission system can be modelled as

$$\mathbf{H}_n(l)=\begin{pmatrix} h_{11}(l) & h_{12}(l) & \cdots & h_{1n'_t}(l) & \cdots & h_{1n_t}(l) \\ h_{21}(l) & h_{22}(l) & \cdots & h_{2n'_t}(l) & \cdots & h_{2n_t}(l) \\ \vdots & \vdots & \ddots & \vdots & \ddots & \vdots \\ h_{m'_r1}(l) & h_{m'_r2}(l) & \cdots & h_{m'_rn'_t}(l) & \cdots & h_{m'_rn_t}(l) \\ \vdots & \vdots & \ddots & \vdots & \ddots & \vdots\cdots \\ h_{m_r1}(l) & h_{m_r2}(l) & \cdots & h_{m_rn'_t}(l) & \cdots & h_{m_rn_t}(l) \end{pmatrix}$$

where $h_{m'_rn'_t}(l)$ is the lth multipath complex channel fading coefficient over the transmission pipe from the n'_tth transmit antenna to the m'_rth receive antenna. Hence, the signal model can therefore be described for a MIMO-multipath channel as

$$\mathbf{r}(n)=\sum_{l=0}^{L-1}\mathbf{H}_n(l)\mathbf{b}(n-l)+\mathbf{v}(n)$$

Herein, the coefficients of the time domain channel matrices $\mathbf{H}_n(l)$ are multiplied with the transmitted signal vector $\mathbf{b}(n)$ to obtain the received signal $\mathbf{r}(n)$, where $l = 0, \ldots, L-1$ and $\mathbf{v}(n)$ is defined as the uncorrelated additive complex white circular zero mean Gaussian noise at sample time n. Hence, ISI appears when the transmission bandwidth exceeds the channel coherence bandwidth so that the channel delay spread exceeds the duration of the transmitted symbol. In this case, the delayed replicas of the transmitted signals interfere with the current transmitted symbols. Therefore direct signal detection is impossible in the rich multipath propagation environment, and equalization techniques are required at the receiver, such as in a GSM system which exploits a maximum likelihood sequence estimation (MLSE)-based equal-

izer. However, the complexity of the equalization can be too high to realize the communications in practical applications, e.g. when realized in the form of an MLSE equalizer it grows exponentially with the number of propagation paths between the transmitter and the receiver. Hence, it is even more difficult in (n_t, m_r) MIMO system for wideband communication, where there are $n_t \times m_r$ radio subchannels. A robust technique to overcome the ISI problem in MIMO systems is orthogonal frequency division multiplexing (OFDM) [31], [20]. In an OFDM-based system, the whole high data rate stream is divided into many low data rate substreams which occupy small bandwidth; and then, each data substream is transmitted using a different subcarrier. OFDM thereby transforms the frequency selective fading channel into many narrowband flat fading channels. Because each substream has low data rate, the symbol transmitting duration is therefore wide enough to mitigate the problem ISI degrading transmitting performance. Otherwise, if ISI remains an issue successive interference cancellation can be applied in the MIMO-OFDM system for further performance improvement.

It is strongly expected that MIMO-OFDM technique will be the basis for the link layer of emerging high-speed data wireless communications. Table 3.1 represents some wideband MIMO standards with the corresponding technology. It is clear to see that with the exception of 3GPP Release 7, all standards work with OFDM and orthogonal frequency division multiple access (OFDMA), where 3GPP Release 8 LTE (long term evolution) is the name given to a project within the third generation partnership project (3GPP) to improve the UMTS mobile phone standard to cope with future requirements. The advantages of OFDM can obviously be linked with MIMO. The table confirms

Table 3.1. MIMO standards and the corresponding technology

Standard	Technology
WLAN 802.11n	OFDM
WiMAX 802.16-2004	OFDM/OFDMA
WiMAX 802.16e	OFDMA
3GPP Release 7	WCDMA
3GPP Release 8 (LTE)	OFDMA
802.20	OFDM
802.22	OFDM

that the combination of MIMO with OFDM is generally the technology of choice to reinforce WLANs and current mobile 3G networks. In 2003, the task group of IEEE 802.11n was established to improve the throughput in 802.11 WLANs by applying a combination of MIMO with OFDM techniques. Some proposals were submitted by different telecom consortia, but none of them was accepted. In May 2006, the last proposed draft was rejected. On the other hand, strong eagerness still exists for the 802.11n standard in the telecommunications industry. Some companies, e.g. Dell and Acer, have announce that they plan to exploit the draft of the 802.11n standard in their products [113], [114].

3.2 Introduction to MIMO-OFDM Systems

Figure 1.2 has illustrated a block diagram of a basic baseband MIMO-OFDM system. Consider this MIMO-OFDM system with n_t transmit and m_r receive antennas. In this system, OFDM techniques add signal processing in the frequency dimension into the MIMO framework which includes the spatial and temporal dimension algorithms. In gen-

eral, the incoming bit stream is first encoded by a channel encoder and interleaved. After PSK/PAM mapping, the incoming bit stream is converted into a mapped symbol stream and then encoded by MIMO coding techniques (e.g. STBC) to engender coded spatial and frequency domain transmitting symbols. A set of subcarriers can be chosen for signal transmission. Despite the fact these carriers effectively overlap in the frequency domain, all the signals can be distinguished at the receiver because of the orthogonality of the carriers. Thus, the whole system is spectrally efficient provided the problems of synchronization (frequency offset) and doubly selective channels are not severe. To provide the transmission with the appropriate frequency carriers, digital signal processing with an IFFT operation is applied at the transmitter for each branch of the output of the MIMO encoder, and then the cyclic prefix (CP) is added on to the OFDM symbols to mitigate ISI before transmission. A quasi-static channel environment for this system where each OFDM block experiences time-invariant but different fading is assumed. The number of multipaths of every fading channel from each transmit antenna to each receive antenna is assumed the same, which is denoted by L. In such a MIMO system the maximum diversity gain is theoretically $n_t \times m_r \times L$, to exploit this diversity additional coding is required at the transmitter [115]. Such coding is not considered in this thesis. Herein, perfect synchronization is assumed for all transmitters and receivers and the high peak-to-average power ratio of OFDM is ameliorated by perfect linear power amplifiers. Hence, at the receive end, the CP is removed and the complementary FFT is performed for each receive branch. Then, at this point, the MIMO decoder/detector must be applied to recover the frequency domain data stream, and then

demapping/deinterleaving and decoding are implemented to obtain binary output data. It is typically assumed that perfect knowledge of channel state information (CSI) is available at the receiver. In principle, MIMO-OFDM can be considered as a parallel set of SISO-OFDM systems. Thus, the received signal across all the receive antennas at discrete frequency tone k after removing the CP and taking the FFT can be written as

$$\mathbf{r}(k) = \mathbf{H}_f(k)\mathbf{x}(k) + \mathbf{v}_f(k) \tag{3.2.1}$$

where $\mathbf{r}(k) = [r_1(k), r_2(k), \ldots, r_{m_r}(k)]^T$, and $k = 0, 1, \ldots, N-1$. $\mathbf{x}(k) = [x_1(k), x_2(k), \ldots, x_{n_t}(k)]^T$ is the frequency domain transmitting data symbol at the kth subcarrier across the n_t'th transmit antenna, $n_t' = 1, 2, \ldots, n_t$; and $\mathbf{v}_f(k) = [\mathbf{v}_{f1}(k), \mathbf{v}_{f2}(k), \ldots, \mathbf{v}_{fm_r'}(k), \ldots, \mathbf{v}_{fm_r}(k)]$ denotes the frequency domain representation for the additive complex white Gaussian noise vector $\mathbf{v}$ at the kth subcarrier. $\mathbf{H}_f(k)$ is the frequency domain channel matrix of the kth tone written as

$$\mathbf{H}_f(k) = \begin{pmatrix} H_{11}(k) & H_{12}(k) & \cdots & H_{1n_t'}(k) & \cdots & H_{1n_t}(k) \\ H_{21}(k) & H_{22}(k) & \cdots & H_{2n_t'}(k) & \cdots & H_{2n_t}(k) \\ \vdots & \vdots & \ddots & \vdots & \ddots & \vdots \\ H_{m_r'1}(k) & H_{m_r'2}(k) & \cdots & H_{m_r'n_t'}(k) & \cdots & H_{m_r'n_t}(k) \\ \vdots & \vdots & \ddots & \vdots & \ddots & \vdots\cdots \\ H_{m_r1}(k) & H_{m_r2}(k) & \cdots & H_{m_rn_t'}(k) & \cdots & H_{m_rn_t}(k) \end{pmatrix} \tag{3.2.2}$$

where $H_{m_r'n_t'}(k) = \sum_{l=0}^{L-1} h_{m_r'n_t'}(l) e^{-\frac{2\pi j}{N} lk}$ and $h_{m_r'n_t'}(l)$ is the lth tap of the fading channel from the n_t'th transmit antenna to the m_r'th receive antenna. From Eq.(3.2.1), assuming the CP is greater than the channel length L, there is no ISI during transmission.

3.3 Capacity of MIMO-OFDM Systems

From the discussion introduced in the previous section, it is known that in OFDM-based spatial multiplexing systems statistically independent data streams are transmitted from different antennas and different tones and the total available power is allocated uniformly across all space-frequency subchannels. Hence, in OFDM-based systems, a (n_t, m_r) MIMO frequency-selective channel can be divided into a number of narrowband MIMO subchannels for which the frequency response of the kth subchannel is represented as $\mathbf{H}_f(k)$ in Eq.(3.2.2). Assuming the CSI is not known at the transmitter, it has been shown in [22] and [30], that the open-loop capacity for MIMO OFDM over a frequency-selective wideband channel which is defined as bps/Hz can be obtained by averaging over the capacity of these narrowband MIMO subchannels. From the discussion in Chapter 2, the capacity of a narrowband MIMO channel of the kth tone is defined as

$$C = \log_2 \det \left[\mathbf{I}_{m_r} + \left(\frac{SNR}{n_t} \right) \mathbf{H}_f(k) \mathbf{H}_f^H(k) \right] \tag{3.3.1}$$

Herein the frequency band is divided in a discrete number of N frequency-flat subchannels, where N denotes the number of subcarriers carried by an OFDM symbol. Then the open-loop capacity of the (n_t, m_r) MIMO OFDM channel can be given by

$$C = \frac{1}{N} \sum_{k=0}^{N-1} \log_2 \det \left[\mathbf{I}_{m_r} + \left(\frac{SNR}{n_t} \right) \mathbf{H}_f(k) \mathbf{H}_f^H(k) \right] \tag{3.3.2}$$

From Eq.(3.3.2), the open-loop capacity of the (n_t, m_r) MIMO OFDM channel is presented as an average channel capacity determined by real-

izations of the subchannels for all subcarriers. Figure 3.1 illustrates the average channel capacity for different MIMO-OFDM configurations. In this figure, the average capacity is determined by independent realizations of MIMO subchannels $\mathbf{H}_f(k)$ for 1024 subcarriers, where the elements of $\mathbf{H}_f(k)$ are assumed to be i.i.d. circularly-symmetric complex Gaussian distributed. The capacity increasing with $min(n_t, m_r)$ can be observed in this figure. Therefore, in open-loop systems, it is observed that the theoretical capacity of the $(2, 4)$ MIMO frequency-selective channels is identical to the capacity of the $(4, 2)$ channels.

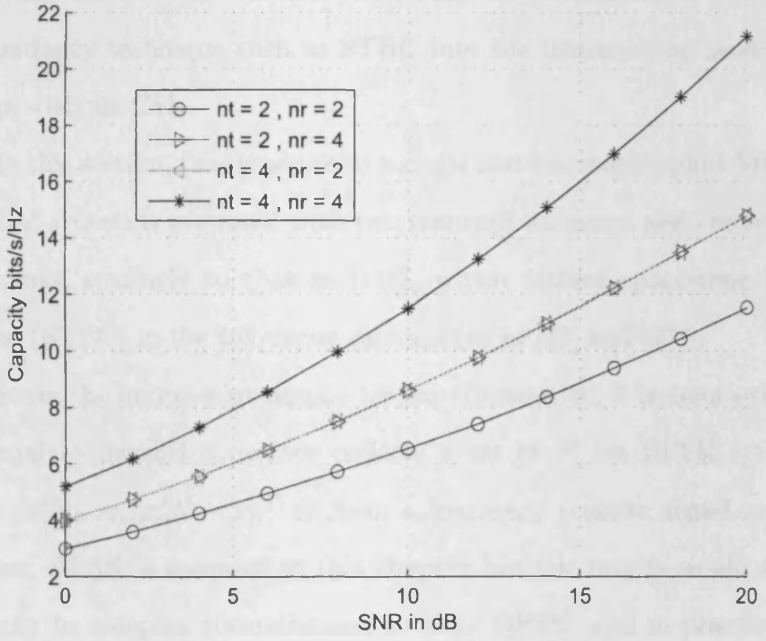

Figure 3.1. Average channel capacity for different MIMO-OFDM configurations.

3.4 Space-Time Block Coded MIMO-OFDM Transceiver Design

To increase the diversity gain and/or to enhance the system capacity, in practice, OFDM may be used in combination with antenna arrays at the transmitter and receiver to form a MIMO-OFDM system, which improves the performance of communication in terms of taking advantage of the spatial diversity assuming a sufficiently rich scattering environment. In most mobile applications, CSI may not be available at the transmitter, hence it is a challenge to extract the full spatial diversity at the transmitter without the knowledge of CSI. However, transmit diversity can still be realized practically by introducing a controlled redundancy technique such as STBC into the transmitting processing stage without CSI.

In this section, the structure of a single user baseband uplink MIMO-OFDM system is proposed with two transmit antennas and two receive antennas, similarly to that in [116], which utilizes space-time block codes (STBC) in the frequency domain (as in [33] and [77]).

From the information source for the transmitter, it is assumed that a serial to parallel convertor collects a set of N bit BPSK symbols $\mathbf{x} = [x(0), \cdots, x(N-1)]^T$ to form a frequency domain signal symbol vector, BPSK is assumed in this chapter but the results would apply equally to complex constellations such as QPSK, and in practice, an explicit OFDM modulating operation will be performed for each sub-channel. To avoid inter-symbol interference (ISI), a sufficiently long cyclic prefix must be chosen, i.e. the guard interval P should satisfy $P > L$, where L is the length of impulse response of each transmit-receive antenna sub-channel, which is the same for each sub-channel. From the previous section, the N time domain received symbols cor-

responding to the receive antenna can be obtained by an OFDM algorithm in terms of vector form as

$$\mathbf{r}_n = \mathbf{H}_c\mathbf{F}^H\mathbf{x}+\mathbf{v} \tag{3.4.1}$$

At each receive antenna, the samples corresponding to the cyclic prefix are first removed and then taking the FFT operation of received signal from Eq.(3.4.1) yields

$$\mathbf{r} = \mathbf{F}\mathbf{r}_n = \mathbf{F}\mathbf{H}_c\mathbf{F}^H\mathbf{x}+\mathbf{F}\mathbf{v} = \mathbf{H}\mathbf{x} + \mathbf{v}_f \tag{3.4.2}$$

where $\mathbf{H}_c$ is the time-domain circular convolutional channel matrix of size $N \times N$, which has been described in Chapter 2, (see also in [108]). Moreover, $\mathbf{F}$ denotes the $N \times N$ DFT matrix and therefore $\mathbf{F}^H$ denotes the IDFT matrix. $\mathbf{H}$ is defined as the *subcarrier coupling matrix* (diagonal for a static channel), where $\mathbf{H}$ is the simplified from $\mathbf{H}_{df}$ in Chapter 2 for clarity, and $\mathbf{v}_f$ is the frequency response of the additive complex Gaussian noise vector.

In the proposed MIMO-OFDM system, the STBC scheme which is similar to the scheme in [77] is adapted for the transmitting terminal. The two consecutive block signal vectors from the data source can be represented as $\mathbf{x}_1 = [x_1(0), \cdots, x_1(N-1)]^T$ and $\mathbf{x}_2 = [x_2(0), \cdots, x_2(N-1)]^T$. Herein, it is assumed that the time domain channel responses are constant during two consecutive signal block intervals, i.e. quasi-static. Here, $[\mathbf{H}_{qj}]$ is defined as *subcarrier coupling matrix* of size $N \times N$, experienced by the signal transmitted from the qth transmit antenna to the jth receive antenna, i.e. the diagonal matrix formed by the channel impulse response in the frequency domain, (as in [117]). The estima-

tion of the time invariant channels is discussed in [107], and this issue is not addressed in this thesis. The coded signal transmitted from the transmit terminal during two block intervals in the frequency domain can be represented in matrix form as follows,

$$\begin{bmatrix} \mathbf{F}^H\mathbf{x}_1 & \mathbf{F}^H\mathbf{x}_2 \\ -\mathbf{F}^H\mathbf{x}_2^* & \mathbf{F}^H\mathbf{x}_1^* \end{bmatrix} \tag{3.4.3}$$

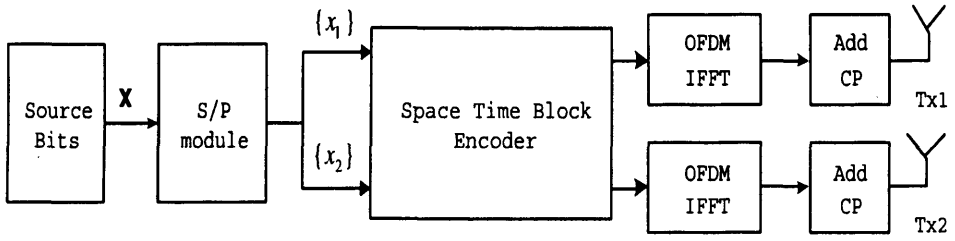

Figure 3.2. STBC MIMO-OFDM baseband transmitter diagram consist of two transmit antennas.

The proposed STBC MIMO-OFDM transmitter is equipped with two transmit antennas for exploiting the above STBC scheme for wireless data transmission, which is shown in Figure 3.2, (as in [116] and [117]). In this transmitter, the source mapped information symbol stream is converted into two consecutive signal blocks of size N, then both signal blocks are encoded by a STBC encoder and each branch of the encoder output needs to be modulated by an OFDM module including IFFT and CP addition, and then these signals are sent from two transmit antennas in two consecutive OFDM time intervals. Two receive antennas are employed at the receiver for collecting the receive signals. If the output of the OFDM demodulator is considered at the first receive antenna after cyclic prefix removal, the frequency domain receive signal vectors during two sequential OFDM time-slots a and

b for the first receive antenna could be obtained as in Eq.(3.4.4) and Eq.(3.4.5), respectively.

$$\mathbf{r}_{1a} = \mathbf{H}_{11}\mathbf{x}_1 + \mathbf{H}_{21}\mathbf{x}_2 + \mathbf{v}_{f1a} \tag{3.4.4}$$

$$\mathbf{r}_{1b}^* = \mathbf{H}_{21}^*\mathbf{x}_1 - \mathbf{H}_{11}^*\mathbf{x}_2 + \mathbf{v}_{f1b}^* \tag{3.4.5}$$

For simplicity of notations, define signal vector $\mathbf{x} = \begin{bmatrix} \mathbf{x}_1 \\ \mathbf{x}_2 \end{bmatrix}$, received vector $\mathbf{r}_1 = \begin{bmatrix} \mathbf{r}_{1a} \\ \mathbf{r}_{1b}^* \end{bmatrix}$, and $\mathbf{v}_{f1} = \begin{bmatrix} \mathbf{v}_{f1a} \\ \mathbf{v}_{f1b}^* \end{bmatrix}$ which is the frequency response of the noise vector for the signal received by the first receive antenna. Therefore, write (3.4.4) and (3.4.5) in a matrix form as

$$\mathbf{r}_1 = \tilde{\mathbf{H}}_1\mathbf{x} + \mathbf{v}_{f1} \tag{3.4.6}$$

The equivalent channel matrix of the transmitting data pipe from transmitter to the first receive antennas could be represented as

$$\tilde{\mathbf{H}}_1 = \begin{bmatrix} \mathbf{H}_{11} & \mathbf{H}_{21} \\ \mathbf{H}_{21}^* & -\mathbf{H}_{11}^* \end{bmatrix}$$

In a similar method, the frequency domain receive signal vectors could also be arranged during the two sequential OFDM time-slots a and b for the second receive antenna as in Eq.(3.4.8) and Eq.(3.4.9), respectively.

$$\mathbf{r}_1 = \tilde{\mathbf{H}}_1\mathbf{x} + \mathbf{v}_{f1} \tag{3.4.7}$$

$$\mathbf{r}_{2a} = \mathbf{H}_{12}\mathbf{x}_1 + \mathbf{H}_{22}\mathbf{x}_2 + \mathbf{v}_{f2a} \tag{3.4.8}$$

$$\mathbf{r}_{2b}^{*} = \mathbf{H}_{22}^{*}\mathbf{x}_1 - \mathbf{H}_{12}^{*}\mathbf{x}_2 + \mathbf{v}_{f2b}^{*} \tag{3.4.9}$$

Eq.(3.4.8) and Eq.(3.4.9) can simply be written in a matrix form as

$$\mathbf{r}_2 = \tilde{\mathbf{H}}_2\mathbf{x} + \mathbf{v}_{f2} \tag{3.4.10}$$

where the received vector for the second receive antenna $\mathbf{r}_2 = \begin{bmatrix} \mathbf{r}_{2a} \\ \mathbf{r}_{2b}^{*} \end{bmatrix}$, and $\mathbf{v}_{f2} = \begin{bmatrix} \mathbf{v}_{f2a} \\ \mathbf{v}_{f2b}^{*} \end{bmatrix}$, and the equivalent channel matrix $\tilde{\mathbf{H}}_2$ to the second receive antennas could be represented as

$$\tilde{\mathbf{H}}_2 = \begin{bmatrix} \mathbf{H}_{12} & \mathbf{H}_{22} \\ \mathbf{H}_{22}^{*} & -\mathbf{H}_{12}^{*} \end{bmatrix}$$

Finally, the overall receive vector can be arranged by combining (3.4.7) and (3.4.10) as

$$\mathbf{r} = \begin{bmatrix} \mathbf{r}_1 \\ \mathbf{r}_2 \end{bmatrix} = \begin{bmatrix} \tilde{\mathbf{H}}_1 \\ \tilde{\mathbf{H}}_2 \end{bmatrix} .\mathbf{x} + \begin{bmatrix} \mathbf{v}_{f1} \\ \mathbf{v}_{f2} \end{bmatrix} = \tilde{\mathbf{H}}.\mathbf{x} + \mathbf{v}_f \tag{3.4.11}$$

Let $N_b = 2N$, so that $\tilde{\mathbf{H}}$ is the overall equivalent channel matrix between transmitter and receiver of size $N_b \times N_b$ and $\mathbf{v}_f$ denotes the whole channel equivalent noise vector of size $N_b \times 1$ with variance σ_n^2.

3.5 Non-Linear Detection Algorithm

Nonlinear detection techniques are usually used in applications where the channel distortion is too stringent for a linear equalizer to handle. That is because a linear equalizer can not deal well with channels

which have deep spectral nulls in the passband. In an attempt to compensate for distortion, the linear equalizer algorithm has to place too much gain near the spectral null, therefore enhancing the noise present in those frequencies. There are three effective nonlinear methods developed for symbol detection: (1) maximum likelihood sequence estimation (MLSE); (2) decision feedback detection algorithm (DF); (3) maximum likelihood symbol detection (ML).

3.5.1 Maximum Likelihood Sequence Detection

The maximum likelihood sequence estimator (MLSE) was first proposed by Forney [118] in 1978, it is an optimal detection algorithm with the concept that it minimizes the probability of sequence error. In the MLSE algorithm, the Viterbi algorithm is exploited to yield computationally efficient estimator structure. The algorithm determines the most likely transmitted sequence from the received sequence corrupted by noise and ISI [54], [110]. An MLSE usually has a large computational requirement, especially when the delay spread of the channel is large. The MLSE equalizer tests all possible data sequences, rather than decoding each received symbol by itself, and chooses the data sequence that is the most probable in all combinations. Therefore, for a memoryless channel, if $Pr(\mathbf{r}, \mathbf{c})$ denotes the conditional probability of receiving $\mathbf{r}$, when code vector $\mathbf{c}$ corresponding to sequence $\{x(n)\}$ of N bits is transmitted, then, the likelihood function can be written as

$$Pr(\mathbf{r}, \mathbf{c}) = \frac{1}{(\pi\sigma_n^2)^N} \prod_{n=1}^{N} e^{-\frac{|r(n)-x(n)|^2}{\sigma_n^2}} \tag{3.5.1}$$

The MLSE is used in the receiver of GSM to mitigate the channel effects for optimal performance [109]. For memory channels, the

MLSE chooses the estimate vector $\hat{\mathbf{c}}$ for which the likelihood function is maximum through the Viterbi algorithm. The likelihood function to maximize can be written as

$$Pr(\mathbf{r}|\mathbf{h},\hat{\mathbf{c}}) = \frac{1}{(\pi\sigma_n^2)^N}\prod_{n=1}^{N} e^{-\frac{|r(n)-\mathbf{x}_n\mathbf{h}|^2}{\sigma_n^2}} \tag{3.5.2}$$

where $\mathbf{x}_n = [x(n), x(n-1), \ldots, x(n-L+1)]$ and $\mathbf{h} = [h(0), h(1), \ldots, h(L-1)]^T$ is the channel impulse response (CIR) of the support L. The MLSE solution is to maximize the likelihood function jointly over the CIR sequence $\{h(n)\}$ and code vector $\mathbf{r}$ corresponding to the transmitted sequence $\{x(n)\}$. Because the MLSE detector has to test all possible data sequences for the most optimal data sequence, hence, its search complexity, measured in number of states, will probably be relatively high, which increases exponentially with the channel support and large constellation order of mapped symbol, e.g. 16PSK or 64QAM. Let M be the order of modulation and L be the support of the channel then the number of states of detector will be M^L.

3.5.2 Decision Feedback Detection

The basic idea of decision feedback detection (DFD) is that once an information symbol has been detected and the decision has been made, the ISI which influences future symbols can be estimated and subtracted out based on previous detection and then detecting the next symbols [54], [1]. The DFD can be realized in a transveral form as shown in Figure 3.3. It consists of a feedforward filter (FFF) and a feedback filter (FBF). Therein, the FFF is adjusted to detect the symbol $x(n)$ from the received symbol $y(n)$ and obtain the equalized information $d(n)$ resulting in detection decision $\hat{x}(n)$. The input of the FBF $\hat{x}_D(n)$

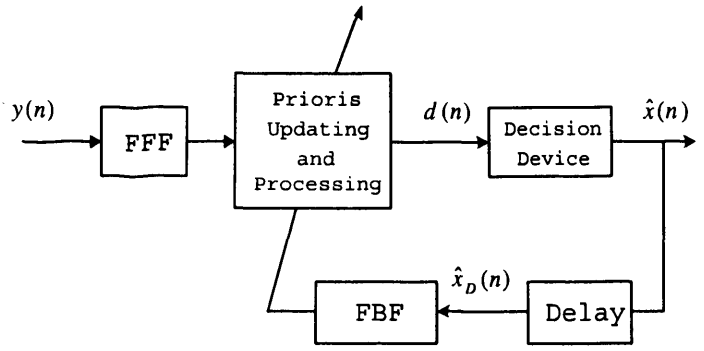

Figure 3.3. Decision Feedback Detector (DFD).

is obtained from delay of the detection decision $\hat{x}(n)$, and the FBF output can be updated by the previous detection information into the DF processor to cancel the ISI on the current symbol $x(n+1)$ from past detected symbols $x(n), x(n-1), \ldots$ and then form $d(n+1)$ and estimation $\hat{x}(n+1)$; i.e. if the previous or past symbols are known, then in the current decision the ISI contribution of these symbols can be removed by subtracting past symbols with appropriate weighting from the equalizer output. The combined output $d(n)$ of a forward and feedback filter can be written as

$$d(n) = \mathbf{G}^H \mathbf{y}(n) - \mathbf{E}^H \hat{\mathbf{x}}_D(n) \tag{3.5.3}$$

which is quantized into a hard decision by a nonlinear decision device

$$\hat{x}(n) = sign(d(n)) \tag{3.5.4}$$

where $\mathbf{G}$ is the FFF weight tap vector and $\mathbf{E}$ is the FBF tap weight vector. As mentioned in Chapter 2, two criteria could be considered for filter optimization with the DF method: the minimum mean-square error (MMSE) criterion and the zero-forcing (ZF) criterion. Herein, since

ZF performs poorly with the presence of noise, under the MMSE criterion, $\mathbf{G}$ and $\mathbf{E}$ can be found so as to minimize the MSE cost function given by

$$\begin{aligned} J(\mathbf{G},\mathbf{E}) &= E\left\{|d(n)-x_D(n+1)|^2\right\} \\ &= E\left\{\left|\mathbf{G}^H\mathbf{y}(n) - \mathbf{E}^H\hat{\mathbf{x}}_D(n)-x_D(n+1)\right|^2\right\} \end{aligned} \quad (3.5.5)$$

where $x_D(n)$ is the delay unit of $x(n)$. Assuming the circulant channel matrix (CCM) $\mathbf{H}$ as

$$\mathbf{H} = \mathbf{H}_u + \mathbf{H}_c \quad (3.5.6)$$

where $\mathbf{H}_u = [\mathbf{h}_1\ \mathbf{h}_2\ \cdots\ \mathbf{h}_k \mid 0\ \cdots\ 0\ ]$ and $\mathbf{H}_c = [0\ \cdots\ 0 \mid \mathbf{h}_{k+1}\ \mathbf{h}_{k+2}\ \cdots\ \mathbf{h}_N\ ]$ are referred to as uncancelled and cancelled symbols respectively and $\mathbf{h}_k$ denotes the kth column of the CCM $\mathbf{H}$. Assuming the feedback decisions are correct, hence taking the gradients of the cost function $J(\mathbf{G},\mathbf{E})$ and equating them to zero, the expression for forward and feedback tap weights can be written as [71]

$$\mathbf{G} = (\mathbf{H}_u\mathbf{H}_u^H + \sigma_n^2\mathbf{I})^{-1}\mathbf{h}_k \quad (3.5.7)$$

$$\mathbf{E} = \mathbf{H}_c^H\mathbf{G} \quad (3.5.8)$$

Although the DFE nearly always outperforms linear equalization of equivalent complexity [111] and mitigates the effects of noise and ISI for better BER performance [71], however, at low SNR condition, the previous detected symbols may have higher probability of errors. Assuming a particular error decision is fed back, the DFE output in-

duces more errors during the next few symbols due to delayed incorrect decision for feedback, which is called error propagation..

3.6 Iterative MMSE Receiver Design for STBC MIMO-OFDM Systems

In this section, a novel iterative MIMO-OFDM detection scheme is proposed, which is based on minimum mean square error (MMSE). The symbols are non-linearly detected in a number of iterations by updating extrinsic information to develop log-likelihood ratios (LLRs). Otherwise, an iterative MMSE updated with decision feedback (MMSE-DF) receiver is also proposed for comparison. The proposed scheme exploits two receive antennas, and suppresses the interference and detect signals. All channel knowledge is assumed known perfectly at the receiver.

3.6.1 Iterative MMSE Receiver Algorithm

Consider an iterative MMSE receiver for joint STBC MIMO-OFDM detection as shown in Figure 3.4. Through utilization of the overall equivalent time domain channel matrix $\tilde{\mathbf{H}}$ in Eq.(3.4.11), estimation of the transmitted symbol $x(n)$ can be obtained. The direct estimation based on the linear MMSE, however, could not offer good enough performance unless the channel is essentially flat. In this work, the transmitted signal can be estimated in an iterative detection process. An MMSE equalizer is structured to first obtain the estimated $x(n)$s, and then those estimated values could be used to maximize the posteriori probability in iterative processing. As shown in Figure 3.4, the whole receive and detection processing can be split into two stages:

(i) In the first stage the CP is removed and then the FFT operation is performed on the received time domain samples on each receive antenna, whereby the frequency domain receive vector $\mathbf{r}$ can be obtained. From the received vector $\mathbf{r}$, an updateable MMSE equalizer is designed for estimating frequency domain transmit symbols $\hat{x}(n)$s.

(ii) In the second stage, the corresponding a posteriori values of the $\hat{x}(n)$s are determined. The a posteriori values are passed to update the MMSE detector of the first stage for better estimation. These two stages iteratively exchange their information learned from each other until the specified number of iterations has passed.

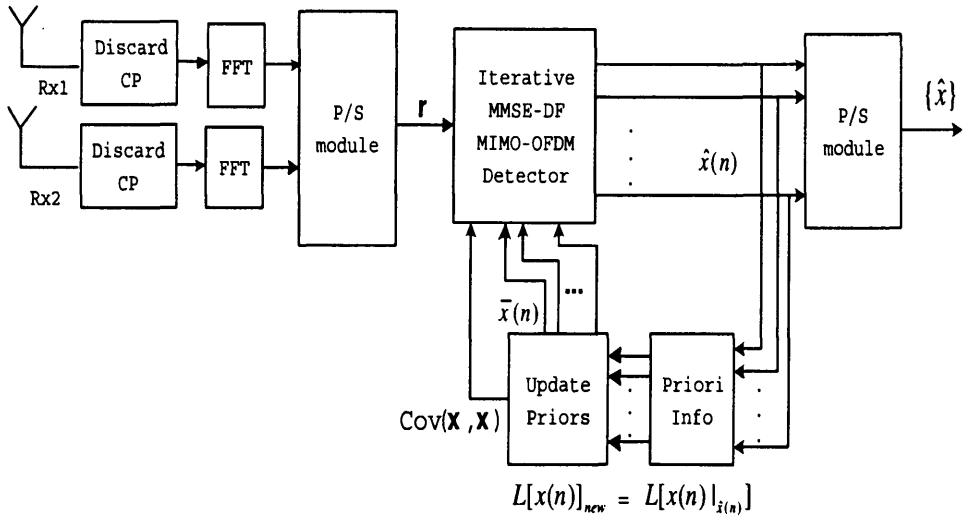

Figure 3.4. Iterative STBC MIMO-OFDM baseband receiver diagram consisting of two receive antennas.

The first step is to estimate the frequency domain transmitted samples through the MMSE equalizer linearly. In order to design this MMSE equalizer, the noise of zero mean in Eq.(3.4.11) is assumed uncorrelated and circularly distributed, therefore $E\{\mathbf{v}_f\} = \mathbf{0}$, $E\{\mathbf{v}_f\mathbf{v}_f^H\} = \sigma_n^2\mathbf{I}_n$ and $E\{x(n)\mathbf{v}_f\} = \mathbf{0}$. The MMSE equalizer $\mathbf{w}_n$ could

be derived through minimizing the following cost function.

$$J(\mathbf{w}_n) = E\{|x(n) - \mathbf{w}_n^H \mathbf{r}|^2\} \tag{3.6.1}$$

which obtains the MMSE equalizer coefficient vector

$$\mathbf{w}_n = (\tilde{\mathbf{H}} Cov(\mathbf{x}, \mathbf{x}) \tilde{\mathbf{H}}^H + \sigma_n^2 \mathbf{I}_n)^{-1} \tilde{\mathbf{H}} Cov(\mathbf{x}, x(n)) \tag{3.6.2}$$

where $Cov(\mathbf{x}, \mathbf{x})$ denotes the covariance matrix of $\mathbf{x}$ in terms of a diagonal matrix as $diag([c_x(0), c_x(1), \ldots, c_x(N_b - 1)])$, here $c_x(n)$ denotes $Cov[x(n), x(n)]$ as the covariance of $x(n)$. $Cov(\mathbf{x}, x(n))$ is equivalent to the nth column of the matrix $Cov(\mathbf{x}, \mathbf{x})$. Hence, define

$$Cov(\mathbf{x}, x(n)) = \mathbf{i}_n Cov[x(n), x(n)]$$

where $\mathbf{i}_n$ is the nth column of an identity matrix. Therefore, Eq.(3.6.2) can be written as

$$\mathbf{w}_n = (\tilde{\mathbf{H}} Cov(\mathbf{x}, \mathbf{x}) \tilde{\mathbf{H}}^H + \sigma_n^2 \mathbf{I}_n)^{-1} \tilde{\mathbf{h}}_n Cov[x(n), x(n)] \tag{3.6.3}$$

where $\tilde{\mathbf{h}}_n$ is the nth column of matrix $\tilde{\mathbf{H}}$, and then the estimated $\hat{x}(n)$ values could be obtained as

$$\hat{x}(n) = \bar{x}(n) + \mathbf{w}_n^H (\mathbf{r} - \tilde{\mathbf{H}} \bar{\mathbf{x}}) \tag{3.6.4}$$

Here, the mean value of sample $x(n)$ is $\bar{x}(n) = E\{x(n)\}$ and the mean value of sample vector $\mathbf{x}$ is $\bar{\mathbf{x}} = E\{\mathbf{x}\}$. From Eq.(3.6.3) and Eq.(3.6.4), estimates of the values of $\{\hat{x}(n)\}$ can be obtained at the first stage. At the start, it is initialized as $\forall \bar{x}(n) = 0$ and $\forall Cov[x(n), x(n)] = 1$.

BPSK constellation is utilized in this work although extension to complex constellations is straightforward. The estimated values obtained in the first stage have high probability of error. To estimate any particular transmitted symbol, the estimator cancels the interference from the other (or *extrinsic information*) symbols, i.e. only the priors from $\{x(k), k \neq n\}$ are used when estimating $x(n)$. This can be implemented with $\bar{x}(n) = 0$ in $\mathbf{x}$ of Eq.(3.6.4) and $Cov[x(n), x(n)] = 1$ in $Cov(\mathbf{x}, \mathbf{x})$ of Eq.(3.6.3), respectively, to find $\hat{x}(n)$. In estimation, on the basis of interference cancellation, the performance of the estimator depends on the accuracy of the mean values of the extrinsic symbols. Therefore, the new mean values after estimation $\bar{x}(n)_{new}$, i.e. posteriori means, can be found by finding the a posteriori probabilities of the transmitted symbols, and the $Cov[x(n), x(n)]_{new}$ could also be found. These posteriori values can be updated into $\bar{\mathbf{x}}$ and $Cov(\mathbf{x}, \mathbf{x})$ for the next estimation, which is shown in Eq.(3.6.3) and Eq.(3.6.4).

A sequential estimation strategy is exploited for the proposed detection algorithm, which includes two different schemes: sequential iterative estimation (SIE) and sequential decision feedback (SDF).

3.6.2 Sequential Iterative Estimation (SIE)

With utilization of BPSK signals, the updating processing of the iterative algorithm could work through finding the log-likelihood ratios (LLR)s from the estimated values of $\{\hat{x}(n)\}$. The prior and posterior LLRs of $x(n)$ as [119]

$$L[x(n)] = \ln \frac{\Pr\{x(n) = 1\}}{\Pr\{x(n) = -1\}} \tag{3.6.5}$$

and

$$L[x(n)|_{\hat{x}(n)}] = \ln \frac{\Pr\{x(n) = 1|_{\hat{x}(n)}\}}{\Pr\{x(n) = -1|_{\hat{x}(n)}\}} \tag{3.6.6}$$

Hence, the difference between the posterior and prior LLRs (which is the extrinsic information) of $x(n)$ is

$$\begin{aligned} \Delta L[x(n)] &= L[x(n)|_{\hat{x}(n)}] - L[x(n)] = L[\hat{x}(n)|_{x(n)}] \\ &= \ln \frac{\Pr\{\hat{x}(n)|_{x(n)=1}\}}{\Pr\{\hat{x}(n)|_{x(n)=-1}\}} \end{aligned} \tag{3.6.7}$$

As the signal $x(n) = b \in \{+1, -1\}$, in order to find the extrinsic LLR, $L[\hat{x}(n)|_{x(n)}]$, the conditional probability density function (PDF) of $x(n)$ is Gaussian distributed and can be expressed as

$$\begin{aligned} &\Pr\{\hat{x}(n)|_{x(n)=b}\} \sim \mathcal{N}\left(m_n(b), \sigma_x^2|_{x(n)=b}\right) \\ &\approx \frac{1}{\sqrt{2\pi}\sigma_x|_{x(n)=b}} \exp\left(-\frac{(\hat{x}(n) - m_n(b))(\hat{x}(n) - m_n(b))^H}{2\sigma_x^2|_{x(n)=b}}\right) \end{aligned} \tag{3.6.8}$$

where the posterior conditional mean and covariance value of $\hat{x}(n)$ could be defined respectively as $m_n(b) = E\{\hat{x}(n)|_{x(n)=b}\}$ and $\sigma_{\hat{x}}^2|_{x(n)=b} = Cov[\hat{x}(n), \hat{x}(n)|_{x(n)=b}]$. Note that

$$\begin{aligned} E\{\mathbf{x}|_{x(n)=b}\} &= E\{\mathbf{x} + \mathbf{i}_n(b - x(n))\} \\ &= \bar{\mathbf{x}} + \mathbf{i}_n(b - \bar{x}(n)) \end{aligned} \tag{3.6.9}$$

Therefore, the conditional mean $m_n(b)$ could be determined by Eq.(3.6.3) and Eq.(3.6.4) as

$$\begin{aligned} m_n(b) &= E\{\hat{x}(n)|_{x(n)=b}\} = E\{\bar{x}(n) + \mathbf{w}_n^H(\mathbf{r} - \tilde{\mathbf{H}}\bar{\mathbf{x}})|_{x(n)=b}\} \\ &= E\left\{\mathbf{w}_n^H\tilde{\mathbf{H}}\mathbf{x}|_{x(n)=b}\right\} - \mathbf{w}_n^H\tilde{\mathbf{H}}\bar{\mathbf{x}}+\bar{x}(n) \\ &= \mathbf{w}_n^H\tilde{\mathbf{H}}\mathbf{i}_n(b - \bar{x}(n)) + \mathbf{w}_n^H\tilde{\mathbf{H}}\bar{\mathbf{x}} - \mathbf{w}_n^H\tilde{\mathbf{H}}\bar{\mathbf{x}}+\bar{x}(n) \\ &= \mathbf{w}_n^H\tilde{\mathbf{h}}_n(b - \bar{x}(n))+\bar{x}(n) \end{aligned} \tag{3.6.10}$$

It should be noted that $m_n(b)$ depends on the conditional value of $x(n) = b$. Similarly, it can be shown that the conditional variance of $x(n) = b$ is

$$\begin{aligned} \sigma_{\hat{x}}^2|_{x(n)=b} &= E\{(\hat{x}(n) - m_n(b))\,(\hat{x}(n) - m_n(b))^H\,|_{x(n)=b}\} \\ &= E\{\hat{x}(n)\hat{x}^H(n)|_{x(n)=b}\} - m_n(b)m_n(b)^H \end{aligned} \tag{3.6.11}$$

Substituting Eq.(3.6.4) and Eq.(3.6.10) in Eq.(3.6.11) yields

$$\sigma_{\hat{x}}^2|_{x(n)=b} = c_x(n)\mathbf{w}_n^H\tilde{\mathbf{h}}_n\left(1 - \tilde{\mathbf{h}}_n^H\mathbf{w}_n\right) \tag{3.6.12}$$

Note that unlike the conditional mean values, the conditional variance is independent of b. Therefore when writing variance in the sequel the conditional value is omitted. Here it is initialized as $\bar{x}(n) = 0$ and $c_x(n) = Cov[x(n), x(n)] = 1$ in Eq.(3.6.10) and Eq.(3.6.12) for finding the posterior LLR of $x(n)$ by only *extrinsic information*, therefore, this yields $L[x(n)] = 0$ at the beginning of the iteration, and hence

$$\begin{aligned}\Delta L[x(n)] &= L[x(n)|_{\hat{x}(n)}] - L[x(n)] \\ &= \ln \frac{\left[\exp\left(-\frac{(\hat{x}(n)-m_n(+1))^2}{\sigma_x^2|_{x(n)=+1}}\right)\right]}{\left[\exp\left(-\frac{(\hat{x}(n)-m_n(-1))^2}{\sigma_x^2|_{x(n)=-1}}\right)\right]} \\ &= \frac{4Re\{\hat{x}(n)\}}{1-\tilde{\mathbf{h}}_n^H \mathbf{w}_n}\end{aligned} \tag{3.6.13}$$

Therefore, the a posteriori LLR of $x(n)$

$$L[x(n)|_{\hat{x}(n)}] = \Delta L[x(n)] + L[x(n)] \tag{3.6.14}$$

Once the LLRs are obtained, the posterior values of $\hat{x}(n)$ such as $\bar{x}(n)|_{\hat{x}(n)}$ and $Cov[x(n), x(n)]|_{\hat{x}(n)}$ can be updated as

$$\begin{aligned}\bar{x}(n)_{new} &= \bar{x}(n)|_{\hat{x}(n)} \\ &= \Pr\{x(n) = +1|_{\hat{x}(n)}\} - \Pr\{x(n) = -1|_{\hat{x}(n)}\} \\ &= \tanh\left(\frac{L[x(n)|_{\hat{x}(n)}]}{2}\right)\end{aligned} \tag{3.6.15}$$

and

$$\begin{aligned}&Cov[x(n), x(n)]_{new} = Cov[x(n), x(n)]|_{\hat{x}(n)} \\ &= \sum_{b\in\{+1,-1\}} \left(b - E\{x(n)|_{\hat{x}(n)}\}\right)^2 \cdot \Pr\{x(n) = b|_{\hat{x}(n)}\} \\ &= 1 - \bar{x}(n)_{new}^2\end{aligned} \tag{3.6.16}$$

By Eq.(3.6.15) and Eq.(3.6.16), the $\bar{x}(n)$ and $Cov[x(n), x(n)]$ in Eq.(3.6.3) and Eq.(3.6.4) can be updated.

In the SIE scheme, $\hat{x}(0)$ is calculated by Eq.(3.6.3) and Eq.(3.6.4),

Table 3.2. Sequential iterative MMSE algorithm for MIMO-OFDM Detection.

$L = zeros(N, 1)$

$\bar{\mathbf{x}} = zeros(N, 1)$

$diag(\mathbf{c}_x) = \mathbf{I}_N$

while $iter \leq$ max

for $n = 1 : N$

$\bar{x}(n) = 0; c_x(n) = 1$

$\mathbf{w}_n = (\tilde{\mathbf{H}} diag(\mathbf{c}_x)\tilde{\mathbf{H}}^H + \sigma_n^2 \mathbf{I}_n)^{-1}\tilde{\mathbf{H}}\mathbf{i}_n c_x(n)$

$\hat{x}(n) = \bar{x}(n) + \mathbf{w}_n^H(\mathbf{r} - \tilde{\mathbf{H}}\bar{\mathbf{x}})$

$\Delta L(n) = \frac{4Re\{\hat{x}(n)\}}{1-\tilde{\mathbf{h}}_n^H \mathbf{w}_n}$

$L(n) = \Delta L(n) + L(n)$

$\bar{x}(n) = \tanh(L(n)/2)$

$c_x(n) = 1 - \bar{x}(n)^2$

end

end

then update $\bar{x}(0)_{new}$ and $Cov[x(0), x(0)]_{new}$ immediately via Eq.(3.6.13)-Eq.(3.6.16). Next $\hat{x}(1)$ is calculated and then $\bar{x}(1)_{new}$ and $Cov[x(1), x(1)]_{new}$ are updated immediately. This continues until $\hat{x}(N_b - 1)$ has been computed and $\bar{x}(N_b - 1)_{new}$ and $Cov[x(N_b - 1), x(N_b - 1)]_{new}$ have been updated. This repeats again starting with estimation of $\hat{x}(0)$ for the next iteration. The algorithm repeats until the specified number of iterations has elapsed. Table 3.2 shows the overall iterative algorithm used for the simulations.

3.6.3 Sequential Decision Feedback (SDF)

Based on the concept of decision feedback detection which is introduced in section 3.5.2, a sequential decision feedback (SDF) scheme [120] can be exploited for iterative signal detection processing. The SDF scheme operates identically to SIE except for the calculation of the value of $\bar{x}(n)_{new}$ and $Cov[x(n), x(n)]_{new}$. In SDF, firstly calculation for $\hat{x}(0)$ is performed by Eq.(3.6.3) and Eq.(3.6.4). Then update $\bar{x}(0)_{new}$ and $Cov[x(0), x(0)]_{new}$ immediately using $\bar{x}(0)_{new} = sgn(\hat{x}(0))$ (BPSK constellation) and $Cov[x(0), x(0)]_{new} = 0$. Next, calculate $\hat{x}(1)$ and then update $\bar{x}(1)_{new}$ and $Cov[x(1), x(1)]_{new}$ immediately by $\bar{x}(1)_{new} = sgn(\hat{x}(1))$ and $Cov[x(1), x(1)]_{new} = 0$. This means to continue updating $\bar{x}(n)_{new}$ and $Cov[x(n), x(n)]_{new}$ the following are used

$$\bar{x}(n)_{new} = sgn(\hat{x}(n))$$

and

$$Cov[x(n), x(n)]_{new} = 0$$

These values are updated for the next estimation until $n = N_b - 1$. This repeats again starting with estimation of $\hat{x}(0)$ for the next iteration. In this algorithm, the estimation is based on assuming the past estimations are correct. Hence, the calculation of LLRs are not necessary. The algorithm terminates when $\bar{x}(n)$ converge or a specified number of iterations has passed. Table 3.3 shows the overall sequential MMSE-DF algorithm used for the simulations.

Table 3.3. Sequential MMSE-DF algorithm for MIMO-OFDM Detection.

$\mathbf{c}_x = ones(N, 1)$

$\bar{\mathbf{x}} = zeros(N, 1)$

$diag(\mathbf{c}_x) = \mathbf{I}_N$

while $iter \leq$ max

for $n = 1 : N$

$\bar{x}(n) = 0; c_x(n) = 1$

$\mathbf{w}_n = (\tilde{\mathbf{H}} diag(\mathbf{c}_x)\tilde{\mathbf{H}}^H + \sigma_n^2 \mathbf{I}_n)^{-1}\tilde{\mathbf{H}}\mathbf{i}_n c_x(n)$

$\hat{x}(n) = \bar{x}(n) + \mathbf{w}_n^H(\mathbf{r} - \tilde{\mathbf{H}}\bar{\mathbf{x}})$

$\bar{x}(n) = sgn(\hat{x}(n))$

$c_x(n) = 0$

end

end

3.6.4 Simulations

In this section, some simulations are implemented for the proposed MMSE-iterative algorithm by the SDF and SIE updating schemes. For all simulations, in order to illustrate the performance of the proposed iterative symbol detection algorithm, a STBC MIMO-OFDM system case with a single user terminal which is equipped with four transmit and two receive antennas is exploited. A 1MHz transmitting data rate is assumed, i.e. the OFDM symbol duration is $T_s = 1\mu s$, which is divided into 128 sub-carriers by OFDM operation, and exploiting a BPSK signal constellation in this work for high speed computation with log-likelihood ratios. Each serial data stream contains 256 symbols, which is coded into two OFDM blocks by a STBC encoding operation. Therefore, the user terminal could transmit two data blocks in parallel

from two transmit antennas, from which the transmitting stream of $N_b = 256$ bits of information symbols are estimated in one detecting iteration.

For OFDM modulation, the length of the CP is kept equal to the order of the channel and the number of carriers is equal to the number of symbols in an OFDM block. A 3-tap wireless $(2, 2)$ MIMO slow fading channel model is used in which each channel tap is represented by a zero mean complex Gaussian random variable. The real and imaginary parts of each channel tap are independently generated with the Doppler spectrum based on Jakes' model (see [76]). The maximum Doppler frequency f_d denotes the characteristic of channel time variations. Hence, the normalized Doppler shift DS can be obtained by $DS = f_d N_b T_s$. Here, it is assumed $\sum_{l=0}^{L-1} \sigma_l^2 = 1$, where σ_l^2 is the variance of the lth path, and the channel fading is assumed to be uncorrelated among different transmitting antennas. Perfect knowledge of the channel state is available at the receiver at any time. However, there is no need for the knowledge of CSI at the transmitter.

Figure 3.5 presents the frame error rate (FER) performance of the proposed iterative receiver over slow fading MIMO wireless channels when $fd = 20Hz$ i.e. DS=0.005. Performance improvement can be observed by iterative processing of both SIE and SDF over the MIMO multipath channel environment after four iterations. The convergence of the iterative algorithm for SIE and SDF can also be shown. It should be noticed that the algorithm takes four iterations to converge and there is no significant improvement in the FER performance after four iterations. Moreover, the comparison of SIE and SDF performances of the proposed algorithm is depicted in this figure as well. It is shown

that the SIE scheme outperforms the SDF scheme with hard decision feedback for symbol detection over MIMO-ISI channels. This confirms the advantage of the use of a soft-symbol based scheme. Note that the performance of non-iterative MMSE receiver corresponds to the single iteration case.

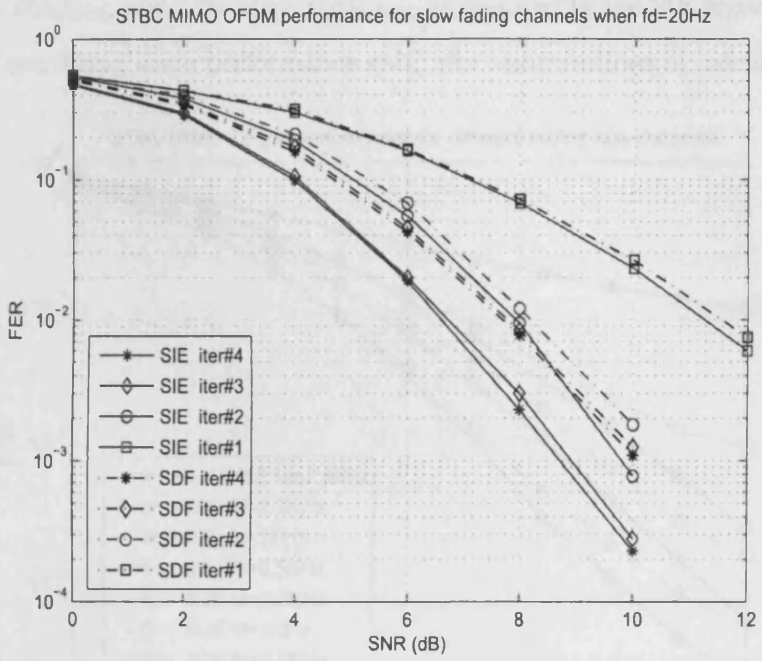

Figure 3.5. The FER vs. SNR performance for a STBC MIMO-OFDM system: the simulation implements two transmit and receive antennas over slow fading channels where $fd = 20Hz$ i.e. DS=0.005 and performs SDF and SIE MMSE detections.

Figure 3.6 shows the comparison of SIE and SDF performance over different fading rate LTV channel environment when the receiver is a three iteration process. The best performance is given when $f_d = 0.5KHz$ which DS is the smallest, and the performance degrades at higher SNR values with maximum Doppler frequency rising for both SIE and SDF. The simple Linear MMSE (LMMSE) based scheme would

have an error floor of 10^{-1} when $f_d = 0.5KHz$ i.e. DS=0.64, and is clearly worse than SIE and SDF schemes at the 3rd iteration. Herein, the SIE scheme still outperforms the SDF scheme in LTV channels. However, in order to find the posteriori values of the frequency domain symbols $L[\hat{x}(n)|_{x(n)}]$, the posteriori mean and variance of the estimator, $\bar{x}(n)|_{\hat{x}(n)}$ and $Cov[x(n), x(n)]|_{\hat{x}(n)}$, is required in the SIE algorithm. By sacrificing some performance gain, the computations of calculating

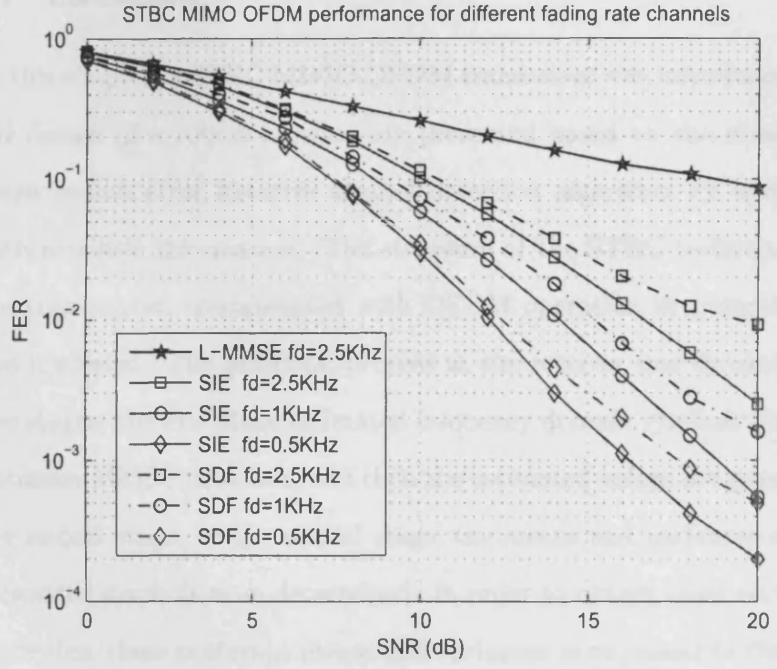

Figure 3.6. The FER vs. SNR performance for the STBC MIMO-OFDM system: the simulation implements two transmit and receive antennas over different fading rate channels (maximum Doppler frequencies are 0.5KHz, 1KHz and 2.5KHz which DS are 0.13, 0.25, 0.64 respectively) and performs SDF and SIE MMSE detections at the 3rd iteration.

the posteriori mean and variance of the estimator can be saved in the SDF scheme. Because, all the posteriori means are calculated as hard decision of the estimation $\hat{x}(n)$ and the variance of the estimator is sup-

posed equal to zero due to assuming estimations completely correct for all symbol detection, then calculating LLRs is not necessary. Therefore it will decrease the overall computational complexity. Moreover, further performance enhancement could be achieved by concatenating another coding technique with the iterative processing, for example, low-density parity-check code (LDPC) or turbo coding.

3.7 Conclusions

In this chapter, a STBC MIMO-OFDM transceiver was introduced and the design of a robust receiver are presented based on the minimum mean square error iterative symbol detection algorithm by updating with extrinsic information. The structure of the STBC techniques at the transmitter, concatenated with OFDM operation to mitigate ISI was exploited. The detection process at the receiver was divided into two stages; the first stage estimated frequency domain symbols with an optimum MMSE equalizer, and then the estimated values are passed to the second stage. In the second stage, the means and variances of the estimated symbols were determined. In order to obtain more accurate estimates, these posteriori means and variances were passed to the first stage to use in the following iteration. The first stage utilizes these values to update equalizer coefficient values and cancel the interference in order to provide more accurate estimates. Thereby both stages iteratively exchanged their information learnt from each other. The simulation results indicate that the proposed SIE and SDF schemes could obtain substantial performance improvement during iteration processing over both quasi-static channels and a slow fading channel environment. In future work, it may still be possible to develop this structure

by introducing channel coding technology into the feedback process for more performance development.

Chapter 4

TWO-STEP MULTIUSER DETECTION SCHEME FOR STBC MIMO-OFDM SYSTEMS

In the previous chapter single user detection for a MIMO wideband channel was investigated. In this chapter the multiuser detection problem for a multicarrier MIMO system is addressed. In particular, performing a parallel interference cancellation (PIC) algorithm to aid multiuser STBC-OFDM systems is the topic of interest.

The outline of this chapter is organized as follows. In Section 4.1, the interference occurring in the multiuser application is introduced. Then the PIC algorithm is discussed to mitigate multiuser interference for signal detections in Section 4.2. A proposed two-step multiuser interference cancellation scheme based on PIC is designed in Section 4.3, which was also proposed in [121]. In order to improve this two-step scheme, a novel joint coded PIC multiuser detection scheme is proposed and assessed in Section 4.4 including simulation results and analysis, which was represented in [122] as well. Finally, conclusions

are provided in Section 4.5.

4.1 Multiuser Interference and Multiuser Detections

In wireless communication systems, the radio spectrum resource has to transmit data by reusing the frequency bands. However, when more than one transmitter operates in one frequency-division channel, they will interfere with each other. This represents so called co-channel interference (CCI). Nowadays, the cross-correlation between users' different multipath channels has become one of the major challenge of loss in wireless system performance.

In practical wireless communications, strong interferers possibly happen in urban areas where the base stations (BS) are closely spaced. Therefore effectively suppressing CCI is important to improve the service quality or minimize the allowable distance among nearby co-channel BSs, and thus increase the system capacity [123] [124]. For example in a two user transmitter case, it will provide ability to allocate two users in the same time-slot if the strong co-channel interferer can be effectively suppressed, and therefore double the uplink capacity. Multiple access interference (MAI) is present in a code-division multiple access (CDMA) system due to the operation over the same waveband. CCI is also an inherent problem for most multiple access schemes, for example OFDMA and TDMA. MAI occurs between subchannels, both in the uplink and downlink. Furthermore, the MAI can also come from other cells (intercell MAI). Hence the ability to allocate a larger number of users can be provided in the cell and among cells by suppressing the MAI due to each user. Otherwise, suppressing MAI and CCI will reduce the transmit power which is required to meet the target signal-to-noise

ratio (SNR), and enable more channels to be used for transmitting with the limited power, thereby resulting in capacity increase. Hence the design of interference-suppression receivers becomes very important for future multiuser mobile systems.

Multiuser receivers can implement robust multiuser signal processing algorithms referred to as multiuser detection (MUD) to effectively suppress or cancel the multiuser interference between users, such as improving upon most conventional single-user receivers which are only designed to operate in thermal noise without CCI or MAI. Therefore, multiuser receivers can potentially substantially outperform single-user receivers in a multiuser environment. Effective multiuser receivers can extract and detect desired user data from the multiuser signal efficiently. Although multiuser detection (MUD) was originally proposed for CDMA systems [62], it can also be employed in TDMA systems [124] and OFDM systems [125]. Nowadays, many types of MUD techniques have been developed. The optimal approaches based on maximum likelihood (ML) or the maximum a posteriori probability (MAP) algorithm can provide performance close to the single-user bound, however, these schemes require high computational complexity [62]. Therefore, some sub-optimal MUD algorithms which have much lower complexity have been developed. By introduction in Chapter 2, zero-forcing (ZF) detection and minimum mean squared error (MMSE) detection are referred to as linear detection which can suppress the interference linearly. On the other hand, there is another class of sub-optimal MUD referred as nonlinear detection such as decision-feedback MUD, successive interference cancellation (SIC) and parallel interference cancellation (PIC). The PIC detector is an iterative multiuser detector, which can perform

more accurate estimation during iterations, which will be introduced in the following sections.

4.2 Parallel Interference Cancellation for Multiuser Detections

As description in Chapter 2, the linear schemes can be used in multiuser detections, on the other hand researchers have also proposed nonlinear detection schemes which exploit the data from the interfering user to detect the signal of the desired user. This strategy is so-called interference cancellation (IC) detection which reconstructs the multiuser interference by temporary data estimations, and then cancels it from the received signal. The IC detection scheme normally includes two types: successive interference cancellation (SIC) and parallel interference cancellation (PIC).

In the SIC detection scheme [126], the detector firstly detects the strongest user (likely most reliable user) in terms of received power by using conventional matched filtering (MF). Then the interference caused by this user is reconstructed and subtracted from the received signal. If the interference is relatively accurately estimated and subtracted from received stream, then the resulting signal term contains one fewer major interfering user. Next the receiver will repeat the same process with the most likely reliable/strongest user among the remaining ones, until the last user is left to be demodulated. This scheme will be introduced in detail in Chapter 6.

PIC detection [127] and [128] simultaneously firstly detects each user's data separately. In order to cancel the MAI for each user, the detector employs the first stage estimations to remove the remaining users' interference for each user from the received signal. Compared

with the SIC, since the IC is performed in parallel for all users, the problem of relatively long processing delay which happens in SIC due to serial cancellation one-by-one can be solved by reducing processing duration. It is clear that the parallel cancellation process should be divided into at least two stages: (1) perform the estimation of all users' signals; (2) reconstruct the MAI and subtracts it from the received signal for each user. Thus the PIC is so-called multi-stage IC. The first stage of PIC can be provided by an MF or linear detection such as MMSE. Figure 4.1 illustrates the structure of the PIC detector in a two-user scenario.

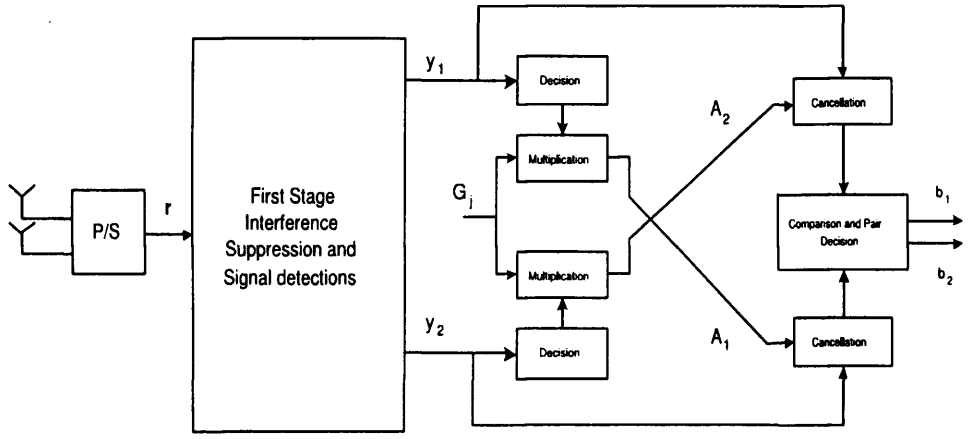

Figure 4.1. The structure of the parallel interference cancellation (PIC) for two user signal detection.

Now suppose that there are K users which are detected in the first stage. Then the signal estimation of the users is given by

$$\mathbf{y} = \mathbf{W}^H \mathbf{r} \tag{4.2.1}$$

where $\mathbf{W}$ is the detection weight matrix where $\mathbf{W} = [\mathbf{w}_1, \mathbf{w}_2, \ldots, \mathbf{w}_K]$ and $\mathbf{w}_k$ is the column weight vector for the kth user. $\mathbf{y} = [y_1, y_2, \ldots, y_K]^T$

is the first stage detection, it is assumed that the complex scalar G_j is reconstructing the MAI parameter of the jth interfering user, so the kth user's MAI caused by the jth interfering user is obtained as

$$A_j = G_j y_j \tag{4.2.2}$$

where $j \neq k$. So for a desired user k, the MAI is subtracted from the received signal as

$$\tilde{y}_k = y_k - \sum\nolimits_{j \neq k} A_j \tag{4.2.3}$$

Assuming that a hard decision is employed, the output of the two-stage PIC detector is:

$$\begin{aligned} b_k &= sgn(\tilde{y}_k) \\ &= sgn\left(y_k - \sum\nolimits_{j \neq k} G_j y_j\right) \end{aligned} \tag{4.2.4}$$

From the discussion above, it can be found that PIC detection can remove the MAI in parallel which can avoid the long delay derived from the serial processing in the SIC. Moreover, the PIC approach can be further improved by iterative processing, which updates the MAI reconstruction with the increasingly reliable temporary decisions of the interfering users. The iteration can be performed as many times as needed. In general, the performance of the detector should continuously improve with increasing number of iterations until convergence as the best performance. Hence PIC detection is considered as one of the most promising MUD techniques [129], [130].

4.3 Two-Step PIC MUD for STBC MIMO-OFDM Systems

In this section, the transceiver design is exploited for a wideband multiuser-multiple-input, multiple-output (MIMO) communication system, where the co-channel users are equipped with multiple transmit and multiple receive antennas. In particular, a two-step hard-decision parallel interference cancellation (PIC) receiver is developed for a multiuser-MIMO synchronous uplink system which employs orthogonal frequency division multiplexing (OFDM) modulation and space-time block coding (STBC). The STBC is implemented either over adjacent tones or adjacent OFDM symbols and the performances of both implementations is tested under slowly time-varying channels. The two-step receiver structure is implemented using a combined interference suppression scheme based on minimum mean-squared error (MMSE) and symbol-wise likelihood detectors, which is then followed by a PIC stage. The receiver can suppress and cancel the interference from the co-channel users effectively without increasing the complexity significantly. Some simulation results are provided that are intended to improve the understanding of specific issues involved in the design of multiuser STBC-OFDM systems. This work has also been published in [121].

The outline of this section is organized as follows. In Section 4.3.1, the two-step PIC multiuser detection is introduced for multiuser STBC-OFDM systems. Then the signal processing of the system model is given in Section 4.3.2. The proposed two-step multiuser receiver scheme is described in Section 4.3.3. In Section 4.3.4, the algorithm complexity is discussed in detail, and finally, simulation results are provided and discussed in Section 4.3.5.

4.3.1 Introduction

In this work, a wide-band uplink system is considered with K synchronous co-channel users, each is equipped with Alamouti's STBC and OFDM modulated transmit antennas (using the same scheme as [33], [116] and [77]). During OFDM modulation, assuming that the channels remain constant over continuous tones of each block, the STBC is employed over the adjacent tones, which is suitable for slow fading environments with large delay spreads. The number of transmit antennas per user is limited to $n_t = 2$. The receiving station is equipped with m_r ($\geq K$) receive antennas. The challenge is to design a receiver that can suppress the CCI and ISI simultaneously. The narrow band two-step PIC scheme proposed in [77] is extended to the proposed wideband channels.

Note that the classical MMSE interference suppression technique has been proposed in [116] for multiuser STBC-OFDM systems. The proposed two-step interference cancellation receiver brings considerable performance gain while maintaining simplicity of symbol estimation without increasing the complexity of the receiver considerably compared to classical MMSE receivers. Moreover, as for the scheme in [116], it employs STBC over two OFDM symbols assuming that the channel is constant over the adjacent OFDM symbols, i.e. quasi-static channels, and its sensitivity to the channel variation within the two symbol period is significantly higher than the proposed transmitter. Further, the iterative PIC receiver schemes for the proposed scenario may achieve better performance but with considerable complexity increase (see in [131], [129], [130]).

4.3.2 Synchronous System Model

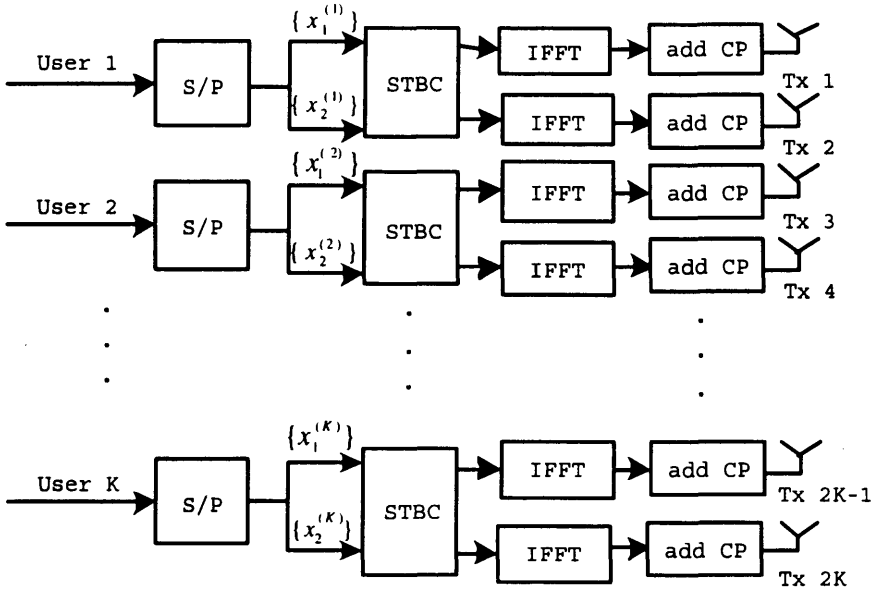

Figure 4.2. Baseband Multiuser STBC MIMO-OFDM transmitters for K users, where each user terminal is equipped with $n_t = 2$ transmit antennas.

A K-user space-time block coded OFDM wireless communication system is considered as illustrated in Figure 4.2, where each user terminal is equipped with $n_t = 2$ transmit antennas. First, the incoming data streams are space-time block encoded and then an OFDM modulator is applied to the outputs of the space time encoders. The outputs of the OFDM modulators after addition of cyclic prefix bits are transmitted using multiple antennas simultaneously.

In general, the frequency selective channel can be converted to multiple flat-fading channels by using OFDM modulation. First, a set of N QPSK symbols forms a frequency domain transmitting signal block $\mathbf{x}^{(i)} = [x^{(i)}(0), \cdots, x^{(i)}(N-1)]^T$ where the superscript (i) denotes the ith user. Then, the time-domain baseband transmitting sig-

nal can be obtained by performing N-point inverse DFT operation $\mathbf{F}^H$ over $\mathbf{x}^{(i)}$, where the $\mathbf{F}$ denotes the $N \times N$ DFT matrix whose mnth $(m, n = 1, 2, \ldots N)$ element [117] is given by

$$\mathbf{F} = \frac{1}{\sqrt{N}} e^{-j2\pi(m-1)(n-1)/N} \tag{4.3.1}$$

The time domain transmitting signal can be written as $\mathbf{F}^H\mathbf{x}^{(i)}$. Therefore, the time domain samples are appended with a cyclic prefix and then serially transmitted over the multipath channel. To avoid inter symbol interference (ISI), a sufficient cyclic prefix interval P, i.e. $P > L$, is inserted prior to the transmission.

Here, there are two popular ways to extend space-time block codes combined with OFDM modulation, which are traditionally designed for single-tone flat fading channels, to multiple-tone OFDM modulation:

(i) STBC is performed on a per-tone basis across consecutive OFDM symbols in time exactly as performed in the flat fading environments (see also in [116]). Hence the STBC scheme implements encoding still on frequency domain symbols. As shown in Figure 4.2, the STBC is taken before OFDM modulation cross n_t OFDM blocks. However, this requires that the channel remains constant over n_t OFDM symbol periods which is equal to the duration of $n_t(N + L - 1)T_s$, where L denotes the frequency-selective sub-channel tap length and T_s denotes transmitted symbol period, i.e. the MIMO-ISI channel keeps quasi-static during n_t consecutive OFDM blocks.

(ii) STBC is performed with the time index replaced by the tone index in OFDM and STBC is performed across n_t continuous subcarriers. This requires that the channel remains constant over a number of

adjacent tones equal to the number of transmit antennas n_t. Compared with the first scheme, this encoding scheme is performed on time domain symbols which are symmetric to the source signal in the frequency domain. Hence, this STBC scheme is a so-called space frequency block coding (SFBC). Both approaches are next considered.

4.3.2.1 STBC Over OFDM Symbols For $n_t = 2$

Consider two consecutive transmitting OFDM symbol blocks $\mathbf{x}_1^{(i)} = [x_1^{(i)}(0), \cdots, x_1^{(i)}(N-1)]^T$ and $\mathbf{x}_2^{(i)} = [x_2^{(i)}(0), \cdots, x_2^{(i)}(N-1)]^T$, which are the frequency domain symbols from the ith user, $i = 1, \ldots, K$. The output of the STBC encoder is converted into the time domain samples by N-point inverse DFT operation $\mathbf{F}^H$. Consequently, the OFDM modulated STBC coded time-domain symbols of the ith user during two consecutive block intervals can be written in the matrix form:

$$\begin{bmatrix} \mathbf{F}^H\mathbf{x}_1^{(i)} & \mathbf{F}^H\mathbf{x}_2^{(i)} \\ -\mathbf{F}^H\mathbf{x}_2^{(i)*} & \mathbf{F}^H\mathbf{x}_1^{(i)*} \end{bmatrix} \tag{4.3.2}$$

At a given block interval, $\mathbf{F}^H\mathbf{x}_1^{(i)}$, and $\mathbf{F}^H\mathbf{x}_2^{(i)}$ denote the signal blocks transmitted by antenna one and two after OFDM modulation, respectively, without cyclic prefix of course. Then, during the next block interval $-\mathbf{F}^H\mathbf{x}_2^{(i)*}$ and $\mathbf{F}^H\mathbf{x}_1^{(i)*}$ are respectively sent by antenna one, and two.

At the receiving end, after the FFT operation and cyclic prefix removal, the N received symbols in the frequency domain are collected from the jth receive antenna during the first and second OFDM inter-

vals which can be represented as

$$\mathbf{r}_{1j} = \sum_{i=1}^{K} \{\mathbf{F}[\mathbf{H}_c^{(i)}]_{1j}\mathbf{F}^H\mathbf{x}_1^{(i)} + \mathbf{F}[\mathbf{H}_c^{(i)}]_{2j}\mathbf{F}^H\mathbf{x}_2^{(i)}\} + \mathbf{v}_{f1j} \quad (4.3.3)$$

$$\mathbf{r}_{2j} = \sum_{i=1}^{K} \{\mathbf{F}[\mathbf{H}_c^{(i)}]_{2j}\mathbf{F}^H\mathbf{x}_1^{(i)^*} - \mathbf{F}[\mathbf{H}_c^{(i)}]_{1j}\mathbf{F}^H\mathbf{x}_2^{(i)^*}\} + \mathbf{v}_{f2j} \quad (4.3.4)$$

where $\mathbf{v}_{f1j}$ and $\mathbf{v}_{f2j}$ are the frequency domain vectors of the zero mean complex white circular Gaussian noise which influences on the jth receive antenna; $[\mathbf{H}_c^{(i)}]_{qj}$ is the channel impulse response circular convolution matrix of size $N \times N$ which is experienced by the ith user's signal transmitted from the qth transmit antenna to the jth receive antenna, and $q \in \{1, 2\}$. The matrix form of $[\mathbf{H}_c^{(i)}]_{qj}$ has been represented in chapter 2 (see also in [108]). Note that, it is assumed that the channel responses are constant during two consecutive signal block intervals, i.e. quasi-static.

The *subcarrier coupling matrix* $\mathbf{H}_{qj}^{(i)}$ for the equivalent frequency response of the channel is defined as

$$\mathbf{H}_{qj}^{(i)} = \mathbf{F}[\mathbf{H}_c^{(i)}]_{qj}\mathbf{F}^H \quad (4.3.5)$$

Because the transmission is considered to be over quasi-static frequency-selective fading channels, i.e. channel impulse response keeps invariant during the OFDM symbol duration, the equivalent frequency channel response is represented in a diagonal matrix form as

$$\mathbf{H}_{qj}^{(i)} = diag[H_{qj}^i(0), H_{qj}^i(1), \ldots, H_{qj}^i(N-1)]$$

Hence, let $H_{1j}^i(k)$ and $H_{2j}^i(k)$ denote the channel frequency response of the kth tone, corresponding to the channel from the $1st$ and $2nd$

transmit antennas of the ith user to the jth receive antenna, respectively, over two continuous signal block intervals. Due to employing a space-time block encoding scheme, the kth tone receive symbol in the frequency domain over the two sequential OFDM time-slots 1 and 2 are obtained in Eq.(4.3.6) and Eq.(4.3.7), where $k = 0, 1, \ldots, N-1$, respectively as

$$r_{1j}(k) = \sum_{i=1}^{K} \{H_{1j}^{i}(k) x_1^{(i)}(k) + H_{2j}^{i}(k) x_2^{(i)}(k)\} + v_{f1j}(k) \tag{4.3.6}$$

$$r_{2j}(k) = \sum_{i=1}^{K} \{H_{2j}^{i}(k) x_1^{(i)^*}(k) - H_{1j}^{i}(k) x_2^{(i)^*}(k)\} + v_{f2j}(k) \tag{4.3.7}$$

where $[v_{f1j}(k)\ v_{f2j}(k)]$ represent the frequency domain representation of the receiver AWGN at the kth tone. Next defining

$$\mathbf{r}_j(k) = [r_{1j}(k), r_{2j}^{*}(k)]^T$$

$$\mathbf{x}^{(i)}(k) = [x_1^{(i)}(k), x_2^{(i)}(k)]^T$$

$$\mathbf{v}_{fj}(k) = [v_{f1j}(k), v_{f2j}^{*}(k)]^T$$

and $\breve{\mathbf{H}}_j^i$ as the equivalent channel response matrix of the kth tone between the ith user terminal and the jth receive antenna as

$$\breve{\mathbf{H}}_j^i = \begin{bmatrix} H_{1j}^{i}(k) & H_{2j}^{i}(k) \\ H_{2j}^{i\,*}(k) & -H_{1j}^{i\,*}(k) \end{bmatrix}$$

Hence, the kth tone receive signals from all receive antennas during two consecutive OFDM periods can be represented in matrix form as

follows:

$$\begin{bmatrix} \mathbf{r}_1(k) \\ \mathbf{r}_2(k) \\ \vdots \\ \mathbf{r}_{m_r}(k) \end{bmatrix} = \begin{bmatrix} \breve{\mathbf{H}}_1^1(k) & \cdots & \breve{\mathbf{H}}_1^K(k) \\ \breve{\mathbf{H}}_2^1(k) & \cdots & \breve{\mathbf{H}}_2^K(k) \\ \vdots & \ddots & \vdots \\ \breve{\mathbf{H}}_{m_r}^1(k) & \cdots & \breve{\mathbf{H}}_{m_r}^K(k) \end{bmatrix} \begin{bmatrix} \mathbf{x}^{(1)}(k) \\ \mathbf{x}^{(2)}(k) \\ \vdots \\ \mathbf{x}^{(K)}(k) \end{bmatrix} + \begin{bmatrix} \mathbf{v}_{f1}(k) \\ \mathbf{v}_{f2}(k) \\ \vdots \\ \mathbf{v}_{fm_r}(k) \end{bmatrix} \tag{4.3.8}$$

The receive signal for simplicity of notation is thereby rewritten, as follows:

$$\tilde{\mathbf{r}}(k) = \tilde{\mathbf{H}}(k)\tilde{\mathbf{x}}(k) + \mathbf{v}_f(k) \tag{4.3.9}$$

where $\tilde{\mathbf{r}}(k)$ is the overall receive signal vector at all receive antennas with $2m_r$ elements, $\tilde{\mathbf{H}}(k)$ is the equivalent overall channel response matrix of size $2m_r \times 2K$, $\tilde{\mathbf{x}}(k)$ is the transmitting signal vector with $2K$ elements including all users at the kth tone, and $\mathbf{v}_f(k)$ is the equivalent complex noise vector of size $2m_r$ which influences the overall channels.

4.3.2.2 SFBC Over OFDM Carriers For $n_t = 2$

An Alamouti type scheme can also be performed across two consecutive tones k and $k+1$ for space frequency encoding. In this context, the channel is assumed to be constant over two adjacent tones i.e. $H_{qj}(k) = H_{qj}(k+1)$. If the transmitting signal from the ith user is defined as $\mathbf{x}^{(i)} = [x^{(i)}(0), \cdots, x^{(i)}(N-1)]^T$, then, the coded signal from two transmit antennas of the ith user could be represented in a matrix form as

$$\begin{bmatrix} x^{(i)}(k) & x^{(i)}(k+1) \\ -x^{(i)^*}(k+1) & x^{(i)^*}(k) \end{bmatrix} \tag{4.3.10}$$

The two symbols $x_1^{(i)}$ and $x_2^{(i)}$ are transmitted over antennas 1 and 2

respectively on tone k and $-x_2^{(i)*}$ and $x_1^{(i)*}$ are transmitted over antennas 1 and 2 respectively on tone $k+1$ within the same OFDM symbol. Hence, the receive signal at the jth receive antenna across two adjacent frequency domain sample time will be given by

$$r_j(k) = \sum_{i=1}^{K} \{H_{1j}^i(k) \cdot x^{(i)}(k) + H_{2j}^i(k) \cdot x^{(i)}(k+1)\} + v_{fj}(k) \quad (4.3.11)$$

$$r_j(k+1) = \sum_{i=1}^{K} \{H_{2j}^i(k+1) \cdot x^{(i)*}(k) - H_{1j}^i(k+1) \cdot x^{(i)*}(k+1)\} + v_{fj}(k+1) \quad (4.3.12)$$

Hence, a vector form similarly to STBC over OFDM could be defined over two adjacent tones k and $k+1$ as

$$\mathbf{r}_j(k) = [r_j(k), r_j^*(k+1)]^T$$

$$\mathbf{x}^{(i)}(k) = [x^{(i)}(k), x^{(i)}(k+1)]^T$$

$$\mathbf{v}_j(k) = [v_{fj}(k), v_{fj}^*(k+1)]^T$$

and define $\breve{\mathbf{H}}_j^i$ as the equivalent channel response matrix between the ith user terminal and the jth receive antenna across the kth and $k+1$th tone as

$$\breve{\mathbf{H}}_j^i = \begin{bmatrix} H_{1j}^i(k) & H_{2j}^i(k) \\ H_{2j}^{i\,*}(k+1) & -H_{1j}^{i\,*}(k+1) \end{bmatrix}$$

Hence, similarly, the receive signal vector from all receive antennas across two adjacent OFDM subcarriers k and $k+1$ in terms of matrix form would be the same form as Eq.(4.3.8). For simplicity of notation, this equation could also be rewritten to obtain the same overall signal processing equation as Eq.(4.3.9).

4.3.3 Two step MMSE Interference Cancellation

The two-step generalized MMSE interference receiver in [77] is therefore extended to the proposed multiuser STBC-OFDM scheme. For simplicity, without loss of generality only the two-user scenario is considered. The receiver structure is illustrated in Figure 4.3.

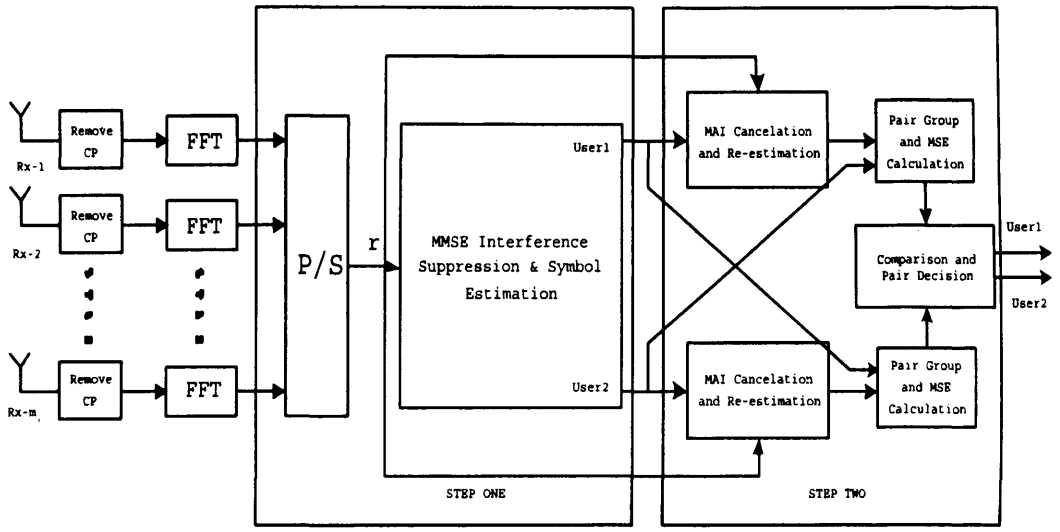

Figure 4.3. Two-step baseband PIC STBC MIMO-OFDM receiver for two users equipped with $m_r = 2$ receive antennas.

In this receiver structure, the OFDM-demodulated received signal will be passed through the following three parts of processing:

(1) Signal estimation based on a combined MMSE and multiuser detector;

(2) Multiple-access interference cancellation and symbol estimation using the modified interference-free received signal;

(3)Decision based on the reliability estimation.

Step 1: Linear MMSE Interference Suppression and Symbol Estimation

In the first step, a Linear MMSE (L-MMSE) interference cancellation and symbol-wise likelihood decoder is used to estimate the transmitted symbols by the users. Considering the ith user terminal, where $i = 1, 2$, the mean squared error cost which incorporates the co-channel interference and noise corresponding to the symbol $\hat{x}^{(i)}$ is defined as

$$J(\mathbf{w}) = E\left\{\left|x^{(i)}(k) - \mathbf{w}^H\tilde{\mathbf{r}}(k)\right|^2\right\} \tag{4.3.13}$$

where $\hat{x}^{(i)}(k) = \mathbf{w}^H\tilde{\mathbf{r}}(k)$ is the estimation of the symbol $x^{(i)}$ and $E\{\cdot\}$ denotes the statistical expectation operator. To minimize the mean squared error, the weight vector $\mathbf{w}$ of size $2m_r$ is chosen based on standard minimization techniques:

$$\frac{\partial J(\mathbf{w})}{\partial \mathbf{w}} = 0 \tag{4.3.14}$$

Hence, the weight vectors $\mathbf{w}_{2i-1} = [w_{2i-1,1}, w_{2i-1,2}, \ldots, w_{2i-1,2m_r}]^T$ and $\mathbf{w}_{2i} = [w_{2i,1}, w_{2i,2}, \ldots, w_{2i,2m_r}]^T$, corresponding to the ith user, can be computed respectively, as

$$\mathbf{w}_{2i-1} = \mathbf{M}^{-1}\tilde{\mathbf{h}}_{2i-1} \tag{4.3.15}$$

$$\mathbf{w}_{2i} = \mathbf{M}^{-1}\tilde{\mathbf{h}}_{2i} \tag{4.3.16}$$

where $\mathbf{M} = \tilde{\mathbf{H}}(k)\tilde{\mathbf{H}}^H(k) + \frac{1}{\tau}\mathbf{I}_{2m_r}$ and $\tau = E_s/N_0$ is the signal to noise ratio, $\tilde{\mathbf{h}}_{2i-1}$ and $\tilde{\mathbf{h}}_{2i}$ are the $(2i-1)$th and $(2i)$th columns of $\tilde{\mathbf{H}}(k)$, respectively. Then, the symbol-wise likelihood decoding equation can be written as

$$\hat{\mathbf{x}}^{(i)}(k) = \arg \min_{\left[x_{c1}^{(i)}\ x_{c2}^{(i)}\right] \in \mathbf{X}} \left\{ \left| \mathbf{w}_{2i-1}^{H} \tilde{\mathbf{r}}(k) - x_{c1}^{(i)}(k) \right|^2 + \left| \mathbf{w}_{2i}^{H} \tilde{\mathbf{r}}(k) - x_{c2}^{(i)}(k) \right|^2 \right\} \tag{4.3.17}$$

where the candidate pair $\left[x_{c1}^{(i)}\ x_{c2}^{(i)}\right]$ is the hypothesised symbols which refer to one of all possible symbol pairs in the transmitted signal. Both $x_{c1}^{(i)}$ and $x_{c2}^{(i)}$ are scalar signal symbols at the kth tone, which can be decided independently, because the metrics separate easily.

Finally, the reliability function for the first step estimation of the symbol from the ith user terminal can be represented as

$$\triangle_{\hat{\mathbf{x}}^{(i)}(k)} = \left| \mathbf{w}_{2i-1}^{H} \tilde{\mathbf{r}}(k) - \hat{x}_1^{(i)}(k) \right|^2 + \left| \mathbf{w}_{2i}^{H} \tilde{\mathbf{r}}(k) - \hat{x}_2^{(i)}(k) \right|^2 \tag{4.3.18}$$

where $\hat{x}_1^{(i)}(k)$ and $\hat{x}_2^{(i)}(k)$ are found in $\hat{\mathbf{x}}^{(i)}(k)$ from Eq. 4.3.17

Step 2: Two-Step Approach for MAI Cancellation and Symbol Re-estimation

In Step 1, the L-MMSE scheme is used to suppress the interferences from the co-channel users in estimating the transmitted information symbols. In the second step, the transmitted symbols are re-estimated based on a modified received signal obtained by parallel cancelling the multiple access interferences for each user. Note that a perfect interference cancellation may be achieved only if the signals from the first step have been decoded correctly. During the PIC for two users, in order to re-estimate the second user symbols, the receiver cancels the multiple access interference (MAI) caused by the first user from the received signal $\mathbf{r}_1(k), \mathbf{r}_2(k), \ldots, \mathbf{r}_{m_r}(k)$ to estimate the transmitted symbols. For the kth tone, the modified received signal vectors after cancelling the MAI from the first user will be represented as

$$\mathbf{a}_1(k) = \mathbf{r}_1(k) - \breve{\mathbf{H}}_1^1(k)\hat{\mathbf{x}}^{(1)}(k) \tag{4.3.19}$$

$$\mathbf{a}_2(k) = \mathbf{r}_2(k) - \breve{\mathbf{H}}_2^1(k)\hat{\mathbf{x}}^{(1)}(k) \tag{4.3.20}$$

$$\cdots\cdots$$

$$\mathbf{a}_{m_r}(k) = \mathbf{r}_{m_r}(k) - \breve{\mathbf{H}}_{m_r}^1(k)\hat{\mathbf{x}}^{(1)}(k) \tag{4.3.21}$$

The second user's kth signals are re-estimated using the above modified received vector:

$$\hat{\hat{\mathbf{x}}}^{(2)}(k) = \arg \min_{\mathbf{x}_c^{(2)} \in \mathbf{X}} \sum_{n=1}^{m_r} \left\{ \left\| \mathbf{a}_n(k) - \breve{\mathbf{H}}_n^2(k)\mathbf{x}_c^{(2)}(k) \right\|^2 \right\} \tag{4.3.22}$$

where $\mathbf{x}_c$ is one of all possible choices of symbols from a QPSK constellation, and $\|\cdot\|^2$ denotes squared Euclidean norm operator. The reliability function for the estimation from this second step of the user 2 will be given by

$$\triangle_{\hat{\hat{\mathbf{x}}}^{(2)}(k)} = \sum_{n=1}^{m_r} \left\{ \left\| \mathbf{a}_n(k) - \breve{\mathbf{H}}_n^2(k)\hat{\hat{\mathbf{x}}}^{(2)}(k) \right\|^2 \right\} \tag{4.3.23}$$

Finally, the total reliability of the first and second step estimation will be the summation of the reliability of the first user at the first step and the reliability of the second user at the second step, which is given by the overall reliability corresponding to $\hat{\mathbf{x}}^{(1)}(k)$ and $\hat{\hat{\mathbf{x}}}^{(2)}(k)$ as

$$\triangle_a = \triangle_{\hat{\mathbf{x}}^{(1)}(k)} + \triangle_{\hat{\hat{\mathbf{x}}}^{(2)}(k)} \tag{4.3.24}$$

This procedure will be repeated for re-estimating the first user's symbol by assuming correct decision of the second user at the first step.

Based upon its estimate $\hat{\mathbf{x}}^{(2)}(k)$ the user 1's signals will be re-estimated as $\hat{\hat{\mathbf{x}}}^{(1)}(k)$. The receiver repeats the MAI interference cancellation and symbol-wise likelihood re-estimation algorithm in parallel, assuming that the estimation of the second user transmitted signal at the kth tone $\hat{\mathbf{x}}^{(2)}(k) = [\hat{x}_1^{(2)}(k), \hat{x}_2^{(2)}(k)]^T$ has been estimated correctly at the first step. In a similar fashion, the reliability function can also be defined as

$$\triangle_b = \triangle_{\hat{\mathbf{x}}^{(2)}(k)} + \triangle_{\hat{\hat{\mathbf{x}}}^{(1)}(k)} \tag{4.3.25}$$

where $\triangle_b$ denotes the overall reliability corresponding to $\hat{\mathbf{x}}^{(2)}(k)$ and $\hat{\hat{\mathbf{x}}}^{(1)}(k)$.

Finally, the symbol pairs based on the best overall reliabilities obtained between $\triangle_a$ and $\triangle_b$ will be selected. When $\triangle_a < \triangle_b$, the pair $[\hat{\mathbf{x}}^{(1)}(k), \hat{\hat{\mathbf{x}}}^{(2)}(k)]$ will be chosen as the estimates, otherwise, it is $[\hat{\hat{\mathbf{x}}}^{(1)}(k), \hat{\mathbf{x}}^{(2)}(k)]$. The table 4.1 shows the proposed two-step PIC MUD algorithm for two user STBC-OFDM detection.

From the discussion in Section 4.2, it is known that the conventional PIC MUD can fully remove the MAI if the temporary decision is correct. However if the temporary decision is wrong, the error will be doubled after the PIC and therefore cause error propagation. Hence the PIC based on hard decisions in each iteration has the risk of oscillation. Compared with a conventional PIC scheme, the proposed two-step PIC MUD includes calculation of overall reliability values for each user branch, across all estimation stages. These operations for overall reliability values provide different decision pairs for comparison in order to choose more reliable results for output. Hence, this strategy avoids error propagation due to the case that one of the users signals is not estimated correctly and thus may improve the FER performance

Table 4.1. Two-step algorithm for two user STBC-OFDM Detection.

for $k = 0 : N-1$

for $i = 1, 2$

$\mathbf{M} = \tilde{\mathbf{H}}(k)\tilde{\mathbf{H}}^H(k) + \frac{1}{\tau}\mathbf{I}_{2m_r}$

$\mathbf{w}_{2i-1} = \mathbf{M}^{-1}\tilde{\mathbf{h}}_{2i-1}$

$\mathbf{w}_{2i} = \mathbf{M}^{-1}\tilde{\mathbf{h}}_{2i}$

$$\hat{\mathbf{x}}^{(i)}(k) = \arg \min_{\left[x_{c1}^{(i)}\ x_{c2}^{(i)}\right] \in \mathbf{X}} \left\{ \left| \mathbf{w}_{2i-1}^H \tilde{\mathbf{r}}(k) - x_{c1}^{(i)}(k) \right|^2 + \left| \mathbf{w}_{2i}^H \tilde{\mathbf{r}}(k) - x_{c2}^{(i)}(k) \right|^2 \right\}$$

$$\triangle_{\hat{\mathbf{x}}^{(i)}(k)} = \left| \mathbf{w}_{2i-1}^H \tilde{\mathbf{r}}(k) - \hat{x}_1^{(i)}(k) \right|^2 + \left| \mathbf{w}_{2i}^H \tilde{\mathbf{r}}(k) - \hat{x}_2^{(i)}(k) \right|^2$$

$\mathbf{a}_1(k) = \mathbf{r}_1(k) - \breve{\mathbf{H}}_1^i(k)\hat{\mathbf{x}}^{(i)}(k)$

$\mathbf{a}_2(k) = \mathbf{r}_2(k) - \breve{\mathbf{H}}_2^i(k)\hat{\mathbf{x}}^{(i)}(k)$

.....

$\mathbf{a}_{m_r}(k) = \mathbf{r}_{m_r}(k) - \breve{\mathbf{H}}_{m_r}^i(k)\hat{\mathbf{x}}^{(i)}(k)$

$j \in \{1, 2\}$ and $j \neq i$

$$\hat{\hat{\mathbf{x}}}^{(j)}(k) = \arg \min_{\mathbf{x}_c^{(j)} \in \mathbf{X}} \sum_{n=1}^{m_r} \left\{ \left\| \mathbf{a}_n(k) - \breve{\mathbf{H}}_n^j(k)\mathbf{x}_c^{(j)}(k) \right\|^2 \right\}$$

$$\triangle_{\hat{\hat{\mathbf{x}}}^{(j)}(k)} = \sum_{n=1}^{m_r} \left\{ \left\| \mathbf{a}_n(k) - \breve{\mathbf{H}}_n^j(k)\hat{\hat{\mathbf{x}}}^{(j)}(k) \right\|^2 \right\}$$

$\triangle_i = \triangle_{\hat{\mathbf{x}}^{(i)}(k)} + \triangle_{\hat{\hat{\mathbf{x}}}^{(j)}(k)}$

end

if $\triangle_1 < \triangle_2$

choose $\left[\hat{\mathbf{x}}^{(1)}(k), \hat{\hat{\mathbf{x}}}^{(2)}(k)\right]$

else

choose $\left[\hat{\hat{\mathbf{x}}}^{(1)}(k), \hat{\mathbf{x}}^{(2)}(k)\right]$

end

end

and be a benefit for estimation in the next iteration. Moreover, because the proposed two-step scheme performs exactly the same interference

cancellation and re-estimating algorithm compared with a conventional MMSE PIC scheme, it has identical order of complexity to the conventional MMSE PIC, therefore it does not increase computational cost.

4.3.4 Algorithm Complexity Discussion

Following the discussion in section 4.3.2, the proposed algorithm is only based on linear MMSE and simple symbol-wise likelihood detection. Therefore, the symbols can be estimated with similar computational complexity compared with the conventional MMSE-PIC multiuser detector [127], [128]. As shown in Eq.(4.3.8) and Eq.(4.3.9), assuming the proposed STBC provides Dth order of diversity for each user terminal (the STBC in this work provides $D = 2$), then the dimensions of matrix $\tilde{\mathbf{H}}$ are $Dm_r \times DK$. Let $N_r = Dm_r$ denote the length of the receive vector $\tilde{\mathbf{r}}$ in Eq.(4.3.9), hence, to find the equalizer coefficient weight vector $\mathbf{w}$ for each linear MMSE cancellation, the algorithm requires the inversion of $[\tilde{\mathbf{H}}.\tilde{\mathbf{H}}^H + \frac{1}{\tau}\mathbf{I}_{N_r}]$ that needs $\mathcal{O}(N_r^3)$ multiplication operations. Hence, for MMSE weight vectors, it requires on the order of $\mathcal{O}(N_r^3 + DN_r)$ multiplication complexity for each estimation pair of the D-elements for each user $[x_1^{(i)}, \ldots, x_D^{(i)}]$. Although symbol-wise estimation based on maximum likelihood detection requires a search for the optimum result for all possible result pairs within the symbol constellation, however, based on the processing in Eq.(4.3.17) it only requires on the order of $\mathcal{O}(N_r + 1)$ real multiplication operations and does not need more multiplications for calculation of the reliability values in Eq.(4.3.18). For the second step PIC processing from Eq.(4.3.19) to Eq.(4.3.25), MAI cancellation only requires $\mathcal{O}(N_r)$ calculations, and re-estimations require the order of $\mathcal{O}((N_r + 1)M)$ real multiplications

to find the re-estimation pairs for each user and no more for reliability calculation, both of which are lower order than the MMSE. M denotes the discrete source constellation size. This processing must be performed N times to estimate each signal block of $N_b = 2N$ length for the K users. Hence, the highest order of complexity in processing for the two-step PIC algorithm is on the order $\mathcal{O}(KN(N_r^3))$ operations to detect each block of signal for K users, the complexity order of which is identical to the L-MMSE algorithm. The simulation results in section 4.3.5 show that the performance of the proposed scheme will be significantly greater than the L-MMSE algorithm. Therefore, the two-step interference cancellation receiver brings considerable performance gain while maintaining decoding simplicity and without increasing the complexity of the receiver considerably compared to classical MMSE receivers.

4.3.5 Numerical Results and Discussions

In order to illustrate the performance of the proposed two-step receiver structure in principle, simulations were run simply based on a two user STBC MIMO-OFDM system case equipped with two transmit antennas for each user and two receive antennas. Each user data stream contains 256 symbols, which are coded into two data blocks by space time encoding. It assumed symbol transmission rate of 1MHz. For the tones orthogonal to each other, the assumed baseband is divided into 128 sub-carriers by IFFT operation on each time slot with $128\mu s$ duration. The QPSK signal modulation is employed at the transmitting stage. Moreover, an additional 22 cyclic prefix symbols are used as a guard interval after each data block. Therefore, in this case, there

contains $512\mu s$ information duration and $88\mu s$ additional cyclic prefix in one transmitting signal frame in total and $150\mu s$ for each OFDM duration. The data transmission is implemented simply over a MIMO frequency selective channel with slow time variant fading, generated by the typical Jakes fading model (see in [76]) and 3-delay taps have been introduced into each sub-channel, i.e. frequency-selective sub-channel tap length $L = 3$ and $\sum_{l=1}^{L} \sigma_l^2 = 1$, where σ_l^2 is the variance of the lth path. The channel fading is also simplified with the assumption of uncorrelation among different transmitting antennas of different users. Moreover, perfect knowledge of the channel state at the receiver is assumed at any time.

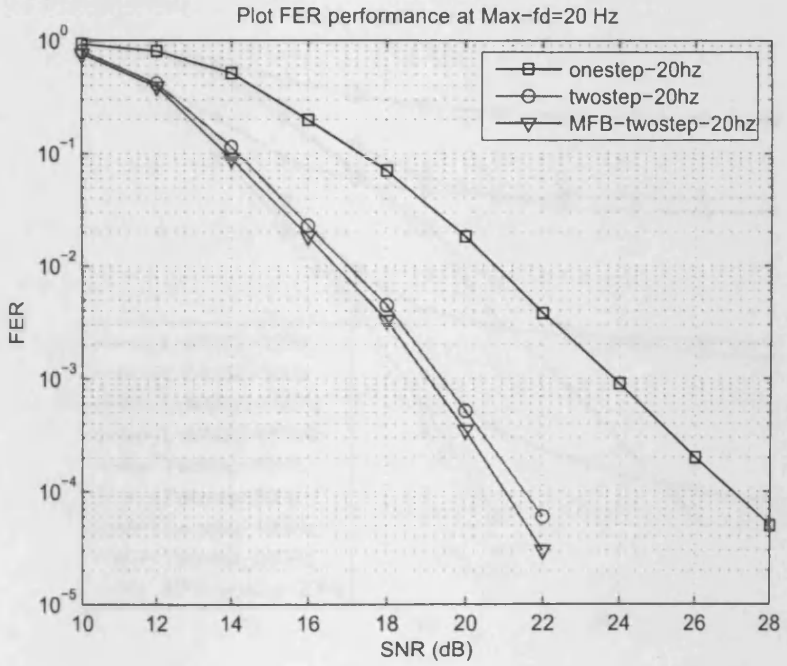

Figure 4.4. The FER vs. SNR performance comparison for two user STBC-OFDM system: implements between typical MMSE and two-step processing over slow fading $(4, 2)$ 3-tap MIMO-ISI channels when maximum Doppler frequency $f_d = 20Hz$, i.e. normalized DS=0.003.

Figure 4.4 shows the frame error rate (FER) performance comparison for two user STBC-OFDM system multiuser detection. The simulations are implemented between L-MMSE interference suppression and PIC cancellation over slow fading channels of 20Hz maximum Doppler frequency, i.e. normalized DS=0.003, this small value avoid an error floor and SNR is used in the simulation for consistency but E_b/N_0 would simply be a 3dB shift for QPSK. As a benchmark, we also evaluate performance of the matched filter for two-step processing, assuming *perfect knowledge of the interfering symbols* [108] at maximum Doppler frequency of 20Hz. The two-step interference cancellation scheme performs very close to the match filter bound (MFB) i.e. MAI-free bound,

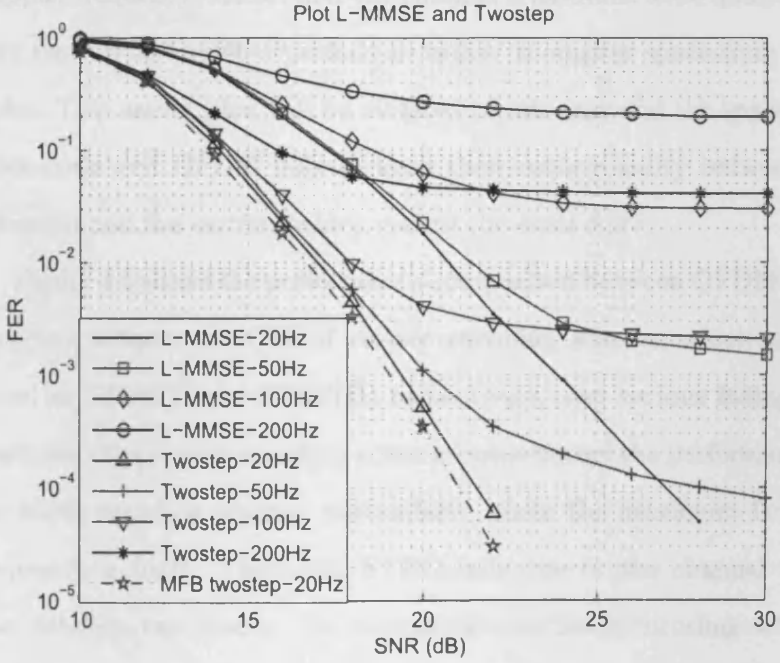

Figure 4.5. The FER vs. SNR performance comparison for two user STBC-OFDM system: implements between typical MMSE and two-step processing over various fading rates (maximum Doppler frequencies f_d are 20Hz, 50Hz, 100Hz and 200Hz respectively).

as a result, the channel variation has not influenced the receiver very much at slow fading rate and the MAI have been cancelled effectively.

Figure 4.5 shows the comparison of system performance between L-MMSE interference cancellation and two-step processing when the system is tested with various fading rate channel environments. The best performance is given at the channel of 20Hz maximum Doppler frequency. In this work, the typical STBC scheme as in [33] is exploited in order to attain double spatial diversity compared with normal MIMO transmission. Hence, by explanation in [33], [77] and [132], this two-step scheme could achieve a diversity order of $2\times(m_r-K+1)$. Otherwise, the performance degrades at higher SNR values with increasing maximum Doppler frequency. Recall that the channel is assumed to be quasi-static over two OFDM symbol periods in order to employ space-time block codes. This assumption will be violated in this case and the space-time block code and OFDM fails to keep their orthogonality between the antennas and the carriers which causes the error floor.

Figure 4.6 shows the performance comparison between OFDM block encoding scheme and OFDM carrier encoding scheme, which are denoted as STBC(I) and STBC(II) respectively, over various fading rate channels. The carrier encoding scheme outperforms the performance of the block encoding scheme, particularly, when the maximum Doppler frequency is high. The block STBC fails due to the channel variation between two blocks. In contrast to the block encoding scheme, the OFDM carrier encoding scheme is essentially not affected by the channel variation between two blocks, but only affected by time variant interference between adjacent subcarriers. However, for the OFDM symbols to be orthogonal, the channel should remain constant within

an OFDM block, which is the reason for the error-floor still occurring in varying channels.

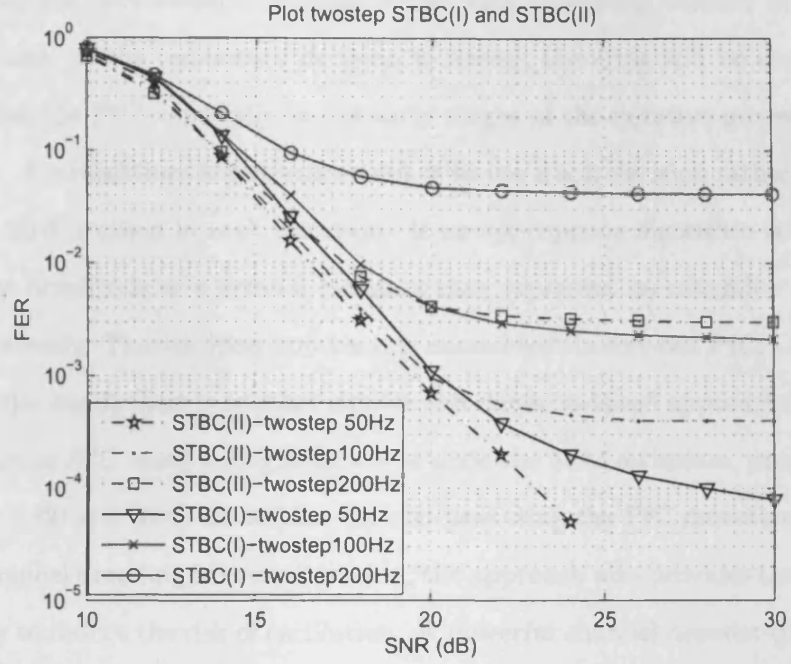

Figure 4.6. The FER vs. SNR performance comparison for two user STBC-OFDM system: implements two-step scheme between OFDM block encoding scheme and OFDM carrier encoding scheme, over various fading rates (maximum Doppler frequencies f_d are 50Hz, 100Hz and 200Hz respectively).

In this work, the design of a two-step interference cancellation receiver has been addressed to cancel multiple access interference (MAI) in a multiuser MIMO wideband wireless communication system within a slow fading channel environment. The simulation results indicate that the proposed scheme could obtain substantial performance improvement without increasing the complexity compared with the L-MMSE scheme. MAI can be suppressed and cancelled effectively. However, the performance of the scheme still suffers significant degradation from the

effect of time variant MIMO-ISI channels. Due to error detection, the PIC based on hard decisions could induce the risk of oscillation such that the performance becomes worse with increasing number of iterations. If the temporary decision is wrong, the error will be doubled after the PIC, especially in the early stages of the iterative processing.

A straightforward enhancement is to use a soft decision rather than a hard decision in each iteration. If an appropriate algorithm is used, the amplitude of a symbol estimate may represent its reliability more correctly. The resulting approach is named soft-in soft-out PIC. On the other hand, there is another similar soft decision-based approach called *partial PIC* using a weight factor to scale the MAI estimates, proposed in [133] and [134]. Otherwise, by concatenating the PIC detection with channel decoding in every iteration, the approach also provides the ability to reduce the risk of oscillation. A powerful channel decoder (for example, convolutional coding technique) can substantially improve the temporary data estimates and achieve more accurate interference reconstruction and subtraction. In addition to the multiple transmit and receive antenna diversities, the frequency selective diversity of order L can also be gained by the proposed receiver. Both of these improving work will be performed in the next section and have been presented in [122]. Another approach to the oscillation problem encourages us to try to improve the performance in the first stage of detection for the beginning iteration. The iterative MMSE or decision feedback detector are both considered to serve as the first stage as presented in [135], which will be introduced in the following chapters.

4.4 A Joint Coded PIC MUD for STBC-OFDM Systems

As discussed in the past sections, reliable communication in multiuser systems is affected by the presence of both MAI and ISI in multi-path channels. In this section, a novel transceiver design is investigated for a wideband multiuser-MIMO communication system. In particular, a PIC scheme is proposed with an error correction coding technique for the receiver of a synchronous multiuser uplink system. The scheme employs OFDM and STBC at the transmitter and the receiver performs as a soft output multiuser detector based on minimum mean-squared error (MMSE) interference suppression at the first stage, and then, MAI cancellation is implemented with a bank of single-user channel decoders.

The outline of this section is organized as follows. In Section 4.4.1, the problem statement for the PIC scheme is discussed for multiuser detections. Then the signal processing of the system model for a joint coded multiuser STBC-OFDM systems is given in Section 4.4.2. The proposed joint multiuser PIC and detection scheme is described in Section 4.4.3. Finally, simulation results are provided and discussed in Section 4.4.4.

4.4.1 Problem Statement for Parallel Interference Cancellation

As discussed in Section 4.2, it is known that PIC detection can improve the performance of MUD continuously with increasing number of iterations. However, sometimes the PIC receiver gives a worse result in the current iteration than in the previous one due to error propagation, which can result in failure of convergence. In a PIC receiver, the temporary decisions of the users' data detected in the current iteration

are used to reconstruct the MAI that is subtracted from the received signal in the next iteration. Hence, it is known that PIC detection provides ability to perform well for MUD, however there are still potential problems located in this algorithm. When some of the decisions for the users' data are not correct, the problem occurs. A wrong decision of a bit will result in a wrong interference reconstruction. And when a wrong value of interference is subtracted from the multiuser signal, MAI can potentially be strengthened, instead of cancelled, which is the so-called doubled error in Section 4.2 and therefore makes error propagated to the corresponding bits of other users' signals. If this is a serious error, it is possible to lead the decision of the data into the wrong direction in the next iteration. Although the two-step PIC scheme which is proposed in Section 4.4 can cancel MAI and detect multiuser signals effectively, however, the performance at the first stage still suffer from the effect of MIMO-ISI channels, which could possibly induce error propagation for future improvement by iterative processing. Here, there are two measures that can be taken to solve this problem:

(1) Employ soft PIC detection instead of hard detection. This can be implemented using two approaches: (i) the temporary estimates can be provided by a soft-in-soft-out (SISO) detection and the reliability values can be calculated based on these soft outputs [136], or in the decoding process outputs which represent the data as well as their reliability can be used such as the LLRs in the maximum a posteriori (MAP) algorithm as shown in [135]. Then the soft outputs, rather than the hard decisions, can be fed to the PIC detector directly. Thus the interference generated can be subtracted from the reliable bits and restrict the influence of the unreliable ones. (ii) The other SISO PIC

approach is partial PIC. It uses a weight factor to scale the MAI estimates obtained from past hard decisions before subtracting them from the received signal, thus reducing the sensitivity to errors in the estimated MAI [133], [134]. In this section, the former approach is adopted, so that the performance of the scheme can be further improved by joint soft error correction techniques.

(2) Try to improve the quality of the data estimates before they are used to reconstruct the interference. In this scheme, forward-error-correction (FEC) decoders are involved in each iteration, such as convolutional or Turbo decoders.

In this section, the wideband parallel interference suppression and cancellation scheme proposed in [121] is extended for quality improvement. Soft PIC detection instead of hard detection is employed which incorporates error correction coding for multiuser STBC OFDM systems. This work was also represented in [122].

4.4.2 Joint System Model for Synchronous Uplink

A K-user space-time block coded OFDM wireless communication system is considered, where each user terminal is equipped with $n_t = 2$ transmit antennas. First, the incoming data stream is encoded by a half rate convolutional encoder, and the code bit will be interleaved and mapped as QPSK. Then, a space-time block encoding processing is implemented on the signal and the OFDM modulator is applied to the outputs of the space time encoder. The outputs of the OFDM modulators are transmitted using multiple antennas simultaneously.

Here, space-time block codes are combined with OFDM modulation. In this scheme, the temporal index in each block corresponds to the tone

index of OFDM. This requires that the channel remains constant over a number, two in this work, of consecutive blocks equal to the number of transmit antennas n_t (see in [116]). The ith user's input, $i = 1, \ldots, K$, is two consecutive blocks, denoted as $\mathbf{s}_1^{(i)}$ and $\mathbf{s}_2^{(i)}$. Each block is then channel encoded, interleaved and symbol mapped to form the two OFDM blocks of length N, denoted as $\mathbf{x}_1^{(i)} = [x_1^{(i)}(0), \cdots, x_1^{(i)}(N-1)]^T$ and $\mathbf{x}_2^{(i)} = [x_2^{(i)}(0), \cdots, x_2^{(i)}(N-1)]^T$ in the frequency domain. The transmission is described in terms of the frequency domain, as the method is extended from [116] and [117], and because the transmission is considered over frequency-selective fading channels; hence, the equivalent frequency channel response is represented in a diagonal matrix form as $diag[H_{qj}^i(0), H_{qj}^i(1), \ldots, H_{qj}^i(N-1)]$ (see in [117] and [108]). Here, $H_{1j}^i(k)$ and $H_{2j}^i(k)$ denote the channel frequency responses of the kth tone, related to the channel from the $1st$ and $2nd$ transmit antennas and corresponding to the ith user and the jth receive antennas, respectively, over two contiguous signal block intervals. Due to employing a space-time block encoding scheme, the kth tone receive symbol is in the frequency domain over the two sequential OFDM time-slots 1 and 2, respectively,

$$r_{1j}(k) = \sum_{i=1}^{K} \{H_{1j}^i(k) x_1^{(i)}(k) + H_{2j}^i(k) x_2^{(i)}(k)\} + v_{f1j}(k) \qquad (4.4.1)$$

$$r_{2j}(k) = \sum_{i=1}^{K} \{H_{2j}^i(k) x_1^{(i)^*}(k) - H_{1j}^i(k) x_2^{(i)^*}(k)\} + v_{f2j}(k) \qquad (4.4.2)$$

where $k = 0, 1, \ldots, N-1$ and $[v_{f1j}(k)\ v_{f2j}(k)]$ denote the frequency domain representation of the receiver AWGN at the kth tone. Next define $\mathbf{r}_j(k) = [r_{1j}(k)\ r_{2j}^*(k)]^T$, $\mathbf{x}^{(i)}(k) = [x_1^{(i)}(k)\ x_2^{(i)}(k)]^T$, $\mathbf{v}_{fj}(k) = [v_{f1j}(k)$

$v^*_{f2j}(k)]^T$ and $\breve{\mathbf{H}}^i_j = \begin{bmatrix} H^i_{1j}(k) & H^i_{2j}(k) \\ H^i_{2j}{}^*(k) & -H^i_{1j}{}^*(k) \end{bmatrix}$, where $\breve{\mathbf{H}}^i_j$ is the equivalent channel response matrix of the kth tone between the ith user terminal and the jth receive antenna. The kth tone receive signals from all receive antennas during two consecutive OFDM periods can be represented in matrix form as follows:

$$\begin{bmatrix} \mathbf{r}_1(k) \\ \mathbf{r}_2(k) \\ \vdots \\ \mathbf{r}_{m_r}(k) \end{bmatrix} = \begin{bmatrix} \breve{\mathbf{H}}^1_1(k) & \cdots & \breve{\mathbf{H}}^K_1(k) \\ \breve{\mathbf{H}}^1_2(k) & \cdots & \breve{\mathbf{H}}^K_2(k) \\ \vdots & \ddots & \vdots \\ \breve{\mathbf{H}}^1_{m_r}(k) & \cdots & \breve{\mathbf{H}}^K_{m_r}(k) \end{bmatrix} \begin{bmatrix} \mathbf{x}^{(1)}(k) \\ \mathbf{x}^{(2)}(k) \\ \vdots \\ \mathbf{x}^{(K)}(k) \end{bmatrix} + \begin{bmatrix} \mathbf{v}_{f1}(k) \\ \mathbf{v}_{f2}(k) \\ \vdots \\ \mathbf{v}_{fm_r}(k) \end{bmatrix} \tag{4.4.3}$$

Re-writing the received signal for simplicity of notation as follows:

$$\tilde{\mathbf{r}}(k) = \tilde{\mathbf{H}}(k)\tilde{\mathbf{x}}(k) + \mathbf{v}_f(k) \tag{4.4.4}$$

where $\tilde{\mathbf{r}}(k)$ is the overall receive signal vector at all receive antennas with $2m_r$ elements, $\tilde{\mathbf{H}}(k)$ is the equivalent overall channel response matrix of size $2m_r \times 2K$, $\tilde{\mathbf{x}}(k)$ is the transmitting signal vector with $2K$ elements including all users at the kth tone, and $\mathbf{v}_f(k)$ is the equivalent complex noise vector of size $2m_r \times 1$ which influences the overall channels.

4.4.3 Joint Coded Two-step Parallel Interference Cancellation

The two-step generalized MMSE interference receiver in [121] and [77] is extended to the proposed joint multiuser STBC-OFDM scheme. For simplicity, without loss of generality, the two-user scenario is considered. The receiver structure is illustrated in Figure 4.7.

In this receiver structure, the OFDM-demodulated received signal will be passed through the following five parts of processing:

(1)Perform soft signal value estimation based on a combined soft output MMSE and multiuser detector.

(2) Exploit soft-input-soft-output (SISO) Viterbi decoding to correct errors and evaluate reliability values for the first stage.

(3) Exploit parallel multiple-access interference cancellation and symbol re-estimation using the modified interference-free received signal.

(4) Compare result pairs and make decision for estimation output based on the reliability comparison.

(5) Perform channel decoding to obtain the final signal estimate.

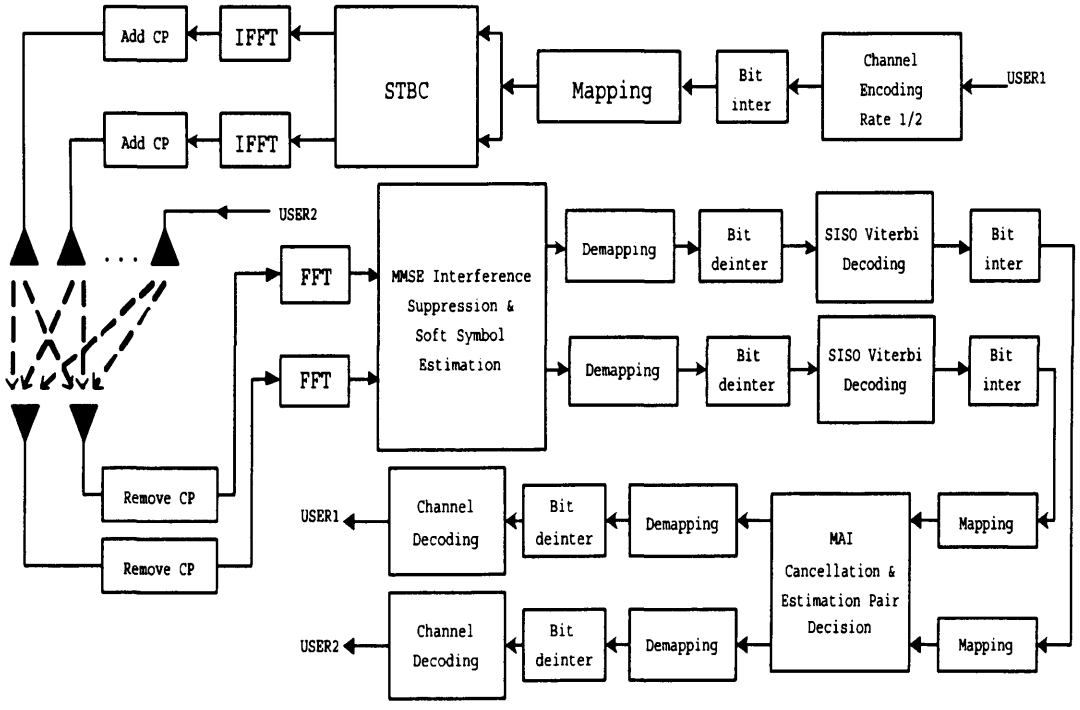

Figure 4.7. Proposed two user joint STBC MIMO-OFDM wireless transmission system equipped with $n_t = 2$ transmit antennas for each user terminal and $m_r = 2$ receive antennas.

Stage 1: Linear MMSE Interference Suppression and Viterbi Decoding

In the first stage, MMSE interference cancellation and error correction by soft input soft output (SISO) Viterbi decoding are to estimate the transmitted symbols. Consider the ith user terminal, where $i = 1, 2$, and define the following mean squared error cost function which includes co-channel interference and noise in the symbol $\hat{x}^{(i)}(k)$, where $\hat{x}^{(i)}(k) = \mathbf{w}^H \tilde{\mathbf{r}}(k)$ is the estimation of the symbol $x^{(i)}(k)$:

$$J(\mathbf{w}) = E\left\{\left|x^{(i)}(k) - \mathbf{w}^H \tilde{\mathbf{r}}(k)\right|^2\right\} \tag{4.4.5}$$

where $E\{\cdot\}$ and $|\cdot|^2$ denote the statistical expectation operator and absolute value, respectively. To minimize the mean squared error, the weight vector $\mathbf{w}$ of size $2m_r$ is chosen based on standard minimization:

$$\frac{\partial J(\mathbf{w})}{\partial \mathbf{w}} = \mathbf{0} \tag{4.4.6}$$

Hence, the weight vectors $\mathbf{w}_{2i-1} = [w_{2i-1,1}, w_{2i-1,2}, \ldots, w_{2i-1,2m_r}]^T$ and $\mathbf{w}_{2i} = [w_{2i,1}, w_{2i,2}, \ldots, w_{2i,2m_r}]^T$, corresponding to the ith user, can be computed respectively, as

$$\mathbf{w}_{2i-1} = \mathbf{M}^{-1} \tilde{\mathbf{h}}_{2i-1} \tag{4.4.7}$$

$$\mathbf{w}_{2i} = \mathbf{M}^{-1} \tilde{\mathbf{h}}_{2i} \tag{4.4.8}$$

where $\mathbf{M} = \tilde{\mathbf{H}}(k)\tilde{\mathbf{H}}^H(k) + \frac{1}{\tau}\mathbf{I}_{2m_r}$ and $\tau = E_s/N_0$ is the signal to noise ratio, $\tilde{\mathbf{h}}_{2i-1}$ and $\tilde{\mathbf{h}}_{2i}$ are the $(2i-1)$th and $(2i)$th columns of $\tilde{\mathbf{H}}(k)$, respectively. Hence, the soft estimation symbols are obtained and written

as

$$\lambda_1^{(i)}(k) = \mathbf{w}_{2i-1}^H \tilde{\mathbf{r}}(k) \tag{4.4.9}$$

and

$$\lambda_2^{(i)}(k) = \mathbf{w}_{2i}^H \tilde{\mathbf{r}}(k) \tag{4.4.10}$$

The $\lambda_1^{(i)}(k)$ and $\lambda_2^{(i)}(k)$ values are passed through the SISO Viterbi decoder for advanced error correction, and then the scalar soft decision symbols $\hat{x}_1^{(i)}(k)$ and $\hat{x}_2^{(i)}(k)$ are obtained, on which independent decisions can be formed.

Finally, one form of error correction reliability value which is based entirely on soft quantities for the whole first step estimation of the ith user's symbol can be represented as

$$\triangle_{\hat{\mathbf{x}}^{(i)}(k)} = \left|\lambda_1^{(i)}(k) - \hat{x}_1^{(i)}(k)\right|^2 + \left|\lambda_2^{(i)}(k) - \hat{x}_2^{(i)}(k)\right|^2 \tag{4.4.11}$$

and this technique is applied in the simulation. Another form would be

$$\triangle_{\hat{x}_1^{(i)}(k)} = \left|\lambda_1^{(i)}(k) - x_{c1}^{(i)}(k)\right|^2 + \left|\hat{x}_{1SISO}^{(i)}(k) - x_{c2}^{(i)}(k)\right|^2 \tag{4.4.12}$$

$$\triangle_{\hat{x}_2^{(i)}(k)} = \left|\lambda_2^{(i)}(k) - x_{c1}^{(i)}(k)\right|^2 + \left|\hat{x}_{2SISO}^{(i)}(k) - x_{c2}^{(i)}(k)\right|^2 \tag{4.4.13}$$

$$\triangle_{\hat{\mathbf{x}}^{(i)}(k)} = \triangle_{\hat{x}_1^{(i)}(k)} + \triangle_{\hat{x}_2^{(i)}(k)} \tag{4.4.14}$$

which would require the calculation of hard decisions $x_{c1}^{(i)}(k)$ and $x_{c2}^{(i)}(k)$, and this could be considered for future work.

Stage 2: Two-Step Approach for MAI Cancellation and Symbol Re-Estimation

In stage 1, a linear MMSE scheme and symbol error correction by SISO Viterbi decoding is used to suppress the interferences from the

co-channel users in estimating the transmitted information symbols. In the second stage, the transmitted symbols are re-estimated based on a modified received signal obtained by cancelling the multiple access interferences. Note that a perfect interference cancellation may be achieved only if the signals from the first step have been decoded correctly. In the case of two users, in order to estimate the second user symbols, the receiver cancels the multiple access interference (MAI) caused by the first user from the received signals $\mathbf{r}_1(k), \mathbf{r}_2(k), \ldots, \mathbf{r}_{m_r}(k)$ to estimate the transmitted symbols. For the kth tone, the modified received signal from the nth receive antenna after cancelling the MAI from the first user will be represented as

$$\mathbf{a}_n(k) = \mathbf{r}_n(k) - \breve{\mathbf{H}}_n^1(k)\hat{\mathbf{x}}^{(1)}(k) \tag{4.4.15}$$

where $n = 1, \ldots, m_r$, hence the second user's kth signals are re-estimated using the above modified received vector:

$$\hat{\hat{\mathbf{x}}}^{(2)}(k) = \arg \min_{\mathbf{x}_c^{(2)} \in \mathbf{X}} \sum_{n=1}^{m_r} \left\{ \left\| \mathbf{a}_n(k) - \breve{\mathbf{H}}_n^2(k)\mathbf{x}_c^{(2)}(k) \right\|^2 \right\} \tag{4.4.16}$$

where $\mathbf{X}$ includes all possible choices of QPSK symbols. The reliability function for the estimation from this second step of user 2 will be given by

$$\triangle_{\hat{\hat{\mathbf{x}}}^{(2)}(k)} = \sum_{n=1}^{m_r} \left\{ \left\| \mathbf{a}_n(k) - \breve{\mathbf{H}}_n^2(k)\hat{\hat{\mathbf{x}}}^{(2)}(k) \right\|^2 \right\} \tag{4.4.17}$$

Finally, the total reliability of the first and second step estimation will be the summation of the reliability of the first user at the first step and the reliability of the second user at the second step, which is given by the overall reliability for $\hat{\mathbf{x}}^{(1)}(k)$ and $\hat{\hat{\mathbf{x}}}^{(2)}(k)$ as

$$\triangle_a = \triangle_{\hat{\mathbf{x}}^{(1)}(k)} + \triangle_{\hat{\tilde{\mathbf{x}}}^{(2)}(k)} \tag{4.4.18}$$

This procedure will be repeated in parallel assuming a correct decision for the second user at the first step and based upon its estimate, the user 1 signals will be re-estimated by repeating the MAI interference cancellation and symbol-wise likelihood re-estimation algorithm, assuming that the estimation of the second user transmitted signal at the kth tone $\hat{\mathbf{x}}^{(2)}(k) = [\hat{x}_1^{(2)}(k), \hat{x}_2^{(2)}(k)]^T$ has been decoded correctly at the first step. In a similar fashion, the reliability function is defined as

$$\triangle_b = \triangle_{\hat{\mathbf{x}}^{(2)}(k)} + \triangle_{\hat{\tilde{\mathbf{x}}}^{(1)}(k)} \tag{4.4.19}$$

where $\triangle_b$ denotes the overall reliability for $\hat{\mathbf{x}}^{(2)}(k)$ and $\hat{\tilde{\mathbf{x}}}^{(1)}(k)$.

Then, the symbol pairs based on the best overall reliabilities obtained between Δ_a and Δ_b will be the focus. When $\triangle_a < \triangle_b$, the pair $[\hat{\mathbf{x}}^{(1)}(k), \hat{\tilde{\mathbf{x}}}^{(2)}(k)]$ will be chosen as the estimates, otherwise, it will be $[\hat{\tilde{\mathbf{x}}}^{(1)}(k), \hat{\mathbf{x}}^{(2)}(k)]$.

Finally, the decision result will be modified by de-mapping, and deinterleaving, and then passed to the channel decoder to obtain the final estimations of input signal $\hat{s}_1^{(i)}$ and $\hat{s}_2^{(i)}$.

4.4.4 Numerical Results and Discussions

In order to illustrate the basic concept of the proposed coded two-step receiver structure, the simulations are simply based on a two user space-time block coded MIMO OFDM system case equipped with two transmit antennas for each user and two receive antennas. Each user data stream contains 256 symbols, for which a standard rate 1/2 and

constraint length 3 convolutional code is used [54]. In order to correct the subcarriers in deep fades, forward error correction and bit interleaving are used across the subcarriers. The QPSK signal mapping is employed at the transmitting stage with symbol transmission rate of 1MHz. For the tones orthogonal to each other, the assumed baseband is divided by the IFFT operation over each OFDM time slot after space-time block encoding. Moreover, an additional 20 cyclic prefix symbols are used as a guard interval after each data block. The data transmission is implemented simply over MIMO frequency selective channels with both quasi-static fading and slow time variant fading, generated by the typical Jakes fading model [76] and 3-delay taps have been introduced into each sub-channel, i.e. a frequency-selective sub-channel tap length $L = 3$ and $\sum_{l=1}^{L} \sigma_l^2 = 1$, where σ_l^2 is the variance of the lth path. The channel fading is also simplified with an assumption of no correlation between different transmitting antennas of different users. Perfect knowledge of the channel state at the receiver is assumed. In order to keep equal signal power under the effect of channel coding, the complex white Gaussian noise was compensated by scaling by the convolutional coding rate for normalization and the soft input Viterbi decoding scheme is used in this simulation.

Figure 4.8 shows the FER performance comparison of system between the joint coded PIC scheme and normal two-step processing, both of which includes L-MMSE interference cancellation. The system is tested in quasi-static channel environments. The best performance is given by the coded two-step interference cancellation scheme. The coded two-step interference cancellation scheme over the range of SNR in the figure shows higher gradient of the frame error rate curve better

than the other scheme, as a result, the ISI and MAI have been cancelled effectively by the two-step processing and coding correction. In this simulation, the typical STBC scheme as in [33] is used in order to attain more spatial diversity compared with normal MIMO transmission. Hence, following the explanations in [33], [77] and [132], this coded two-

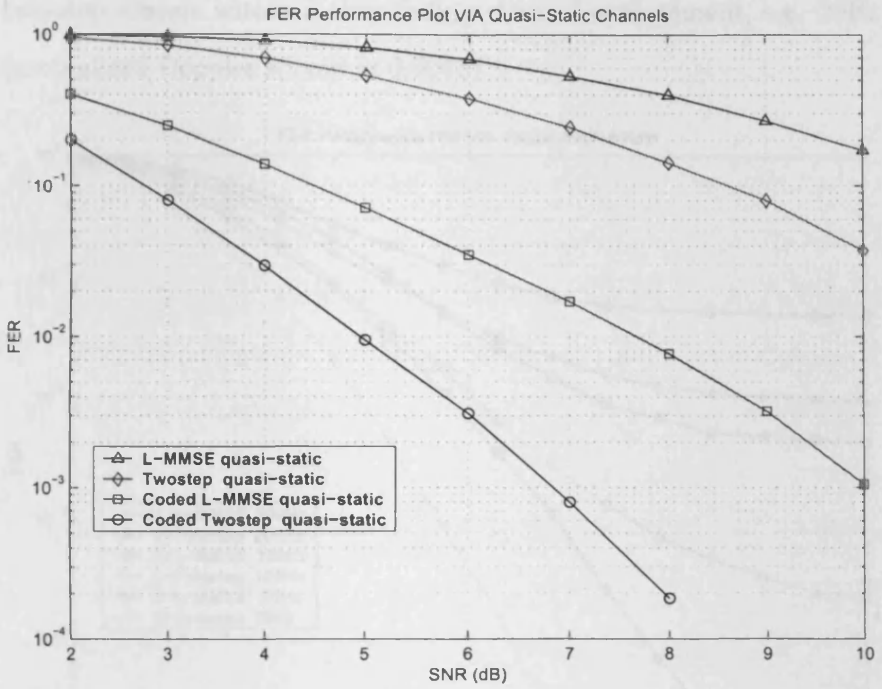

Figure 4.8. The FER vs. SNR performance comparison for two user STBC-OFDM system: implements joint PIC scheme over quasi-static MIMO-ISI channels where channel tap length $L = 3$.

step scheme could almost achieve a diversity order of $2 \times (m_r - K + 1)$. In addition to the multiple transmit and receive antenna diversities, the frequency selective diversity of order L can also be gained by the effect of coding correction.

Secondly, the performance is seen to degrade at higher SNR values with increasing maximum Doppler frequency which is shown in Fig.4.9. Recall that the channel is assumed to be quasi-static over

two OFDM symbol periods in order to employ space-time block codes. This assumption will be violated in this case and the space-time block code and OFDM fails to keep their orthogonality between the antennas and the carriers which causes the error floor. However, the MAI and time variant interference are still suppressed effectively by the coding two-step scheme within a slow fading channel environment, e.g. 20Hz (normalized Doppler spread is 0.0055)

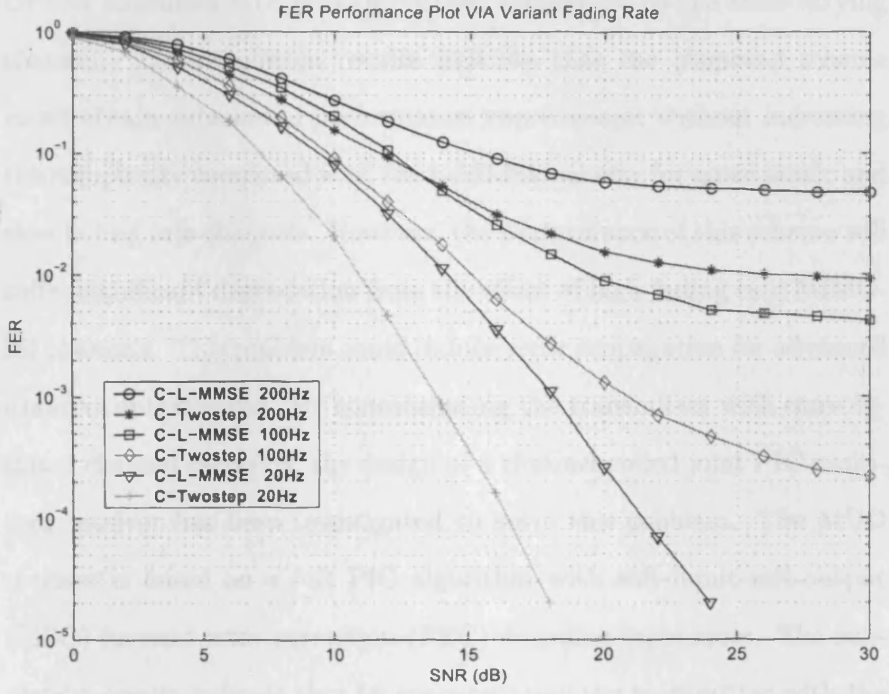

Figure 4.9. The FER vs. SNR performance comparison for two user STBC-OFDM system: implements joint PIC scheme over channels with different maximum Doppler frequency fading rates.

4.5 Conclusions

In this chapter, a novel and robust MUD technique called parallel interference cancellation is introduced for multiuser STBC-OFDM detec-

tions. Firstly, the design of a two-step interference cancellation receiver has been addressed to cancel MAI in a multiuser MIMO wideband wireless communication system within both quasi-static and variant fading channel environment. In this approach, the transmitter serially concatenates STBC with OFDM for each user terminal and the receiver is based on a two-step hard-interference cancellation algorithm. Otherwise, another approach would be to use space-frequency block codes and OFDM modulation to provide further robustness to the time-varying channel. The simulation results indicate that the proposed scheme could obtain substantial performance improvement without increasing the complexity compared with the L-MMSE scheme for quasi-static and slow fading rate channels. However, the performance of this scheme will suffer significant degradation from the effect of high fading rate MIMO-ISI channels. This problem could induce error propagation for advanced iterative optimization. By concatenating the transmitter with convolutional channel encoding, the design of a channel coded joint PIC multiuser receiver has been investigated to solve this problem. The MUD receiver is based on a soft PIC algorithm with soft-input-soft-output (SISO) forward error correction (FEC) decoding techniques. The simulation results indicate that by concatenating the transmitter with the half rate outer channel code, the proposed scheme obtained significant performance gain rather than the normal scheme, which obtains benefit for performing more iterations reliably for performance improvement. In addition to the multiple transmit and receive antenna diversities, the frequency selective diversity of order L can also be gained by the effect of coding correction rather than the normal two-step scheme.

Chapter 5

ITERATIVE MULTIUSER DETECTION FOR STBC MIMO-OFDM SYSTEMS

In recent years, iterative processing techniques with soft-input-soft-output components have received considerable attention. These iterative schemes have been also introduced in signal detection, as shown in Chapter 3. In this chapter, multiuser detection by iterative signal estimation scheme will be addressed. This scheme is performed iteratively based on the extrinsic feedback of information to obtain optimum performance.

The outline of this chapter is organized as follows. In Section 5.1, the concept of conventional iterative MUD and Turbo MUD is introduced. Then a proposed iterative MMSE MUD scheme for Multiuser STBC-OFDM systems is discussed in Section 5.2. This work was also proposed in [135]. Then this iterative MUD algorithm is extended to a type of turbo MUD by concatenating a SISO channel decoder, which is represented in Section 5.3 and [137]. Section 5.4 provides relative simulation results and analysis. Finally, conclusions are provided in Section 5.5.

5.1 Iterative Multiuser Detections

Normally, iterative MUD performs signal estimation in an iterative process by updating extrinsic information such as log-likelihood ratios (LLRs) as shown in Chapter 3. In conventional iterative multiuser receivers, the SISO MUD and the channel decoding are performed separately based on joint signal detection signal processing, depicted in Figure 5.1(a). Each user's data can be detected iteratively at the first stage in the SISO multiuser detector for optimum estimation and then passed into the channel decoder for error correction. Recently, following the development of powerful Turbo codes [138], the "Turbo Principle" [73], [74] has been extended to other aspects of the reception technique. It was found that the combination of two types of components (channel decoding and MUD elements) in the receiver brought a substantial performance gain. Thus the basic idea is to break up joint signal processing into separate components and iterate between them with the exchange of probabilities (or soft extrinsic information). This approach typically results in almost no loss of information.

Two types of forward-error-correction (FEC) codes are considered for Turbo MUD: convolutional codes and Turbo codes. Some researchers construct iterative receivers using a SISO multiuser detector and a convolutional decoder. As assumed, iterative reception is proposed following the principle of Turbo decoding. Hence the straightforward approach is to take advantage of the multiuser detector for the first stage decoder (Figure 5.1(b)) and then concatenating a convolutional decoder. In this receiver structure, continuous performance improvement with increasing number of iterations comes from the refreshed detection results. As is well known, the better the signal source provided

to the channel decoder, the more accurate the data gained, i.e. having improved the detection results with more accurate MUD, and fed them to the convolutional decoder, the decoder will yield better decoding results. And then the output of decoder can be fed back to multiuser detection to achieve better detection result for the next iteration. In this thesis, my work will focus on this type of iterative turbo MUD.

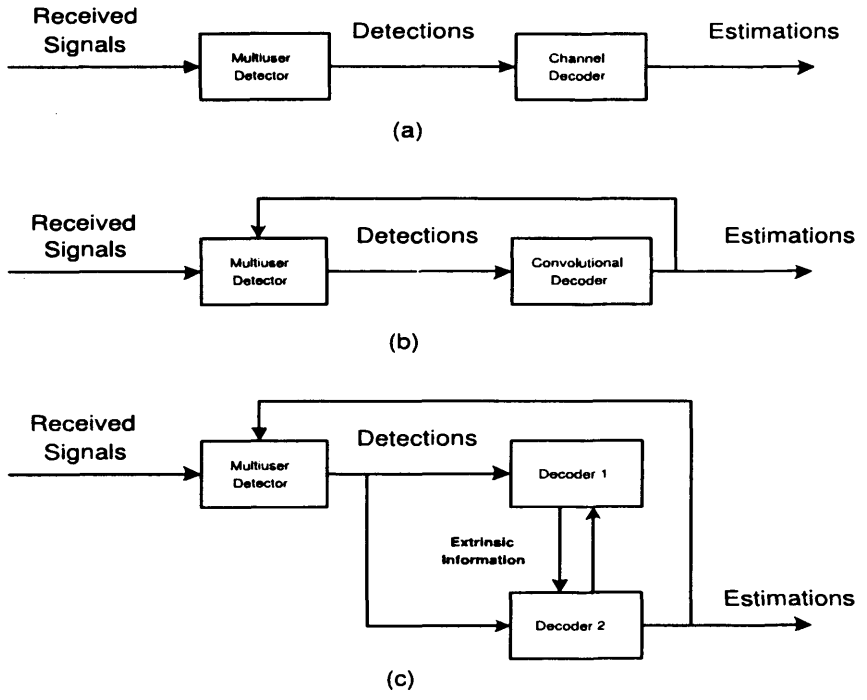

Figure 5.1. Multiuser detection (MUD) techniques: (a) Conventional MUD scheme; (b) Joint MUD and Convolutional Decoding; (c) Joint MUD and Turbo Decoding

On the other hand, some research on the Turbo receiver is based on Turbo codes. The internal iterative structure of the Turbo decoder (as shown in Figure 5.1(c)) is retained and its powerful correction scheme based on the exchange of extrinsic information. In this case, there are two factors to drive the convergence of the receiver: MUD and exchange

of extrinsic information. Hence, there are two types of iterations which are performed in the receiver: The outer iteration exchanges information between the multiuser detector and the Turbo decoder; the inner iteration exchanges extrinsic information between the two component decoders.

The cost of this improved performance is that the Turbo-coded receivers have higher complexity than the convolutional-coded ones. However, it is not caused by the use of the iterative structure, but due to the use of inner Turbo codes, i.e. the complexity increasing in iterative MUD of the first stage is introduced into both the convolutional-coded system and Turbo-coded system with iteration increase. Moreover, the convolutional decoding is repeated in each iteration (complexity $\mathcal{O}(2^{K\eta})$), where η is the code constraint length. Therefore, for the same outer iterations, the turbo decoding scheme brings a larger complexity with inner iteration increase, but obtains improvement of performance. In general, a larger number of iterations will further improve the data estimates, and then lead to more accurate interference reconstruction and cancellation. As a cost, this will increase the complexity of the receiver. It will be interesting to discuss the tradeoff between the complexity increase and the performance improvement relative to the use of complexity reduced multi-iteration decoding scheme.

5.2 Iterative MMSE MUD for Multiuser STBC OFDM Systems

In this section, an iterative multiuser detection structure for STBC MIMO-OFDM scheme is exploited over slow fading channels. The multiuser detection structure of STBC-OFDM system in [116] is extended with an iterative estimating method over slow fading chan-

nels. A MIMO OFDM system with two users is implemented in this work, which utilizes STBC (see [33] and [77]) and iterative MMSE [108] multiuser detection by updating extrinsic information to develop log-likelihood ratios (LLRs), whereas the proposed STBC MIMO-OFDM scheme exploits two transmit antennas for each user terminal for signal transmission which is similar as in Chapter 4. The multiuser receiver is equipped with two receive antennas to collect the propagation signal for interference suppression and cancellation, and then to estimate the signals. All channel knowledge is assumed known perfectly throughout, the work could be also seen in [135].

5.2.1 Synchronous System Models

Here, a multi-user MIMO OFDM uplink wireless communication system is exploited for k users as in Chapter 4. On the ith user, a serial to parallel convertor collects a set of N bit information symbols in the frequency domain $\mathbf{x}^{(i)} = [x^{(i)}(0), \cdots, x^{(i)}(N-1)]^T$ (which can be simply converted to QPSK) and explicit OFDM modulating operation is performed for each sub-channel. To avoid inter symbol interference (ISI), a sufficiently long cyclic prefix is added, i.e. the guard interval P should satisfy $P > L$, where L is the length of the impulse response of each transmit-receive antennas sub-channel. Hence, the N time domain received symbols in terms of vector form can be written as

$$\mathbf{r}_n = \mathbf{H}_c^{(i)}\mathbf{s}^{(i)} + \mathbf{v}^{(i)} = \mathbf{H}_c^{(i)}\mathbf{F}^H\mathbf{x}^{(i)} + \mathbf{v}^{(i)} \tag{5.2.1}$$

At each receive antenna, the samples corresponding to the cyclic prefix are first removed and then the FFT operation of the received signal from Eq.(5.2.1) is taken which yields

$$\mathbf{r} = \mathbf{F}\mathbf{r}_t = \mathbf{F}\mathbf{H}_c^{(i)}\mathbf{F}^H\mathbf{x}^{(i)} + \mathbf{F}\mathbf{v}^{(i)} = \mathbf{H}^{(i)}\mathbf{x}^{(i)} + \mathbf{v}_f^{(i)} \tag{5.2.2}$$

$$\mathbf{H}_c^{(i)} = \begin{bmatrix}
h_0^0 & 0 & \cdots & & 0 & & & h_0^{N_h-1} & h_0^{N_h-2} & \cdots & h_0^1 \\
h_1^1 & h_1^0 & 0 & \cdots & & 0 & & 0 & h_1^{N_h-1} & \cdots & h_1^2 \\
\vdots & & \ddots & & & \ddots & & & \ddots & & \vdots \\
h_{N_h-2}^{N_h-2} & \cdots & h_{N_h-2}^0 & 0 & \cdots & 0 & & \cdots & & 0 & h_{N_h-2}^{N_h-1} \\
h_{N_h-1}^{N_h-1} & h_{N_h-1}^{N_h-2} & \cdots & h_{N_h-1}^0 & 0 & \cdots & 0 & & \cdots & & 0 \\
0 & h_{N_h}^{N_h-1} & h_{N_h}^{N_h-2} & \cdots & h_{N_h}^0 & 0 & \cdots & 0 & & \cdots & 0 \\
\vdots & & \ddots & & & \ddots & & & \ddots & & \vdots \\
0 & \cdots & & \cdots & & 0 & h_{N-2}^{N_h-1} & h_{N-2}^{N_h-2} & \cdots & h_{N-2}^0 & 0 \\
0 & 0 & \cdots & & \cdots & & 0 & h_{N-1}^{N_h-1} & h_{N-1}^{N_h-2} & \cdots & h_{N-1}^0
\end{bmatrix}_{N\times N} \tag{5.2.3}$$

where $\mathbf{H}_c^{(i)}$ is the time-domain channel circular convolution matrix of size $N \times N$ passed by the ith user's signal, which is described in Eq.(5.2.3), (see also in [108]). Moreover, F denotes the $N \times N$ DFT matrix and $\mathbf{H}^{(i)} = \mathbf{F}\mathbf{H}_c^{(i)}\mathbf{F}^H$ is defined as the frequency channel response called the *subcarrier coupling matrix* [108]. $\mathbf{v}_f^{(i)}$ is the frequency domain representation of the additive Gaussian complex noise vector $\mathbf{v}^{(i)}$ for the ith user.

In this work, the STBC scheme which is similar to the scheme in [77] is adopted for each MIMO OFDM system terminal. The two consecutive block signal vectors from ith user can be represented as $\mathbf{x}_1^{(i)} = [x_1^{(i)}(0), x_1^{(i)}(1), \cdots, x_1^{(i)}(N-1)]^T$ and $\mathbf{x}_2^{(i)} = [x_2^{(i)}(0), x_2^{(i)}(1), \cdots, x_2^{(i)}(N-1)]^T$ of size N. Here, the time domain channel responses are assumed constant during two consecutive signal block intervals, i.e. quasi-static. Hence, $\mathbf{H}_{jq}^{(i)}$ is the frequency channel coefficient matrix experienced by the ith user's signal transmitted from the qth transmit antenna to the

jth receive antenna, and $q \in \{1,2\}$, in terms of the diagonal matrix when the channel is quasi-static in the time domain, (see in [117]). The coded signal from two transmit antennas of the ith user's terminal during two block intervals in the frequency domain could be represented in matrix form as follows,

$$\begin{bmatrix} \mathbf{F}^H\mathbf{x}_1^{(i)} & \mathbf{F}^H\mathbf{x}_2^{(i)} \\ -\mathbf{F}^H\mathbf{x}_2^{(i)^*} & \mathbf{F}^H\mathbf{x}_1^{(i)^*} \end{bmatrix} \tag{5.2.4}$$

Next consider a STBC MIMO-OFDM transmitter for two user terminals (as in [116], [121] and [135]). Each user terminal is equipped with two transmit antennas for exploiting the above STBC scheme for wireless data transmission, and therefore, four antennas are required at the transmitter.

Considering the output of the OFDM demodulator at the first receive antenna after cyclic prefix removal, the signal vectors during the two sequential OFDM time-slots a and b could be obtained in Eq.(5.2.5) and Eq.(5.2.6), respectively, as

$$\mathbf{r}_a^1 = \mathbf{H}_{11}\begin{bmatrix} \mathbf{x}_1^{(1)} \\ \mathbf{x}_1^{(2)} \end{bmatrix} + \mathbf{H}_{21}\begin{bmatrix} \mathbf{x}_2^{(1)} \\ \mathbf{x}_2^{(2)} \end{bmatrix} + \mathbf{v}_{f1a} \tag{5.2.5}$$

$$\mathbf{r}_b^{1^*} = \mathbf{H}_{21}^*\begin{bmatrix} \mathbf{x}_1^{(1)} \\ \mathbf{x}_1^{(2)} \end{bmatrix} - \mathbf{H}_{11}^*\begin{bmatrix} \mathbf{x}_2^{(1)} \\ \mathbf{x}_2^{(2)} \end{bmatrix} + \mathbf{v}_{f1b}^* \tag{5.2.6}$$

where $\mathbf{H}_{qj} \triangleq [\mathbf{H}_{qj}^{(1)}, \mathbf{H}_{qj}^{(2)}]$. For simplicity of notation, let us define signal vector $\mathbf{x} = [\mathbf{x}_1^{(1)^T}, \mathbf{x}_1^{(2)^T}, \mathbf{x}_2^{(1)^T}, \mathbf{x}_2^{(2)^T}]^T$, receive vector $\mathbf{r}^1 = \begin{bmatrix} \mathbf{r}_a^1 \\ \mathbf{r}_b^{1^*} \end{bmatrix}$, and

$\mathbf{v}_{f1} = \begin{bmatrix} \mathbf{v}_{f1a} \\ \mathbf{v}^*_{f1b} \end{bmatrix}$. Therefore, write Eq.(5.2.5) and Eq.(5.2.6) in a matrix form as

$$\mathbf{r}^1 = \tilde{\mathbf{H}}_1 \mathbf{x} + \mathbf{v}_{f1} \tag{5.2.7}$$

The equivalent channel matrix from transmitter to the first receive antennas could be represented as $\tilde{\mathbf{H}}_1 = \begin{bmatrix} \mathbf{H}_{11} & \mathbf{H}_{21} \\ \mathbf{H}^*_{21} & -\mathbf{H}^*_{11} \end{bmatrix}$. In a similar method, arrange the output at the second receive antennas as

$$\mathbf{r}^2 = \tilde{\mathbf{H}}_2 \mathbf{x} + \mathbf{v}_{f2} \tag{5.2.8}$$

where the equivalent channel matrix $\tilde{\mathbf{H}}_2$ to the second receive antennas could be represented as $\tilde{\mathbf{H}}_2 = \begin{bmatrix} \mathbf{H}_{12} & \mathbf{H}_{22} \\ \mathbf{H}^*_{22} & -\mathbf{H}^*_{12} \end{bmatrix}$. Here, the overall receive vector is arranged by combining Eq.(5.2.7) and Eq.(5.2.8) as

$$\mathbf{r} = \begin{bmatrix} \mathbf{r}^1 \\ \mathbf{r}^2 \end{bmatrix} = \begin{bmatrix} \tilde{\mathbf{H}}_1 \\ \tilde{\mathbf{H}}_2 \end{bmatrix} .\mathbf{x} + \begin{bmatrix} \mathbf{v}_{f1} \\ \mathbf{v}_{f2} \end{bmatrix} = \tilde{\mathbf{H}} . \mathbf{x} + \mathbf{v}_f \tag{5.2.9}$$

Let $N_b = 2KN$, where K is the number of users. $\tilde{\mathbf{H}}$ is the overall equivalent channel matrix between transmitter and receiver of size $N_b \times N_b$ and $\mathbf{v}_f$ denotes the whole channel equivalent noise vector of size N_b with variance σ_n^2.

5.2.2 Iterative MMSE MUD Algorithms

An iterative MMSE MUD scheme is now considered, in which the multiuser receiver is equipped with two receive antennas, as shown in Figure 5.2 (see also in [135]). Through utilization of the overall equivalent

time domain channel matrix $\tilde{\mathbf{H}}$ in Eq.(5.2.9), estimation of the transmitted symbol $\hat{x}(n)$ could be obtained. The direct estimation based on

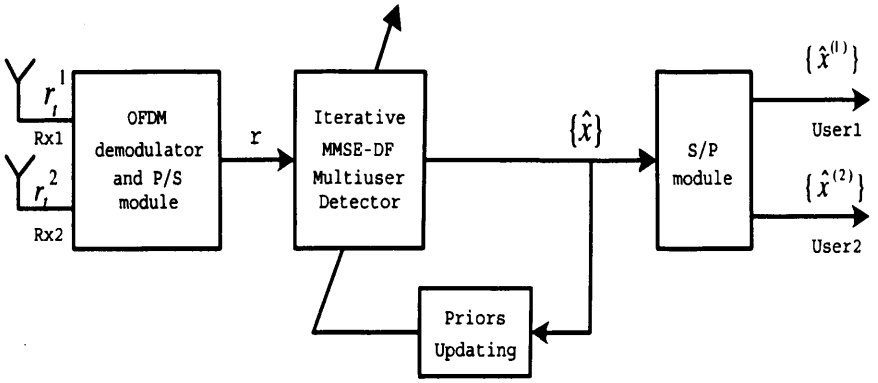

Figure 5.2. The iterative MMSE multiuser receiver structure equipped with two receive antennas for two user applications.

L-MMSE, however, could not offer good enough performance due to the presence of MAI and ISI. In this work, the transmitted signal can be estimated in an iterative detection process. An MMSE equalizer is structured to get signal estimations $\hat{x}(n)$s at first, and then those estimated values could be used to maximize the posteriori probability in iterative processing.

The first step is to estimate the frequency domain samples through the L-MMSE equalizer. The noise in Eq.(5.2.9) is assumed uncorrelated and zero mean, therefore $E\{\mathbf{v}_f\} = \mathbf{0}$, $E\{\mathbf{v}_f\mathbf{v}_f{}^H\} = \sigma_n^2\mathbf{I}_{N_b}$ and $E\{x(n)\mathbf{v}_f\} = \mathbf{0}$. As discussed in Chapter 3, the MMSE equalizer $\mathbf{w}_n$ can be derived through minimizing the following cost function

$$J(\mathbf{w}_n) = E\{|x(n) - \mathbf{w}_n^H\mathbf{r}|^2\} \tag{5.2.10}$$

and thereby obtain the MMSE equalizer coefficient vector

$$\mathbf{w}_n = (\tilde{\mathbf{H}} Cov[\mathbf{x}, \mathbf{x}] \tilde{\mathbf{H}}^H + \sigma_n^2 \mathbf{I}_{N_b})^{-1} \tilde{\mathbf{H}} Cov[\mathbf{x}, x(n)] \tag{5.2.11}$$

and then the estimated value $\hat{x}(n)$s could be obtained as

$$\hat{x}(n) = \bar{x}(n) + \mathbf{w}_n^H (\mathbf{r} - \tilde{\mathbf{H}} \bar{\mathbf{x}}) \tag{5.2.12}$$

Here, $\bar{x}(n) = E\{x(n)\}$ and $\bar{\mathbf{x}} = E\{\mathbf{x}\}$. By Eq.(5.2.11) and Eq.(5.2.12), the values of $\{\hat{x}(n)\}$ are estimated at the first step. In order to apply an iterative algorithm, next, updated values for $\{\bar{x}(n)\}$ and $\{Cov[x(n), x(n)]\}$ are obtained based on the estimates $\hat{x}(n)$s. With these values, only *extrinsic information* is chosen to find the posterior values of SISO MUD as updated priors of the next iteration, which leads to update $\{\bar{x}(n)\}$ and $\{Cov[x(n), x(n)]\}$ into $\bar{\mathbf{x}}$ and $Cov[\mathbf{x}, \mathbf{x}]$, as shown in Eq.(5.2.11) and Eq.(5.2.12). Here, a sequential iterative estimation (SIE) approach is chosen. Initialize by setting $\forall \bar{x}(n) = 0$ and $\forall Cov[x(n), x(n)] = 1$ when estimating $x(n)$. With utilization of BPSK signals, the updating processing of the iterative algorithm could work through finding the log-likelihood ratios (LLR)s from the estimated values of $\{\hat{x}(n)\}$. Defining the prior and posterior LLR of $x(n)$ respectively, as

$$L[x(n)] = \ln \frac{\Pr\{x(n) = 1\}}{\Pr\{x(n) = -1\}} \tag{5.2.13}$$

$$L[x(n)|_{\hat{x}(n)}] = \ln \frac{\Pr\{x(n) = 1|_{\hat{x}(n)}\}}{\Pr\{x(n) = -1|_{\hat{x}(n)}\}} \tag{5.2.14}$$

Hence, the extrinsic LLR is defined as the difference between the posterior and prior LLRs of $x(n)$:

$$\begin{aligned}\Delta L[x(n)] &= L[x(n)|_{\hat{x}(n)}] - L[x(n)] \\ &= \ln \frac{\Pr\{\hat{x}(n)|_{x(n)=1}\}}{\Pr\{\hat{x}(n)|_{x(n)=-1}\}}\end{aligned} \tag{5.2.15}$$

As the signal $x(n) = b \in \{+1, -1\}$, the conditional probability density function (PDF) of $x(n)$ is Gaussian distributed and can be expressed as

$$\begin{aligned}&\Pr\{\hat{x}(n)|_{x(n)=b}\} \sim \mathcal{N}\left(m_n(b), \sigma_x^2|_{x(n)=b}\right) \\ &\approx \frac{1}{\sqrt{2\pi}\sigma_x|_{x(n)=b}} \exp\left(-\frac{(\hat{x}(n) - m_n(b))(\hat{x}(n) - m_n(b))^H}{2\sigma_x^2|_{x(n)=b}}\right)\end{aligned} \tag{5.2.16}$$

where the posterior conditional mean and covariance value of $\hat{x}(n)$ could be defined as $m_n(b) = E\{\hat{x}(n)|_{x(n)=b}\}$ and $\sigma_x^2|_{x(n)=b} = Cov[\hat{x}(n), \hat{x}(n)|_{x(n)=b}]$, respectively. They could be determined by (5.2.11) and (5.2.12) as

$$E\{\hat{x}(n)|_{x(n)=b}\} = \mathbf{w}_n^H \tilde{\mathbf{h}}_n b \tag{5.2.17}$$

$$\begin{aligned}\sigma_x^2|_{x(n)=b} &= E\{\hat{x}(n)\hat{x}^H(n)|_{x(n)=b}\} - m_n(b)m_n(b)^H \\ &= \mathbf{w}_n^H \tilde{\mathbf{h}}_n - \mathbf{w}_n^H \tilde{\mathbf{h}}_n \tilde{\mathbf{h}}_n^H \mathbf{w}_n\end{aligned} \tag{5.2.18}$$

where $\tilde{\mathbf{h}}_n$ is the nth column of $\tilde{\mathbf{H}}$. Moreover, because there are not available priors before the first estimation, therefore, $L[x(n)] = 0$ at the beginning of iteration. Now, obtain

$$\begin{aligned}\Delta L[x(n)] &= L[x(n)|_{\hat{x}(n)}] - L[x(n)] \\ &= \ln \frac{\left[\exp\left(-\frac{(\hat{x}(n)-m_n(+1))^2}{\sigma^2_{\tilde{x}|x(n)=+1}}\right)\right]}{\left[\exp\left(-\frac{(\hat{x}(n)-m_n(-1))^2}{\sigma^2_{\tilde{x}|x(n)=-1}}\right)\right]} \\ &= \frac{4Re\{\hat{x}(n)\}}{1-\tilde{\mathbf{h}}_n^H \mathbf{w}_n}\end{aligned} \tag{5.2.19}$$

Therefore, the a posteriori LLR of x(n) can be obtained as

$$L[x(n)|_{\hat{x}(n)}] = \Delta L[x(n)] + L[x(n)] \tag{5.2.20}$$

Once the posteriori LLRs are obtained, it will lead to the update of the priors for the next iteration in terms of $\bar{x}(n)$ and $Cov[x(n), x(n)]$:

$$\begin{aligned}\bar{x}(n)_{new} &= \Pr\{x(n) = +1|_{\hat{x}(n)}\} - \Pr\{x(n) = -1|_{\hat{x}(n)}\} \\ &= \tanh\left(\frac{L[x(n)|_{\hat{x}(n)}]}{2}\right)\end{aligned} \tag{5.2.21}$$

$$\begin{aligned}&Cov[x(n), x(n)]_{new} \\ &= \sum_{b\in\{+1,-1\}} (b - E\{x(n)|_{\hat{x}(n)}\})^2 \cdot \Pr\{x(n) = b|_{\hat{x}(n)}\} \\ &= 1 - \bar{x}(n)^2_{new}\end{aligned} \tag{5.2.22}$$

Then, the equalizer Eq.(5.2.12) receives updates as the posterior values $\bar{x}(n)_{new}$ obtained by Eq.(5.2.21) and $Cov[x(n), x(n)]_{new}$ obtained by Eq.(5.2.22). These values are updated as relative values into the diagonal matrix $Cov[\mathbf{x}, \mathbf{x}]$ of Eq.(5.2.11). These updating coefficients are

used to estimate the next value $\hat{x}(n+1)$ and the next posteriori values are updated by repeating the steps from Eq.(5.2.11) to Eq.(5.2.22). The estimation starts at $\hat{x}(0)$ until $\hat{x}(N_b - 1)$ is obtained, and then repeated again starting with $\hat{x}(0)$ for next iteration. The iterative updating process does not stop until the specified number of iterations has elapsed or the reliability value of LLRs surpasses a threshold.

5.3 Joint Iterative MMSE MUD and Convolutional Decoder

In this section, the transmitter structure of the STBC MIMO-OFDM system in Section 5.2 has been extended for K user applications and the proposed joint iterative multiuser detection scheme with forward error correction coding techniques. The transmitter terminal implements MIMO-OFDM with space-time block codes (STBC), and the receiver joint iterative MMSE multiuser detection with convolutional channel decoding by exchanging extrinsic information in terms of log-likelihood ratios (LLRs), whereas the proposed scheme exploits two transmit antennas for each user terminal and two receive antennas at the receiver. This work was also proposed in [137].

5.3.1 System Model for Joint Iterative MUD

The proposed K user STBC MIMO OFDM transmission system is described in Figure 5.3. Firstly, the incoming data stream is encoded by a half rate convolutional encoder, and then, passed through an interleaving stage. The ith user's continuous input signal blocks $\mathbf{s}_1^{(i)}$ and $\mathbf{s}_2^{(i)}$ will be encoded as two consecutive transmitting OFDM symbol blocks $\mathbf{x}_1^{(i)} = [x_1^{(i)}(0), \cdots, x_1^{(i)}(N-1)]^T$ and $\mathbf{x}_2^{(i)} = [x_2^{(i)}(0), \cdots, x_2^{(i)}(N-1)]^T$, which are the frequency domain symbols, $i = 1, 2, \ldots, K$. Then, space-

time block encoding processing is implemented on the signal and the OFDM modulator is applied to the outputs of the space time encoder. The outputs of the OFDM modulators are transmitted using multiple antennas simultaneously. All channel knowledge is assumed known perfectly throughout. At each of the receive antennas, the samples corresponding to the cyclic prefix are first removed and one received OFDM block in the frequency domain can be represented as

$$\mathbf{r}=\mathbf{F}\mathbf{r}_{\mathbf{t}}=\mathbf{F}\mathbf{H}_{\mathbf{c}}^{(\mathbf{i})}\mathbf{F}^{H}\mathbf{x}^{(i)}+\mathbf{F}\mathbf{v}^{(i)}=\mathbf{H}^{(i)}\mathbf{x}^{(i)}+\mathbf{v}_{f}^{(i)} \tag{5.3.1}$$

where $\mathbf{H}_c^{(i)}$ is the time-domain circular convolution channel matrix of size $N \times N$, denoted as the ith user's data transmitting pipe. $\mathbf{H}^{(i)}$ is defined as the frequency response of the channel coefficients, which is the so-called *subcarrier coupling matrix*. In this work, the STBC scheme which is similar to the scheme in Section 5.2 is adapted for each user terminal. Here, the time domain channel responses could be assumed to be constant during two consecutive OFDM block intervals, i.e. quasi-static. Next consider a STBC MIMO-OFDM transmitter for two user terminals, which is shown in Figure 5.3, (see also in [116], [121] and [135]). Each user terminal is equipped with two transmit antennas for exploiting the above STBC scheme for wireless data transmission, and therefore, $2K$ antennas are required at the transmitter. Hence, the signal vectors during the two sequential OFDM time-slots a and b could be obtained as

$$\mathbf{r}_a^1 = \mathbf{H}_{11}\mathbf{x}_1 + \mathbf{H}_{21}\mathbf{x}_2 + \mathbf{v}_{f1a} \tag{5.3.2}$$

$$\mathbf{r}_b^{1^*} = \mathbf{H}_{21}^*\mathbf{x}_1 - \mathbf{H}_{11}^*\mathbf{x}_2 + \mathbf{v}_{f1b}^* \tag{5.3.3}$$

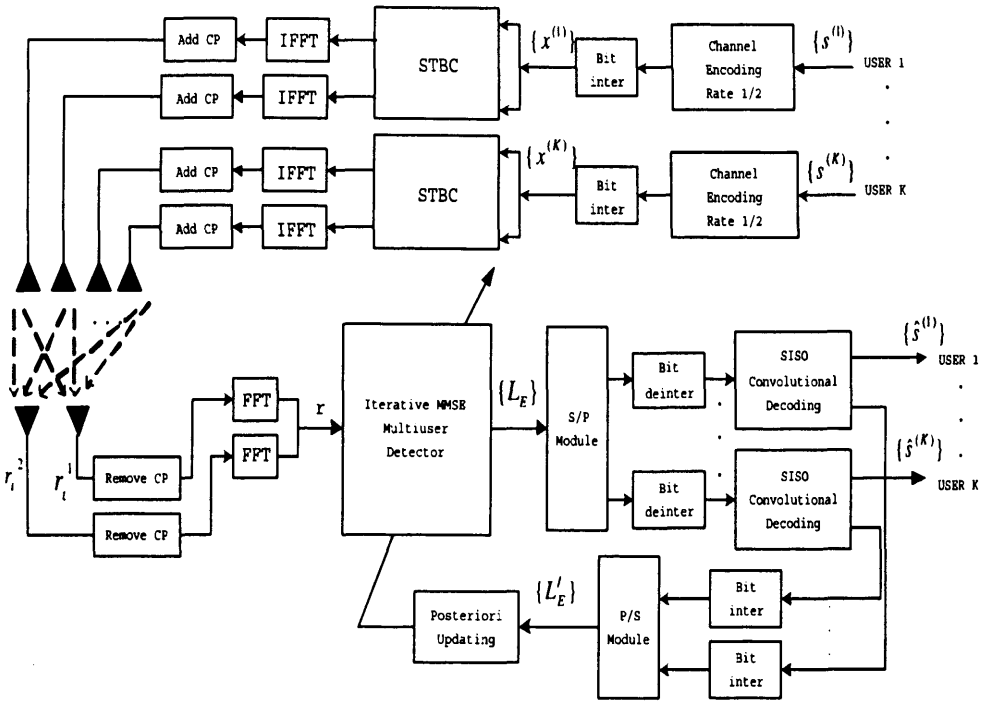

Figure 5.3. K user STBC-OFDM transmission system with joint iterative MMSE MUD and convolutional coded multiuser receiver equipped with two receive antennas.

where $\mathbf{H}_{qj} \triangleq [\mathbf{H}_{qj}^{(1)}, \mathbf{H}_{qj}^{(2)}, \ldots, \mathbf{H}_{qj}^{(K)}]$, and $\mathbf{H}_{jq}^{(i)}$ is the frequency channel coefficient matrix experienced by the ith user's signal transmitted from the qth transmit antenna to the jth receive antenna, and $q \in \{1, 2\}$, in terms of the diagonal matrix when the channel is quasi-static in the time domain, (see in [117]). In addition, $\mathbf{x}_1 = [\mathbf{x}_1^{(1)^T}, \mathbf{x}_1^{(2)^T}, \ldots, \mathbf{x}_1^{(K)^T}]^T$, and $\mathbf{x}_2 = [\mathbf{x}_2^{(1)^T}, \mathbf{x}_2^{(2)^T}, \ldots, \mathbf{x}_2^{(K)^T}]^T$. For simplicity of notation, define the transmitted signal vector $\mathbf{x} = \begin{bmatrix} \mathbf{x}_1^T \\ \mathbf{x}_2^T \end{bmatrix}$, received vector $\mathbf{r}^1 = \begin{bmatrix} \mathbf{r}_a^1 \\ \mathbf{r}_b^{1*} \end{bmatrix}$, and $\mathbf{v}_{f1} = \begin{bmatrix} \mathbf{v}_{f1a} \\ \mathbf{v}_{f1b}^* \end{bmatrix}$. Therefore, also write Eq.(5.3.2) and Eq.(5.3.3) in a matrix form as in Section 5.2

$$\mathbf{r}^1 = \tilde{\mathbf{H}}_1 \mathbf{x} + \mathbf{v}_{f1} \tag{5.3.4}$$

The equivalent channel matrix from transmitter of K users to the first receive antennas could be represented as $\tilde{\mathbf{H}}_1 = \begin{bmatrix} \mathbf{H}_{11} & \mathbf{H}_{21} \\ \mathbf{H}_{21}^* & -\mathbf{H}_{11}^* \end{bmatrix}$. In a similar method, arrange the output at the second receive antennas as

$$\mathbf{r}^2 = \tilde{\mathbf{H}}_2 \mathbf{x} + \mathbf{v}_{f2} \tag{5.3.5}$$

where the equivalent channel matrix $\tilde{\mathbf{H}}_2$ for K users to the second receive antennas could be represented as $\tilde{\mathbf{H}}_2 = \begin{bmatrix} \mathbf{H}_{12} & \mathbf{H}_{22} \\ \mathbf{H}_{22}^* & -\mathbf{H}_{12}^* \end{bmatrix}$. Here, the overall receive vector for K users is arranged by combining Eq.(5.3.4) and Eq.(5.3.5) as

$$\mathbf{r} = \begin{bmatrix} \mathbf{r}^1 \\ \mathbf{r}^2 \end{bmatrix} = \begin{bmatrix} \tilde{\mathbf{H}}_1 \\ \tilde{\mathbf{H}}_2 \end{bmatrix} .\mathbf{x} + \begin{bmatrix} \mathbf{v}_{f1} \\ \mathbf{v}_{f2} \end{bmatrix} = \tilde{\mathbf{H}}.\mathbf{x} + \mathbf{v}_f \tag{5.3.6}$$

Let $N_b = 2KN$, where K is the number of users. $\tilde{\mathbf{H}}$ is the overall equivalent channel matrix between K user transmitting terminals and receiver of size $N_b \times N_b$ and $\mathbf{v}_f$ notes the whole channel equivalent noise vector of size N_b with variance σ_n^2.

5.3.2 Joint Iterative MUD and Decoding Scheme

The structure of the iterative multiuser receiver is shown in the lower half of Figure 5.3. It consists of two stages: a soft input soft output (SISO) multiuser detector and parallel single-user SISO channel decoders. The SISO multiuser detector calculates the marginal prob-

abilities for the ith decoder for the ith user. Then all the single-user SISO channel decoders, according to the marginal probabilities, generate the a posteriori coded bit probabilities, which are then used as the a priori information for the SISO multiuser detector on the next iteration.

Through utilization of the overall channel matrix $\tilde{\mathbf{H}}$, the transmitted signal can be estimated by maximizing the posteriori probability in iterative processing at the first stage. As described similarly in Section 5.2, at first, a linear MMSE equalization is performed to estimate the frequency domain samples. The noise in Eq.(5.3.6) is assumed that it is uncorrelated and circularly distributed. The MMSE equalizer $\mathbf{w}_n$ is derived through minimizing the cost function $J(\mathbf{w}_n) = E\{|x(n)-\mathbf{w}_n^H\mathbf{r}|^2\}$. Hence, the MMSE equalizer coefficient vector $\mathbf{w}_n$ is obtained and the estimated value $\hat{x}(n)$s as follows

$$\mathbf{w}_n = (\tilde{\mathbf{H}}Cov[\mathbf{x},\mathbf{x}]\tilde{\mathbf{H}}^H + \sigma_n^2\mathbf{I}_{N_b})^{-1}\tilde{\mathbf{H}}Cov[\mathbf{x},x(n)] \tag{5.3.7}$$

and

$$\hat{x}(n) = \bar{x}(n) + \mathbf{w}_n^H(\mathbf{r} - \tilde{\mathbf{H}}\bar{\mathbf{x}}) \tag{5.3.8}$$

Here, $\bar{x}(n) = E\{x(n)\}$ and $\bar{\mathbf{x}} = E\{\mathbf{x}\}$. By Eq.(5.3.7) and Eq.(5.3.8), the values of $\{\hat{x}(n)\}$ are estimated at first. Next, the *extrinsic information* of each code bit can be found based on the $\hat{x}(n)$s, and then these extrinsic values should be fed to the channel decoder of each user branch. Thus correct extrinsic values will be obtained at the output of the channel decoder, which is used to obtain posterior values $\{\bar{x}(n)\}$ and $\{Cov[x(n),x(n)]\}$ for updating the iterative multiuser detector. Initialization of $\forall\bar{x}(n) = 0$ and $\forall Cov[x(n),x(n)] = 1$ are known. With

utilization of BPSK signals, the iterative updating processing could start through finding the log-likelihood ratios (LLR)s based on $\{\hat{x}(n)\}$. The difference between the posterior and prior LLRs of $x(n)$ could be defined as the extrinsic information as

$$\begin{aligned} L_E[x(n)] &= L[x(n)|_{\hat{x}(n)}] - L[x(n)] = \Delta L[x(n)] \\ &= \ln \frac{\Pr\{x(n)=1|_{\hat{x}(n)}\}}{\Pr\{x(n)=-1|_{\hat{x}(n)}\}} - \ln \frac{\Pr\{x(n)=1\}}{\Pr\{x(n)=-1\}} \\ &= \ln \frac{\Pr\{\hat{x}(n)|_{x(n)=1}\}}{\Pr\{\hat{x}(n)|_{x(n)=-1}\}} \end{aligned} \tag{5.3.9}$$

With utilization of the signal $x(n) = b \in \{+1, -1\}$, as shown in Section 5.2 the conditional probability density function (PDF) of $x(n)$ is Gaussian distributed and can be expressed as,

$$\begin{aligned} &\Pr\{\hat{x}(n)|_{x(n)=b}\} \sim \mathcal{N}\left(m_n(b), \sigma_x^2|_{x(n)=b}\right) \\ &\approx \frac{1}{\sqrt{2\pi}\sigma_x|_{x(n)=b}} \exp\left(-\frac{(\hat{x}(n)-m_n(b))(\hat{x}(n)-m_n(b))^H}{2\sigma_x^2|_{x(n)=b}}\right) \end{aligned} \tag{5.3.10}$$

where the posterior conditional mean and covariance value of $\hat{x}(n)$ could be defined as $m_n(b) = E\{\hat{x}(n)|_{x(n)=b}\}$ and $\sigma_x^2|_{x(n)=b} = Cov[\hat{x}(n), \hat{x}(n)|_{x(n)=b}]$, respectively. They could be determined by Eq.(5.3.7) and Eq.(5.3.8) as

$$E\{\hat{x}(n)|_{x(n)=b}\} = \mathbf{w}_n^H \tilde{\mathbf{h}}_n b \tag{5.3.11}$$

$$\begin{aligned} \sigma_x^2|_{x(n)=b} &= E\{\hat{x}(n)\hat{x}^H(n)|_{x(n)=b}\} - m_n(b)m_n(b)^H \\ &= \mathbf{w}_n^H \tilde{\mathbf{h}}_n - \mathbf{w}_n^H \tilde{\mathbf{h}}_n \tilde{\mathbf{h}}_n^H \mathbf{w}_n \end{aligned} \tag{5.3.12}$$

where $\tilde{\mathbf{h}}_n$ is the nth column of $\tilde{\mathbf{H}}$. Moreover, set initialization as $\bar{x}(n) =$

0 and $Cov[x(n), x(n)] = 1$ for finding the posterior LLR of $x(n)$. Since no prior information is available, the prior information $L[x(n)] = 0$ at the first iteration. Now, obtaining extrinsic information as

$$\begin{aligned} L_E[x(n)] &= L[x(n)|_{\hat{x}(n)}] - L[x(n)] \\ &= \ln \frac{\left[\exp\left(-\frac{(\hat{x}(n)-m_n(+1))^2}{\sigma^2_{\tilde{x}|x(n)=+1}}\right)\right]}{\left[\exp\left(-\frac{(\hat{x}(n)-m_n(-1))^2}{\sigma^2_{\tilde{x}|x(n)=-1}}\right)\right]} \\ &= \frac{4Re\{\hat{x}(n)\}}{1 - \tilde{\mathbf{h}}_n^H \mathbf{w}_n} \end{aligned} \tag{5.3.13}$$

When the extrinsic information $\{L_E[x(n)]\}$ has been obtained for the whole signal block where $n = 0, \ldots, N_b - 1$, these values will be separated to parallel branches as $\{L_E[x^{(i)}(n)]\}$, $i = 1, \ldots, K$ corresponding to each code bit of the ith user. Only extrinsic information is known to be used for exchanging between the SISO multiuser detector and the SISO convolutional channel decoder. Therefore then these extrinsic values for each code bit of each user will be de-interleaved as $\{L_E[\tilde{x}^{(i)}(n)]\}$, where $\tilde{x}^{(i)}(n)$ denotes de-interleaved extrinsic LLR for the code bit of the ith user. The $\{L_E[\tilde{x}^{(i)}(n)]\}$ is delivered to each SISO single user channel decoder as the a priori information. Thus the de-interleaved posterior information of the corrected code bit of each user $L'[\tilde{x}^{(i)}(n)|_{\hat{\tilde{x}}^{(i)}(n)}]$ can be obtained from the trellis structure of the SISO convolutional decoding, and then the extrinsic LLRs for each corrected code bit of each user $L'_E[\tilde{x}^{(i)}(n)]$ can be extracted after the output of channel decoder as,

$$L'_E[\tilde{x}^{(i)}(n)] = L'[\tilde{x}^{(i)}(n)|_{\hat{\tilde{x}}^{(i)}(n)}] - L_E[\tilde{x}^{(i)}(n)] \tag{5.3.14}$$

Then $\{L'_E[\tilde{x}^{(i)}(n)]\}$ are interleaved at each single user branch in terms of $\{L'_E[x^{(i)}(n)]\}$ and then combined to a serial block $\{L'_E[x(n)]\}$ of size N_b as the same order with $\{L_E[x(n)]\}$, where $L'_E[x(n)]$ is considered as feedback extrinsic LLR of code bit which leads to the updating of the priors of the SISO multiuser detector.

When starting at the next iteration, the feedback extrinsic LLRs $\{L'_E[x(n)]\}$ are delivered to the SISO multiuser detector as new a prior information $L[x(n)]_{new}$ to reconstruct an a priori update value of the SISO MMSE detector in Eq.(5.2.11) and Eq.(5.2.12) as,

$$\begin{aligned}\bar{x}(n)_{new} &= \sum_{b\epsilon\{+1,-1\}} b \cdot \Pr\{x(n)=b\} \\ &= \Pr\{x(n)=+1\} - \Pr\{x(n)=-1\} \\ &= \tanh\left(\frac{L[x(n)]_{new}}{2}\right)\end{aligned} \tag{5.3.15}$$

$$\begin{aligned}&Cov[x(n),x(n)]_{new} \\ &= \sum_{b\epsilon\{+1,-1\}} (b - E\{x(n)\})^2 \cdot \Pr\{x(n)=b\} \\ &= 1 - \bar{x}(n)^2_{new}\end{aligned} \tag{5.3.16}$$

The iterative updating process does not stop until the specified number of iterations has elapsed or the reliability value of LLRs surpass a threshold, and the a posteriori LLR $L'[\tilde{x}^{(i)}(n)|_{\hat{\tilde{x}}^{(i)}(n)}]$ is used to make the decision on the decoded bit at the last iteration, which make the final source symbol estimations $\{\hat{\mathbf{s}}^{(i)}\}$ from the output of the SISO channel decoder of each user.

5.4 Numerical Results and Discussions

To illustrate the performance of the proposed iterative receiver structure, a STBC MIMO-OFDM system for a two user case using four transmit and two receive antennas is simulated in this section. A BPSK signal constellation is exploited in this work, which can be easily mapped into QPSK. Each source data frame contains 1000 bit information symbols. The simulations utilize 1MHz symbol transmission rate, i.e. the OFDM symbol duration is $T_s = 1\mu s$, which is divided into 16 sub-carriers by OFDM operation for the tones orthogonal to each other. Each serial data stream contains 32 symbols, which is coded into two OFDM blocks by STBC encoding operation. An additional 4 cyclic prefix symbols are used as a guard interval after each data block. Therefore, the user terminal could transmit two data blocks in parallel from two transmit antennas, so that the transmitting stream of 64 bit information symbols are estimated in one detecting iteration. A 3-tap wireless MIMO slow fading channel model is used in which each channel tap is represented by a complex Gaussian random variable. The real and imaginary parts of each channel tap are independently generated with the Doppler spectrum based on Jakes model (see [76]). The maximum Doppler frequency f_d notes the characteristic of channel time variations. Moreover, we assume $\sum_{l=0}^{L-1} \sigma_l^2 = 1$, where σ_l^2 is the variance of the lth path, and the channel fading is assumed to be uncorrelated among different transmitting antennas. Perfect knowledge of the channel state is available at the receiver at any time.

Figure 5.4 presents the frame error rate performance of the proposed iterative receiver over a time-variant fading channel with maximum Doppler frequency $fd = 2.5kHz$, i.e. normalized DS=0.05. As

a performance benchmark, performance is evaluated considering the match filter bound (MFB) which is obtained from the model given in (5.2.9) by assuming the symbols $\{x(u)|_{u\neq n}\}$ are perfectly known. By comparison with L-MMSE in Chapter 4, significant improvement of system performance is observed for the first stage MUD, when iterative processing is performed over slow fading channel environment after three iterations.

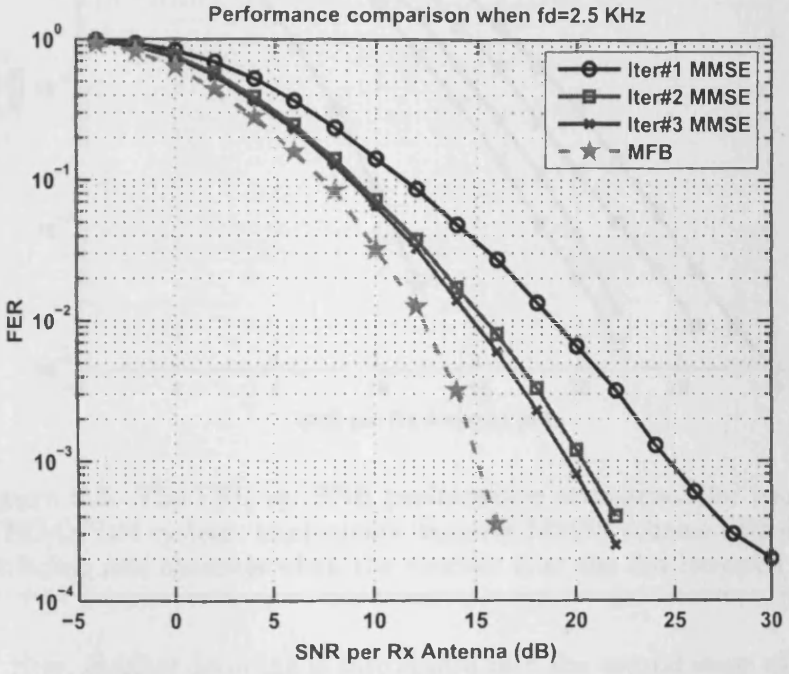

Figure 5.4. The FER vs. SNR performance comparison for two user STBC-OFDM system: implements iterative MMSE scheme with different number of iterations when maximum Doppler frequency is 2.5 KHz (DS=0.05) and channel tap length $L = 3$.

Figure 5.5 shows the comparison of system performance over different fading rate channel environment when the receiver exploits a three iteration process. The best performance is given in a quasi-static channel, and the performance degrades at higher SNR values with maximum

Doppler frequency rising. However, further performance enhancement could be achieved by concatenating channel coding technique into iterative processing.

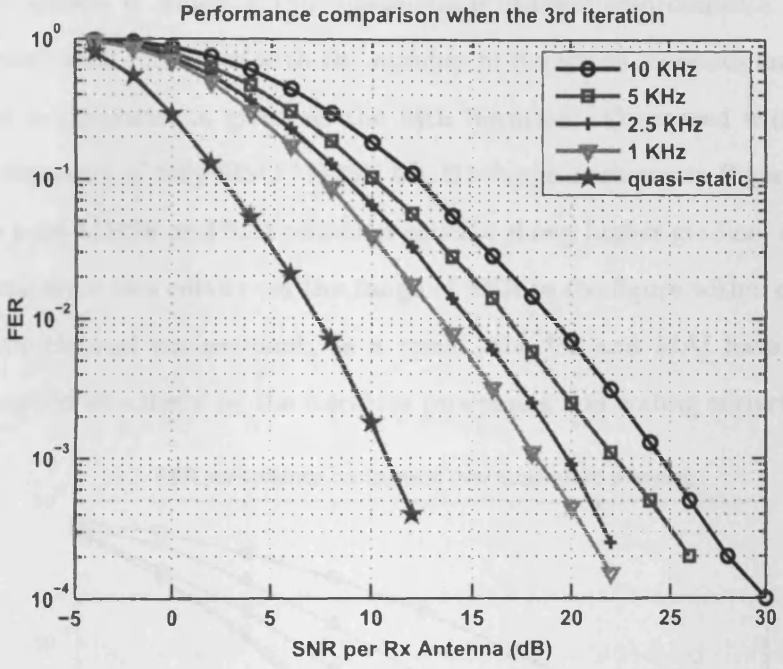

Figure 5.5. The FER vs. SNR performance comparison for two user STBC-OFDM system: implements iterative MMSE scheme with different fading rate channels when the receiver is at the 3rd iteration.

Now, channel decoding is introduced into the second stage of joint iterative detection-decoding scheme. All the users in the system employ a standard rate 1/2 and constraint length 3 convolutional code. In order to correct the subcarriers in deep fades, forward error correction and bit interleaving are used across the subcarriers. In order to keep equal signal power under the effect of channel coding, the complex white Gaussian noise was compensated by scaling by convolutional coding rate for normalization and the soft input soft output convolutional decoder is used in this simulation. Figure 5.6 shows FER vs. SNR

performance comparison for two user STBC MIMO-OFDM system in which the multiuser receiver implements joint iterative MMSE and convolutional channel decoding scheme with different number of iterations. The system is tested within quasi-static channel environments. The performance converges with the number of iterations increases and the best performance is given at the fifth iteration. Compared with the performance of only SISO MMSE MUD scheme as shown in Figure 5.5, the joint MMSE and SISO decoder scheme shows higher gradient of the frame error rate curve over the range of SNR in the figure within quasi-static channel environment, as a result, the ISI and MAI have been cancelled effectively by the iterative processing and coding correction.

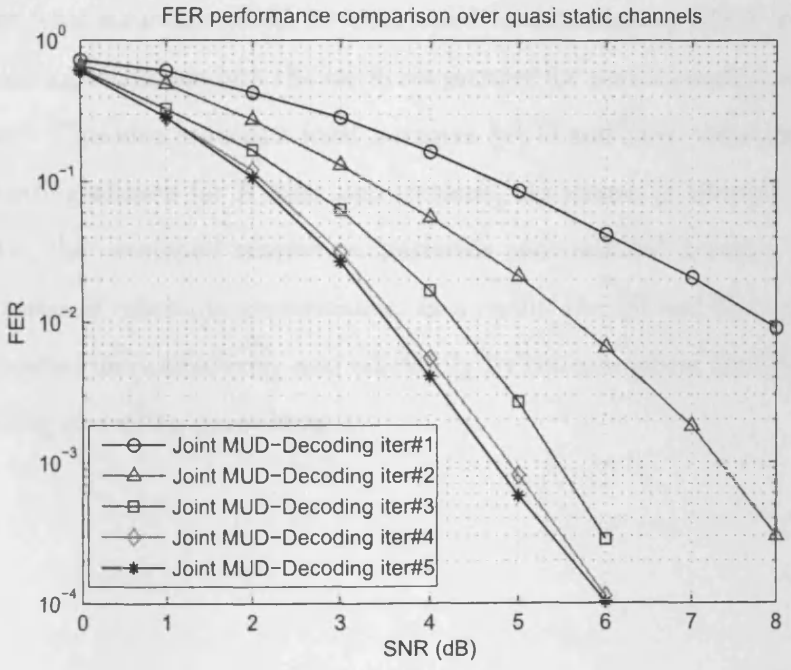

Figure 5.6. The FER vs. SNR performance comparison for two user STBC-OFDM system: implements joint iterative MMSE and channel decoding scheme with different number of iterations over quasi-static channels.

5.5 Conclusions

In this chapter, some iterative MUD schemes have been introduced into a synchronous uplink multiuser MIMO-OFDM wireless communication system over both quasi-static and slow fading rate MIMO-ISI channels. The design of the multiuser receiver was first addressed based on MMSE iterative algorithm by updating with extrinsic information. The structure of STBC techniques at transmitter was exploited, concatenated with OFDM operation to suppress interference. The simulation results indicate that the proposed scheme could obtain substantial performance improvement over slow fading channel environment (including quasi-static channels) rather than the MUD based on L-MMSE. Moreover, this structure could be developed by introducing SISO channel decoding technique into the iterative process for performance enhancement. This idea induces a joint iterative MUD and SISO convolutional decoding scheme for K user applications. As shown in simulation results, the developed scheme outperforms conventional iterative MUD in terms of reliability performance, as a result, the ISI and MAI can be cancelled more effectively and efficiently by concatenating the iterative coding correcting processing.

Chapter 6

LOW COMPLEXITY ITERATIVE INTERFERENCE CANCELLATION AND MULTIUSER DETECTIONS

6.1 Introduction

As discussion in Chapter 5, iterative turbo processing between the detection and decoding operations provide potentially substantial performance improvement for multiuser STBC-OFDM applications. However, combining iterative processing with front-end SISO multiuser detection is particularly challenging because the front-end maximum a posteriori (MAP) algorithm has a computational complexity that is exponential in the array size.

In this chapter, a novel low complexity iterative successive soft interference cancellation based on linear MMSE (SIC-LMMSE) and a multiuser detection (MUD) algorithm is proposed for wideband multiuser MIMO-OFDM communication in the context of synchronous uplink transmission. The proposed algorithm not only achieves performance

close to the conventional iterative multiuser detection and decoding scheme which is represented in Chapter 5 ([69], [135] and [137]), but also reduces the computational complexity by estimation evaluation and selected MAI cancellation processing. Simulation results confirm that the proposed low-complexity MUD-decoding algorithm offers good trade-off between performance and computational expense.

The outline of this chapter is organized as follows. After introduction in Section 6.1, a proposed K user STBC MIMO OFDM transceiver scheme is described in Section 6.2. Then a proposed iterative multiuser receiver based on low-complexity SIC and MUD scheme is designed in Section 6.3. The discussions of complexity issues are given in Section 6.4 and the Section 6.5 provides simulation results and relative discussions. Finally, conclusions are given in Section 6.6.

6.2 Baseband System Model

6.2.1 K User Coded STBC MIMO-OFDM Transmitter

A K-user uplink synchronous space-time block coded MIMO-OFDM wireless communication system is considered, where each user terminal is equipped with two transmit antennas due to Alamouti's STBC scheme, i.e. $n_t = 2K$ transmit antennas and m_r receive antennas are used in total. As shown in the left part of Figure 6.1, the source information stream from the ith user $\mathbf{b}^{(i)}$, $i = 1, \ldots, K$, can be encoded by a half rate $R_c = 1/2$ convolutional encoder and interleaved to yield $\varepsilon^{(i)}$. These can be mapped in terms of the symbol constellation of M_c bit modulation, in order to form frequency domain transmitted symbol $x^{(i)}$ of the ith user's, where ε_b denotes the bth binary value of

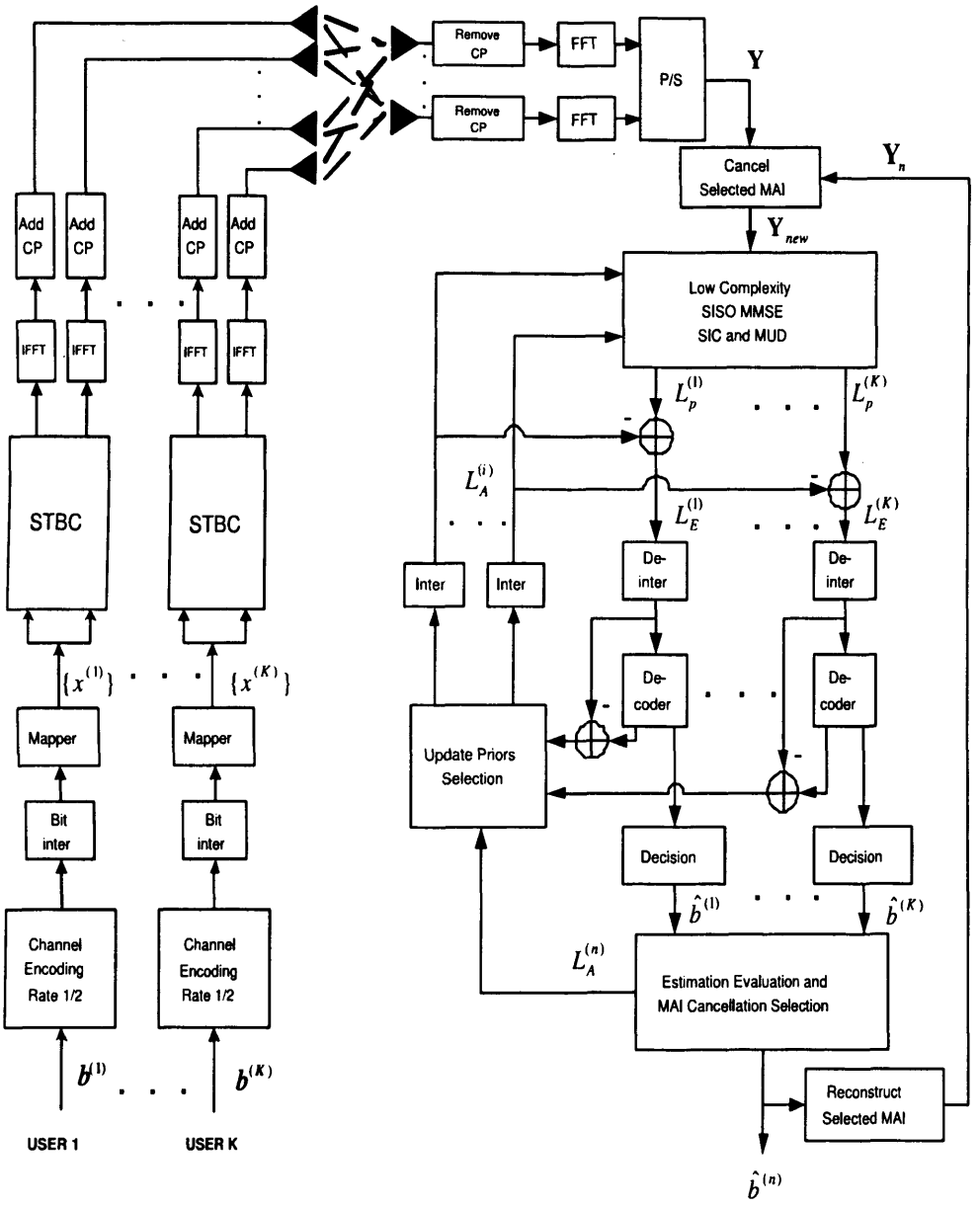

Figure 6.1. The block diagram of K user coded STBC MIMO-OFDM transmitter and the proposed receiver of iterative SIC multiuser detection-decoding and MAI selected cancellation.

mapped transmitted symbol x and $b = 1, \ldots, M_c$. Then, space-time block encoding [33] is combined with OFDM modulation. Thus, the order of D transmit diversity, without loss of generality $D = 2$ in this work, can be provided by the proposed STBC for each user transmitting terminal. Similarly, with the scheme as discussion in Chapter 4, the index k in each N symbol block corresponds to the tone index of OFDM, where $k = 0, 1, \ldots, N-1$. This assumes that the channel remains constant over a number, two in this work, of consecutive blocks equal to the number of transmit antennas in each user terminal, i.e. quasi-static (as in [116]). Hence, these consecutive frequency domain OFDM blocks of N symbol length from the ith user can be denoted as $\mathbf{x}_q^{(i)} = [x_q^{(i)}(0), \cdots, x_q^{(i)}(N-1)]^T$, where $q = 1, 2$ is the antenna number for each transmit terminal. The outputs of the OFDM modulators are transmitted using multiple antennas simultaneously. In this work, the baseband transmission is described in terms of the frequency domain. Due to the assumption of quasi-static channels, the equivalent frequency-selective channel response through the qth transmit antenna of the ith user terminal to the jth receive antenna, is represented in a diagonal matrix form as $diag[H_{qj}^i(0), H_{qj}^i(1), \ldots, H_{qj}^i(N-1)]$, where $j = 1, 2, \ldots, m_r$ (see in [117] and [108]). Here, $H_{1j}^i(k)$ and $H_{2j}^i(k)$ denote the channel frequency responses of the kth tone, related to the channel from the $1st$ and $2nd$ transmit antennas and corresponding to the ith user and the jth receive antennas, respectively, over two contiguous signal block intervals. Due to employing a space-time block encoding scheme, the kth tone receive symbol is in the frequency domain over the two sequential OFDM time-slots 1 and 2, respectively,

$$y_{1j}(k) = \sum_{i=1}^{K} \{H_{1j}^{i}(k)x_1^{(i)}(k) + H_{2j}^{i}(k)x_2^{(i)}(k)\} + v_{f1j}(k) \qquad (6.2.1)$$

$$y_{2j}(k) = \sum_{i=1}^{K} \{H_{2j}^{i}(k)x_1^{(i)*}(k) - H_{1j}^{i}(k)x_2^{(i)*}(k)\} + v_{f2j}(k) \qquad (6.2.2)$$

where $k = 0, 1, \ldots, N-1$ and $[v_{f1j}(k)\ v_{f2j}(k)]$ denote the frequency domain representation of the receiver complex circular symmetric AWGN at the kth tone. Next define $\mathbf{y}_j(k) = [y_{1j}(k)\ y_{2j}^{*}(k)]^T$, $\mathbf{x}^{(i)}(k) = [x_1^{(i)}(k)\ x_2^{(i)}(k)]^T$, $\mathbf{v}_{fj}(k) = [v_{f1j}(k)\ v_{f2j}^{*}(k)]^T$ and $\breve{\mathbf{H}}_j^i = \begin{bmatrix} H_{1j}^{i}(k) & H_{2j}^{i}(k) \\ H_{2j}^{i*}(k) & -H_{1j}^{i*}(k) \end{bmatrix}$, where $\breve{\mathbf{H}}_j^i$ is the equivalent frequency response matrix at the kth tone for the data pipe between the ith user terminal and the jth receive antenna. The kth tone receive signals from all receive antennas during two consecutive OFDM periods can be represented in matrix form as follows:

$$\begin{bmatrix} \mathbf{y}_1(k) \\ \mathbf{y}_2(k) \\ \vdots \\ \mathbf{y}_{m_r}(k) \end{bmatrix} = \begin{bmatrix} \breve{\mathbf{H}}_1^1(k) & \cdots & \breve{\mathbf{H}}_1^K(k) \\ \breve{\mathbf{H}}_2^1(k) & \cdots & \breve{\mathbf{H}}_2^K(k) \\ \vdots & \ddots & \vdots \\ \breve{\mathbf{H}}_{m_r}^1(k) & \cdots & \breve{\mathbf{H}}_{m_r}^K(k) \end{bmatrix} \begin{bmatrix} \mathbf{x}^{(1)}(k) \\ \mathbf{x}^{(2)}(k) \\ \vdots \\ \mathbf{x}^{(K)}(k) \end{bmatrix} + \begin{bmatrix} \mathbf{v}_{f1}(k) \\ \mathbf{v}_{f2}(k) \\ \vdots \\ \mathbf{v}_{fm_r}(k) \end{bmatrix} \qquad (6.2.3)$$

For simplicity of notation, the received signal in Eq.(6.2.3) can be re-written as follows:

$$\mathbf{y}(k) = \tilde{\mathbf{H}}(k)\mathbf{x}(k) + \mathbf{v}_f(k) \qquad (6.2.4)$$

where $\mathbf{y}(k)$ is the overall receive signal vector at all receive antennas

with $N_r = Dm_r$ elements and without loss of generality $D = 2$ in this work. Hence, $\mathbf{y}(k)$ is represented as

$$\begin{aligned}\mathbf{y}(k) &= [y_1(k), y_2(k), \ldots, y_{N_r}(k)]^T \\ &= [y_{11}(k), y_{22}^*(k), \ldots, y_{1_j}(k), y_{2_j}^*(k)]^T\end{aligned}$$

In addition, $\tilde{\mathbf{H}}(k)$ is the equivalent overall channel response matrix of size $N_r \times n_t$, which can also be represented as

$$\tilde{\mathbf{H}}(k) = \left[\tilde{\mathbf{h}}_1(k), \tilde{\mathbf{h}}_2(k), \ldots, \tilde{\mathbf{h}}_{2K-1}(k), \tilde{\mathbf{h}}_{2K}(k)\right]$$

where $\tilde{\mathbf{h}}_n(k)$ denotes the nth column of matrix of $\tilde{\mathbf{H}}(k)$, and $\mathbf{x}(k) = [x_1(k), x_2(k), \ldots, x_{n_t}(k)]$ is the transmitting signal vector with n_t elements including all users at the kth tone, and $\mathbf{v}_f(k)$ is a vector of the overall equivalent zero-mean complex Gaussian noise with size $N_r \times 1$, for which the entries have variance $\sigma^2 = N_0/2$ per each real component. In this chapter, it is assumed that the average symbol energy $E_s \equiv \mathbf{E}\,|x_n(k)|^2 = 1$, and then the spectral efficiency R is defined as $R = n_t M_c R_c$ bits/channel-use (BPCU). The signal to noise ratio is defined as E_b/N_0, where E_b is the energy per transmitted information bit per receive antenna. Hence, the total energy of $n_t E_s$ is collected by each receive antenna at one time, and thus E_b can be obtained as

$$E_b = E_s/(M_c R_c) \tag{6.2.5}$$

6.2.2 Iterative (Turbo) MUD-Decoding Structure

As discussion in Chapter 5, the idea of conventional iterative (Turbo) multiuser detection-decoding (MUD-Decoding) scheme is to concate-

nate SISO multiuser detector with a convolutional decoder and exchange extrinsic information iteratively between detector and decoder to obtain optimal signal estimation in a number of iterations. In this work, a similar iterative MUD-decoding structure for a K user STBC-OFDM receiver is proposed as in the right part of Figure 6.1. After CP removal and FFT operation of OFDM demodulation, the frequency domain receive signal at the kth tone $\mathbf{y}(k)$ is delivered into the front-end SISO multiuser detector. A maximum a posteriori (MAP) multiuser detection algorithm is introduced to the proposed front-end MUD stage, which maximizes the a posteriori probability (APP) of the given code bits and determines the estimate of $x_n(k)$ sequentially by incorporating the outcomes of previous estimates as prior information for subsequent estimates.

Hence, at the first stage, the SISO MUD algorithm takes advantage of the estimate $\widehat{x}_n(k)$ and a priori log-likelihood ratio (LLR) of code bits ε_bs of the transmitted symbol to compute APP and find the extrinsic information. The a priori LLR for each code bit of symbol is defined as

$$L_A(\varepsilon_b) := \ln \frac{\Pr[\varepsilon_b = +1]}{\Pr[\varepsilon_b = -1]} \tag{6.2.6}$$

and after computation is delivered as the extrinsic LLR $L_E(\varepsilon_b)$ for each of the M_c bits per subsequent estimated symbol, into the convolutional channel decoder, where $\varepsilon_b = +1$ represents a binary one and $\varepsilon_b = -1$ represents a binary zero. Herein, an a posteriori LLR is obtained at the output of the front-end SISO detector as $L_P(\varepsilon_b|\widehat{x}_n(k))$ for bit ε_b, which is defined as

$$L_P(\varepsilon_b|\widehat{x}_n(k)) := \ln \frac{\Pr[\varepsilon_b = +1|\widehat{x}_n(k)]}{\Pr[\varepsilon_b = -1|\widehat{x}_n(k)]} \tag{6.2.7}$$

where $\Pr[\varepsilon_b = u|\widehat{x}_n(k)], u = \pm 1$ is the so-called APP of bit ε_b. Using Bayes' theorem, the extrinsic LLR $L_E(\varepsilon_b)$ can be represented as

$$\begin{aligned} L_E(\varepsilon_b) &= L_P(\varepsilon_b|\widehat{x}_n(k)) - L_A(\varepsilon_b) \\ &= \ln \frac{\Pr[\varepsilon_b = +1|\widehat{x}_n(k)]}{\Pr[\varepsilon_b = -1|\widehat{x}_n(k)]} - \ln \frac{\Pr[\varepsilon_b = +1]}{\Pr[\varepsilon_b = -1]} \\ &= \ln \frac{\Pr[\widehat{x}_n(k)|\varepsilon_b = +1]}{\Pr[\widehat{x}_n(k)|\varepsilon_b = -1]} \end{aligned} \tag{6.2.8}$$

In the view of Eq.(6.2.8), the front-end multiuser detector computes and delivers the extrinsic information for code bits of each user $L_E^{(i)}(\varepsilon_b)$ and feeds them into a branch of single user convolutional channel decoders, respectively, as a priori information. As shown in Figure 6.1, the new extrinsic values can be extracted at the output of each single user decoder after code bit error correction, and these extrinsic values will be delivered back to the SISO multiuser detector as updates of the priors for estimation in the next iteration.

6.3 Low Complexity Iterative SIC MUD-Decoding Scheme

In order to obtain multiuser signal estimations, an iterative soft interference cancellation MMSE (SIC-LMMSE) detection algorithm is performed as the front-end detection scheme in this work, see also in [60]. Moreover, this SIC-LMMSE algorithm is developed as a sub-optimal algorithm derived from the MAP but with more manageable complexity and computational efficiency by using reliability evaluation and selected MAI cancellation strategy. The completed low complexity SIC-LMMSE

MUD-decoding scheme as in the right part of Figure 6.1 consists of five distinct stages of processing:

(1) Perform soft interference cancellation (SIC) in parallel.

(2) Soft-input-soft-output (SISO) LMMSE multiuser detection and symbol estimation.

(3) Extrinsic information $L_E(\varepsilon_b)$ computation.

(4) Convolutional channel decoding by using $L_E(\varepsilon_b)$ delivered from the front-end detector.

(5) Estimation evaluation and cancel the selected reconstructed MAI.

(6) A priori information update for next iteration.

6.3.1 SIC-LMMSE MUD-Decoding Algorithm

At the beginning of the first detection-decoding iteration, because the a priori LLR is not available for each code bit ε_b of the transmit symbol $x_n(k)$, therefore the first iteration is starting as the initialization of $\forall L_A(\varepsilon_b) = 0$. Thus it is natural to assume that $\bar{x}(n) \equiv \mathbf{E}\{x(n)\} = 0$. Herein, as more detection-decoding iterations are invoked, a priori information about the current detection estimate $\bar{x}_n(k)$ does become available and $\bar{x}(n) \neq 0$ after the first iteration. Thus a priori information should also be taken into account in the iterative front-end detection algorithm. Based on a priori LLR in terms of $L_A(\varepsilon_b)$s, the transmitted symbol mean $\bar{x}_n(k)$ can be computed as the update of the prior at this step for estimate $\bar{x}_n(k)$

$$\bar{x}_n(k) = \sum\nolimits_{x \in \chi} x \Pr[x_n(k) = x] \tag{6.3.1}$$

where symbol x is equally likely chosen from a complex constellation χ with cardinality $|\chi| = 2^{M_c}$, and $\Pr[x_n(k) = x]$ refers to the a priori symbol probability for $x_n(k) = x$, represented as

$$\Pr[x_n(k) = x] = \prod_{b=1}^{M_c} \frac{1}{1 + e^{-x_b L_A(\varepsilon_b)}} \tag{6.3.2}$$

where x_b denotes the bth value of the M_c modulation bits for the likely chosen symbol x, assumed as statistical independent of the others bits. $x_b = +1$ represents the bth bit value of symbol x is binary one, and $x_b = -1$ represents binary zero, where $b = 1, 2, \ldots, M_c$. Then the variance of the transmit symbol $\sigma^2_{x_n(k)}$ can be obtained as

$$\sigma^2_{x_n(k)} = \sum\nolimits_{x \in \chi} \|x - \overline{x}_n(k)\|^2 \Pr[x_n(k) = x] \tag{6.3.3}$$

Then the interference in the receive vector $\mathbf{y}(k)$ can be cancelled corresponding to $x(n)$ from different transmit antennas in parallel and an equivalent single input receive vector corresponding to the nth transmit antenna can be obtained, as

$$\begin{aligned} \mathbf{y}_n(k) &= \mathbf{y}(k) - \sum_{t=1, t\neq n}^{t=n_t} \overline{x}_t(k)\widetilde{\mathbf{h}}_t(k) \\ &= x_n(k)\widetilde{\mathbf{h}}_n(k) + \sum_{t=1, t\neq n}^{t=n_t} (x_t(k) - \overline{x}_t(k))\widetilde{\mathbf{h}}_t(k) + \mathbf{v}_f(k) \end{aligned} \tag{6.3.4}$$

where the $\widetilde{\mathbf{h}}_n(k)$ denotes the nth column vector of the MIMO channel matrix $\tilde{\mathbf{H}}(k)$. From the representation in Eq.(6.3.4), the observation vector $\mathbf{y}_n(k)$ contains a contribution not only from the desired detected symbol $x_n(k)$, but also from the other transmit symbols and noise. Here an optimal detector weight vector $\mathbf{f}_n(k)$ is chosen to minimize the mean

square error (MSE) between $x_n(k)$ and $\widehat{x}_n(k)$, given the observation vector $\mathbf{y}_n(k)$. Because of the nature of $\bar{x}(n) \neq 0$ after the first iteration, these optimizations can be stated as:

$$\begin{aligned} &\text{minimize } E\left\{|x_n(k) - \widehat{x}_n(k)|^2\right\} \\ &\text{subject to } \widehat{x}_n(k) - \bar{x}_n(k) = \mathbf{f}_n^H(k)(\mathbf{y}_n(k) - \bar{\mathbf{y}}_n(k)) \end{aligned} \tag{6.3.5}$$

For the unbiased detector, $\mathbf{E}\{\widehat{x}_n(k)\} = \bar{x}_n(k)$. Hence, $\bar{\mathbf{y}}_n(k)$ can be calculated as

$$\bar{\mathbf{y}}_n(k) = \mathbf{E}\{\mathbf{y}_n(k)\} = \bar{x}_n(k)\widetilde{\mathbf{h}}_n(k) \tag{6.3.6}$$

Because the noise is assumed uncorrelated and circularly zero-mean complex Gaussian distributed, i.e. $E\{\mathbf{v}_f\} = \mathbf{0}$, $E\{\mathbf{v}_f\mathbf{v}_f^H\} = N_0\mathbf{I}_{N_r}$ and $E\{x(n)\mathbf{v}_f\} = \mathbf{0}$. By solving Eq.(6.3.5), the solution of the optimal L-MMSE equalizer coefficient vector $\mathbf{f}_n(k)$ can be obtained as

$$\mathbf{f}_n(k) = \left(N_0\mathbf{I}_{N_r} + \widetilde{\mathbf{H}}(k)\mathfrak{D}(\mathbf{w})\widetilde{\mathbf{H}}^H(k)\right)^{-1}\sigma^2_{x_n(k)}\widetilde{\mathbf{h}}_n(k) \tag{6.3.7}$$

where $\mathfrak{D}(\cdot)$ denotes a constructing diagonal matrix operation $diag(\cdot)$ and the transmit symbol variance vector $\mathbf{w}$ can be defined as

$$\mathbf{w} = [\sigma^2_{x_1(k)}, \ldots, \sigma^2_{x_n(k)}, \ldots, \sigma^2_{x_{n_t}(k)}]^T$$

The optimal solution to find estimate $\hat{x}_n(k)$ in Eq.(6.3.5) is given by

$$\hat{x}_n(k) = \mathbf{f}_n^H(k)(\mathbf{y}_n(k) - \bar{\mathbf{y}}_n(k)) + \bar{x}_n(k) \tag{6.3.8}$$

where $\mathbf{f}_n(k)$ is obtained in Eq.(6.3.7). By expressing Eq.(6.3.8), the

solution can be rewritten in separated terms as

$$\begin{aligned}\widehat{x}_n(k) &= \mathbf{f}_n^H(k)(\mathbf{y}_n(k) - \overline{\mathbf{y}}_n(k)) + \overline{x}_n(k) \\ &= \mathbf{f}_n^H(k)\widetilde{\mathbf{h}}_n(k)(x_n(k) - \overline{x}_n(k)) + \overline{x}_n(k) \\ &\quad + \underbrace{\sum_{t=1,t\neq n}^{t=n_t} \mathbf{f}_n^H(k)\widetilde{\mathbf{h}}_t(k)(x_t(k) - \overline{x}_t(k)) + \mathbf{f}_n^H(k)\mathbf{v}_{fn}(k)}_{residual\ MAI-plus-noise} \quad (6.3.9)\end{aligned}$$

In view of Eq.(6.3.9), the last two terms of the lower equation can be viewed as residual MAI-plus-noise term, Due to the Gaussian approximation of interference-plus-noise term represented in [139], the output of the proposed optimal parallel SIC-LMMSE detector is approximated as complex Gaussian distributed based on the given knowledge of $x_n(k)$,

$$\begin{aligned}\Pr[\hat{x}_n(k)|x_n(k) = x] &\sim \mathcal{N}(\mu_n(x), \varphi_n^2(x)) \\ &\approx \frac{1}{\varphi_n^2(x)}\Gamma\left(\frac{\widehat{x}_n(k) - \mu_n(x)}{\varphi_n(x)}\right) \quad (6.3.10)\end{aligned}$$

where $\Gamma(z) = e^{-z^2}/\pi$ is the proper complex Gaussian density, $\mu_n(x)$ is the conditional mean and $\varphi_n^2(x)$ is the conditional variance, represented in Eq.(6.3.11) and Eq.(6.3.12) respectively, as

$$\mu_n(x) = \mathbf{f}_n^H(k)\widetilde{\mathbf{h}}_n(k)(x - \bar{x}_n(k)) + \bar{x}_n(k) \quad (6.3.11)$$

$$\varphi_n^2(x) = \sigma_{x_n(k)}^2\mathbf{f}_n^H(k)\widetilde{\mathbf{h}}_n(k)(1 - \widetilde{\mathbf{h}}_n^H(k)\mathbf{f}_n(k)) \quad (6.3.12)$$

By Bayes' theorem, substituting Eq.(6.3.2) and Eq.(6.3.10) into Eq.(6.2.7), an a posteriori LLR $L_P(\varepsilon_b|\widehat{x}_n(k))$ for each code bit, $b =$

$1, 2, \cdots, M_c$, is computed from the SISO estimator for each symbol estimate $\hat{x}_n(k)$, in terms of

$$\begin{aligned} L_P(\varepsilon_b|\widehat{x}_n(k)) &= \ln \frac{\Pr[\varepsilon_b = +1|\widehat{x}_n(k)]}{\Pr[\varepsilon_b = -1|\widehat{x}_n(k)]} \\ &= \ln \frac{\sum_{x\in\chi_b^{+1}} \{\Pr[\widehat{x}_n(k)|x_n(k) = x] \Pr[x_n(k) = x]\}}{\sum_{x\in\chi_b^{-1}} \{\Pr[\widehat{x}_n(k)|x_n(k) = x] \Pr[x_n(k) = x]\}} \\ &= \ln \frac{\sum_{x\in\chi_b^{+1}} \left\{ \Gamma\left(\frac{\widehat{x}_n(k)-\mu_n(x)}{\varphi_n(x)}\right) \left(\prod_{b=1}^{M_c} \frac{1}{1+e^{-x_b L_A(\varepsilon_b)}}\right)\right\}}{\sum_{x\in\chi_b^{-1}} \left\{ \Gamma\left(\frac{\widehat{x}_n(k)-\mu_n(x)}{\varphi_n(x)}\right) \left(\prod_{b=1}^{M_c} \frac{1}{1+e^{-x_b L_A(\varepsilon_b)}}\right)\right\}} \end{aligned} \tag{6.3.13}$$

where $x \in \chi_b^{+1}$ is the set of 2^{M_c-1} actual constellation symbols which have the bth bit as binary $+1$ (i.e. $x_b = +1$), and $x \in \chi_b^{-1}$ refers to $x_b = -1$ similarly. By Eq.(6.3.13) and Eq.(6.2.8), the optimal SIC-MMSE detector delivers the extrinsic LLR $L_E(\varepsilon_b)$ for each code bit as

$$L_E(\varepsilon_b) = L_P(\varepsilon_b|\widehat{x}_n(k)) - L_A(\varepsilon_b) \tag{6.3.14}$$

in turn, to the concatenated single user convolutional decoder as its a priori information for each user. At the decoding stage, the a posteriori information computed at the output of the decoder can also be decomposed into extrinsic and a priori components, and only the "new" extrinsic information will be fed back into the front-end multiuser detector as update of priori information. A "new" transmit symbol variance $\sigma^2_{x_n(k)new}$ and "new" symbol mean $\bar{x}_n(k)_{new}$ can also be obtained by these updates of priors with Eq.(6.3.1) and Eq.(6.3.3), respectively. The iterative updating process does not stop until the specified number of iterations has elapsed or the reliability value of LLRs surpass a

Table 6.1. Developed SIC-LMMSE MUD-Decoding Algorithm.

$\forall L_A = 0$

$\forall \bar{x} = 0$

$diag(\mathbf{c}_x) = \mathbf{I}_{N_r}$

while $iter \leq$ max

for $n = 1 : n_t$

(1) Find a priori symbol probability $\Pr[x_n(k) = x]$ for $x \in \chi$ by (6.3.2)

(2) Find symbol mean $\bar{x}_n$ by (6.3.1)

(3) Find symbol variance $c_x(n)$ by (6.3.3)

(4) Perform soft interference cancellation for $\mathbf{y}_n$ by (6.3.4)

(5) Obtain $\bar{\mathbf{y}}_n$via $\bar{\mathbf{y}}_n = \bar{x}_n \widetilde{\mathbf{h}}_n$ in (6.3.6)

(6) Obtain $\mathbf{f}_n = \left(N_0 \mathbf{I}_{N_r} + \widetilde{\mathbf{H}} diag(\mathbf{c}_x) \widetilde{\mathbf{H}}^H\right)^{-1} c_x(n) \widetilde{\mathbf{h}}_n$

(7) From SIC-MMSE estimate $\widehat{x}_n = \mathbf{f}_n^H(\mathbf{y}_n - \overline{\mathbf{y}}_n) + \overline{x}_n$ in (6.3.8)

(8) Compute conditional symbol mean $\mu_n(x)$ for $x \in \chi$ by (6.3.11)

(9) Compute conditional symbol variance $\varphi_n^2(x)$ for $x \in \chi$ by (6.3.12)

(10) Find $\Pr[\hat{x}_n | x_n = x]$ for $x \in \chi$ by (6.3.10)

(11) Form a posteriori LLR $L_P(\varepsilon_b | \widehat{x}_n)$ by (6.3.13)

(12) Extract extrinsic information $L_E(\varepsilon_b)$ by (6.3.14)

end

(13) Deliver $L_E(\varepsilon_b)$ referred to each user to outer decoder

(14) Extract new extrinsic information as $L_A(\varepsilon_b)$ for $n = 1 : n_t$

end

threshold, and the decoded bits are obtained at the last iteration, which make the final source symbol estimates $\hat{\mathbf{b}}^{(i)}$ from the output of outer channel decoder of each user. The proposed developed SIC-LMMSE detection-decoding algorithm can be shown in Table 6.1.

The computational complexity for the proposed SIC-LMMSE MUD-decoding algorithm is still high. The SIC-LMMSE detector needs to repeat the detection process n_t times for each $\mathbf{y}_n(k)$. This is because the LMMSE equalizer coefficient weight vector $\mathbf{f}_n(k)$ is different for each $x_n(k)$. This process induces high computational expense at the cost of cubic complexity, and this problem can be further optimized by selected MAI cancellation strategy.

6.3.2 Sub-optimal Selected Interference Cancellation Strategy

Because finding the LMMSE equalizer coefficient weight vector $\mathbf{f}_n(k)$ often involves solving the inversion of a high dimension of matrix, which is the most "expensive" step in the algorithm in terms of computational complexity (cubic order), therefore exploiting an efficient method such as QR decomposition is necessary in practice for solving such equations, however still at the cost of cubic complexity. There is an interesting way to perform matrix inversion via a recursive update algorithm. Generally, solving the equalizer equations would be inverting an $N_r \times N_r$ matrix of

$$\mathbf{M}(k) = \left(N_0\mathbf{I}_{N_r} + \widetilde{\mathbf{H}}(k)\mathfrak{D}(\mathbf{w})\widetilde{\mathbf{H}}^H(k)\right)^{-1} \tag{6.3.15}$$

and compute $\mathbf{f}_n(k) = \mathbf{M}(k)\sigma^2_{x_n(k)}\widetilde{\mathbf{h}}_n(k)$. In what follows, the recursive update algorithm is proposed to construct $\mathbf{M}(k)$ directly. As discussed in Chapter 3, $\mathbf{i}_n$ is defined as the nth column of an identity matrix, then define the following matrices

$$\mathbf{M}^{(n_t-1)}(k) = \left(\mathbf{I}_{N_r} + \sum_{n=1}^{n_t-1}\frac{\sigma^2_{x_n(k)}}{N_0}\widetilde{\mathbf{h}}_n(k)\widetilde{\mathbf{h}}_n^H(k)\right)^{-1} \tag{6.3.16}$$

$$\mathbf{M}^{(n_t)}(k) = \left(\mathbf{I}_{N_r} + \sum_{n=1}^{n_t} \frac{\sigma^2_{x_n(k)}}{N_0} \widetilde{\mathbf{h}}_n(k) \widetilde{\mathbf{h}}_n^H(k) \right)^{-1} \tag{6.3.17}$$

Because the term $\widetilde{\mathbf{H}}(k)\mathfrak{D}(\mathbf{w})\widetilde{\mathbf{H}}^H(k)$ in Eq.(6.3.15) can be rewritten as

$$\begin{aligned} \widetilde{\mathbf{H}}(k)\mathfrak{D}(\mathbf{w})\widetilde{\mathbf{H}}^H(k) &= \widetilde{\mathbf{H}}(k) \left(\sum_{n=1}^{n_t} \frac{\sigma^2_{x_n(k)}}{N_0} \mathbf{i}_n \mathbf{i}_n^H \right) \widetilde{\mathbf{H}}^H(k) \\ &= \sum_{n=1}^{n_t} \frac{\sigma^2_{x_n(k)}}{N_0} \widetilde{\mathbf{h}}_n(k) \widetilde{\mathbf{h}}_n^H(k) \end{aligned} \tag{6.3.18}$$

Hence, $\mathbf{f}_n(k)$ can be expressed as

$$\begin{aligned} \mathbf{f}_n(k) &= \frac{\sigma^2_{x_n(k)}}{N_0} \left(\mathbf{I}_{N_r} + \sum_{n=1}^{n_t} \frac{\sigma^2_{x_n(k)}}{N_0} \widetilde{\mathbf{h}}_n(k) \widetilde{\mathbf{h}}_n^H(k) \right)^{-1} \widetilde{\mathbf{h}}_n(k) \\ &= \frac{\sigma^2_{x_n(k)}}{N_0} \mathbf{M}^{(n_t)}(k) \widetilde{\mathbf{h}}_n(k) \end{aligned} \tag{6.3.19}$$

Exploiting the "degenerate" matrix inversion lemma [93] (proof of the algorithm as in Appendix 6.7), a recursive update relation between $\mathbf{M}^{(n_t-1)}(k)$ and $\mathbf{M}^{(n_t)}(k)$ can be found as

$$\mathbf{M}^{(n)}(k) = \mathbf{M}^{(n-1)}(k) - \frac{\frac{\sigma^2_{x_n(k)}}{N_0} \left(\mathbf{M}^{(n-1)}(k) \widetilde{\mathbf{h}}_n(k) \right) \left(\mathbf{M}^{(n-1)}(k) \widetilde{\mathbf{h}}_n(k) \right)^H}{1 + \frac{\sigma^2_{x_n(k)}}{N_0} \widetilde{\mathbf{h}}_n^H(k) \left(\mathbf{M}^{(n-1)}(k) \widetilde{\mathbf{h}}_n(k) \right)} \tag{6.3.20}$$

Therefore, $\mathbf{f}_n(k)$ can be constructed by a recursive update algorithm which is outlined in Table 6.2.

In this recursive processing, $\mathbf{M}^{(n)}(k)$ at the state n, depends on $\mathbf{M}^{(n-1)}(k)$ at the previous state $n-1$. Moreover, with the initialization of $\mathbf{M}^{(0)}(k) = \mathbf{I}_{N_r}$, $\mathbf{M}(k)$ can be directly constructed by recursion to compute $\mathbf{f}_n(k)$. Because of this update algorithm, the MIMO-OFDM MUD algorithm can be transformed into a structure more suitable for the iterative SIC-LMMSE MUD-decoding algorithm. Compared with

the last section, the SIC-LMMSE equalizer coefficient $\mathbf{f}_n(k)$ can be obtained by solving Eq.(6.3.7) without incorporating a priori information, thus, the amount of computational complexity keeps constant through the normal iterative MUD-decoding processing. However, in the processing of SIC-LMMSE with recursive update, the $\mathbf{f}_n(k)$ can be constructed recursively depends on a priori information. At the begin-

Table 6.2. Recursive update algorithm for calculating $\mathbf{f}_n(k)$

Initialization $\mathbf{M}^{(0)}(k) = \mathbf{I}_{N_r}$
for $n = 1 : n_t$
Updating $\mathbf{M}^{(n)}(k)$ from $\mathbf{M}^{(n-1)}(k)$ by (6.3.20)
end
Obtain $\mathbf{f}_n(k) = \frac{\sigma^2_{x_n(k)}}{N_0}\mathbf{M}^{(n_t)}(k)\widetilde{\mathbf{h}}_n(k)$

ning of processing without a priori information, recursive SIC-LMMSE is still a cubic complexity algorithm to obtain $\mathbf{f}_n(k)$, however, when a priori information becomes available, the recursion state $\mathbf{M}^{(n)}(k)$ is only updated from the previous information $\mathbf{M}^{(n-1)}(k)$ in Eq.(6.3.20), when $\sigma^2_{x_n(k)}/N_0 \gg 0$ and $\sigma^2_{x_n(k)}$ is obtained from the a priori LLR. In particular, since the a priori LLR becomes more and more reliable with increasing iteration, the $\bar{x}_n(k)$ computed from the a priori LLR becomes more likely to be the true transmit symbol while $\sigma^2_{x_n(k)}$ is approaching zero. When $\sigma^2_{x_n(k)} = 0$ (i.e. perfect cancellation and $\sigma^2_{x_n(k)}/N_0 = 0$), recursive processing achieves complexity reduction because it costs little to construct $\mathbf{M}^{(n)}(k)$ from $\mathbf{M}^{(n-1)}(k)$. Hence, recursive SIC-LMMSE MUD allows a more flexible allocation of computational complexity depending upon the reliability of the a priori information, i.e. this algorithm is mainly a function of the symbol variance-to-noise ratio,

SVNR(n),

$$SVNR(n) = \frac{\sigma^2_{x_n(k)}}{N_0} \tag{6.3.21}$$

The SVNR(n) is varying depending on the number of iterations and E_b/N_0. Herein, a sub-optimal selected interference cancellation (SSIC) strategy is introduced by parameterizing the reliability threshold θ in the MUD-decoding processing, which enables a trade-off between achieving a lower complexity and better performance. In this scheme, if $SVNR(n) < \theta$, perfect interference cancellation is assumed, i.e. let $\sigma^2_{x_n(k)} = 0$. This means that, in the branch of estimate $\hat{x}_n(k)$, the detection processing is performed the same as the SDF detection described in Chapter 3 for estimating $\hat{x}_n(k)$ when $SVNR(n) < \theta$. Instead of feeding soft information of decoding bits of $\hat{x}_n(k)$ from the outer channel decoder, hard decision of the coded bits of $\hat{x}_n(k)$ can be sent back to the inner multiuser detector. Assuming these hard decision are correct, then interference from other antennas are perfectly cancelled. This is a so-called hard interference cancellation LMMSE (HIC-LMMSE). Hence when estimating $\hat{x}_n(k)$, if $SVNR(n) < \theta$ i.e. a priori information feed back from outer channel decoder becomes very reliable, then the $\hat{x}_n(k)$ can be constructed directly only by $\hat{x}_n(k) = sgn(\bar{x}_n(k))$ [140], and hence the steps Eq.(6.3.3)-Eq.(6.3.12) can be skipped. On the other hand, the recursive SIC-LMMSE detecting process will still be performed to form $\hat{x}_u(k)$, $u \neq n$, when $SVNR(u) \geqslant \theta$ i.e. utilizing "unreliable" a priori information. However, the recursive update algorithm could still skip the step of index n, and achieve further complexity reduction since it costs little for recursion from $\mathbf{M}^{(n-1)}(k)$ to $\mathbf{M}^{(n)}(k)$. This scheme is so-called sub-optimal selected interference cancellation LMMSE (SSIC-LMMSE)

MUD-decoding scheme, which is described in Table 6.3.

Replacing the original SIC-LMMSE MUD-decoding scheme by SSIC-LMMSE MUD-decoding scheme will allow a more efficient computation of the detection symbol estimate as the number of iteration increases. The complexity issue will be discussed in the next section.

6.4 Complexity Issues

Following the discussion in Section 6.2, $\tilde{\mathbf{H}}(k)$ is the equivalent overall channel response matrix of size $N_r \times n_t$. Because the proposed algorithms described in Section 6.3 are all based on L-MMSE. For the conventional SIC-LMMSE MUD algorithm described in Section 6.3.1, it is necessary to perform $\left(N_0\mathbf{I}_{N_r} + \tilde{\mathbf{H}}(k)\mathfrak{D}(\mathbf{w})\tilde{\mathbf{H}}^H(k)\right)^{-1}$ to find the equalizer coefficient weight vector $\mathbf{f}_n(k)$ for each estimate $\hat{x}_n(k)$, which needs $\mathcal{O}(N_r^3)$ multiplication operations. Then computing the a posteriori LLR $L_P(\varepsilon_b|\widehat{x}_n(k))$ in Eq.(6.2.8) requires complexity of $\mathcal{O}(M_c 2^{M_c})$. Hence, the asymptotic computational complexity of the proposed conventional SIC-LMMSE MUD on $\hat{\mathbf{x}}(k)$ is $\mathcal{O}(n_t N_r^3) + \mathcal{O}(n_t M_c 2^{M_c})$, and the amount of computational complexity keeps constant for the subsequent iterations. Comparing with the conventional SIC-LMMSE MUD algorithm, the SSIC-LMMSE MUD scheme has obvious advantage in computational complexity. At the beginning of the first iteration, no a priori information is available and the SSIC-LMMSE detector shares the same complexity as the SIC-LMMSE MUD algorithm, which is $\mathcal{O}(n_t N_r^3) + \mathcal{O}(n_t M_c 2^{M_c})$. However, for subsequent iterations at reasonable E_b/N_0, detection estimate $\hat{x}_n(k)$ may be directly constructed by $\bar{x}_n(k)$ depending on the level of a priori LLR $L_A(\varepsilon_b)$, i.e. when $SVNR(n) < \theta$, perfect interference cancellation is assumed, the dom-

Table 6.3. Outline of SSIC-LMMSE MUD-Decoding Algorithm

$\forall L_A = 0$

$\forall \bar{x} = 0$

$diag(\mathbf{c}_x) = \mathbf{I}_{N_r}$

while $iter \leq$ max

for $n = 1 : n_t$

Find a priori symbol probability $\Pr[x_n(k) = x]$ for $x \in \chi$ by (6.3.2)

Find symbol mean $\bar{x}_n$ by (6.3.1)

Find symbol variance $c_x(n)$ by (6.3.3)

if $SVNR(n) < \theta$ then

$c_x(n) = 0$

$\widehat{x}_n = sgn(\bar{x}_n)$

end

else then

Perform soft interference cancellation for $\mathbf{y}_n$ by (6.3.4)

Obtain $\bar{\mathbf{y}}_n$via $\bar{\mathbf{y}}_n = \bar{x}_n \widetilde{\mathbf{h}}_n$ in (6.3.6)

Obtain $\mathbf{f}_n$ by performing recursive algorithm in Table 6.2

From SIC-MMSE estimate $\widehat{x}_n = \mathbf{f}_n^H(\mathbf{y}_n - \bar{\mathbf{y}}_n) + \bar{x}_n$ in (6.3.8)

Compute conditional symbol mean $\mu_n(x)$ for $x \in \chi$ by (6.3.11)

Compute conditional symbol variance $\varphi_n^2(x)$ for $x \in \chi$ by (6.3.12)

end

Find $\Pr[\hat{x}_n | x_n = x]$ for $x \in \chi$ by (6.3.10)

Form a posteriori LLR $L_P(\varepsilon_b | \widehat{x}_n)$ by (6.3.13)

Extract extrinsic information $L_E(\varepsilon_b)$ by (6.3.14)

end

Deliver $L_E(\varepsilon_b)$ referred to each user to outer decoder

Extract new extrinsic information as $L_A(\varepsilon_b)$ for $n = 1 : n_t$

end

inant computation on detection $\hat{x}_n(k)$ only involves calculation of a posteriori LLR $L_P(\varepsilon_b|\hat{x}_n(k))$ with complexity of $\mathcal{O}(M_c 2^{M_c})$. On the other hand, a recursive update algorithm will still be performed to find $\mathbf{f}_u(k)$ for the estimation $\hat{x}_u(k)$, $u \neq n$, when $SVNR(u) \geqslant \theta$ i.e. those estimates utilizing "unreliable" a priori information, moreover, the calculation of a posteriori LLR $L_P(\varepsilon_b|\hat{x}_u(k))$ is also involved. For full process of the recursive algorithm, it requires computational complexity of $\mathcal{O}(n_t N_r^2)$ for each estimate. However, the recursive process for finding $\mathbf{f}_u(k)$ could still skip the step of index n when $SVNR(n) < \theta$, and achieve further complexity reduction since it costs little for recursion from $\mathbf{M}^{(n-1)}(k)$ to $\mathbf{M}^{(n)}(k)$. Thus, the recursive update processing requires complexity of $\mathcal{O}(\Psi(\theta)N_r^2)$, where $\Psi(\theta)$ is the integer chosen function defined as

$$\Psi(\theta) = 0, 1, 2 \ldots, n_t \qquad 0 \leqslant \theta \leqslant 1 \tag{6.4.1}$$

The value of $\Psi(\theta)$ may be an integer in the range of 0 to n_t depending on the value of $SVNR(n)$ and selected θ. The smaller the value selected for θ, the smaller number of estimates that are constructed directly and fewer skipped steps, which implies more computational complexity. On the other hand, a larger selected value of θ, will induce more advantage of reduced complexity, but may cause degradation of performance. Therefore, the SSIC-LMMSE MUD requires computational complexity of $\mathcal{O}(\Psi^2(\theta)N_r^2) + \mathcal{O}(n_t M_c 2^{M_c})$ for estimating $\hat{\mathbf{x}}(k)$ in the following iteration. As the number of iterations increases, a priori information becomes more and more reliable, i.e. the $\bar{x}_n(k)$ becomes more likely to be the true transmit symbol $x_n(k)$ while more $\sigma^2_{x_n(k)}$s are approaching zero, the value of $\Psi(\theta)$ is approaching zero. Therefore, the

SSIC-LMMSE MUD achieves an asymptotic complexity of $\mathcal{O}(n_t M_c 2^{M_c})$ per iteration.

6.5 Numerical Results and Discussions

To evaluate the performance of the proposed iterative MUD-decoding scheme, the simulations are run simply based on a two user space-time block coded OFDM system case equipped with two receive antennas. Each user data stream contains 256 symbols, for which a code rate 1/2 and constraint length 3 convolutional code is used. In order to correct the subcarriers in deep fades, forward error correction and bit interleaving are used across the subcarriers. The QPSK signal mapping is employed at the transmitting stage and assumed symbol transmission rate is 1MHz. The assumed bandwidth is divided by the IFFT operation over each OFDM interval. Moreover, additional 22 cyclic prefix symbols are used as a guard interval. The data transmission is implemented simply over MIMO frequency selective channels with 3-delay taps and $\sum_{l=1}^{L} \sigma_l^2 = 1$, where σ_l^2 is the variance of the lth path. The channel fading is also simplified with an assumption of no correlation between different transmitting antennas of different users. Perfect knowledge of the channel state at the receiver is assumed.

Figure 6.2 presents a frame error rate (FER) performance comparison between SIC-LMMSE detector and the proposed SSIC-LMMSE MUD-decoding scheme. For each frame transmission, five iterations are performed to estimate each symbol. The SSIC-LMMSE scheme is implemented at the zero-threshold $\theta = 0$. Both schemes can achieve almost the same performance with iteration increases. At 10^{-2} FER, both conventional SIC-LMMSE and proposed SSIC-LMMSE obtain

4dB gain over single iteration (i.e. MMSE suppression detector and decoding), and the performance curves converge at the 5th iteration.

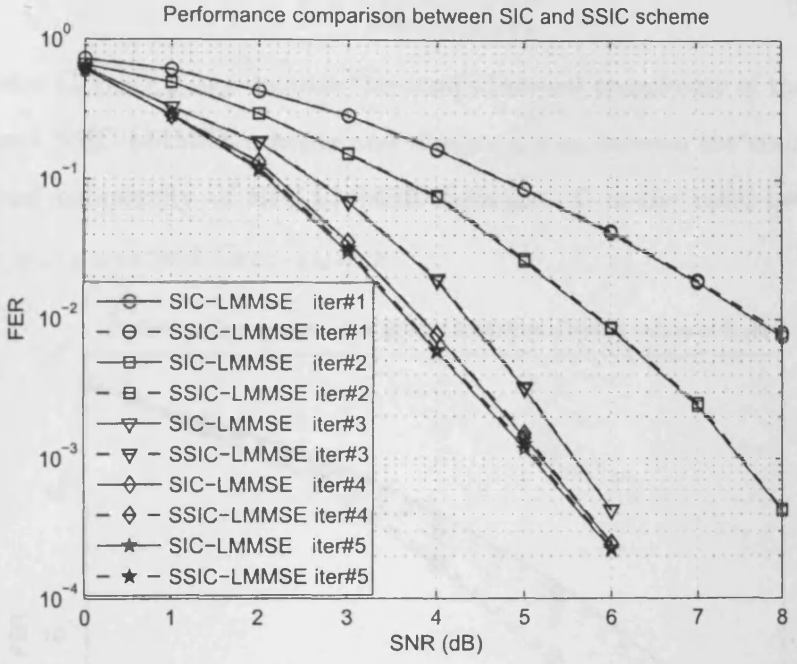

Figure 6.2. The FER vs. SNR performance comparison for two user STBC-OFDM system: implements between SIC-LMMSE and SSIC-LMMSE MUD-decoding scheme at $\theta = 0$.

Figure 6.3 presents a FER performance comparison of the proposed SSIC-LMMSE MUD-decoding algorithm with different values of the zero-threshold θ at the 4th iteration. By having a higher value of θ, the SSIC-LMMSE scheme is expected to achieve lower complexity but suffer a potential performance degradation. From Figure 6.3, an efficient trade-off can be obtained up to $\theta = 0.1$, where the scheme achieves lower complexity without visible performance degradation. At values of θ above 0.1, the performance sacrifices degradation despite lower complexity. Therefore the SSIC-LMMSE algorithm allows a more flexible trade-off between performance and complexity.

Figure 6.4 presents complexity comparison by evaluating the complexity-ratio Γ, defined as

$$\Gamma = \frac{C_{SSIC-LMMSE}}{C_{HIC-LMMSE}} \tag{6.5.1}$$

where $C_{SSIC-LMMSE}$ denotes the computational complexity of the proposed SSIC-LMMSE scheme and $C_{HIC-LMMSE}$ denotes the computational complexity of HIC-LMMSE detector. Γ is the ratio between $C_{HIC-LMMSE}$ and $C_{HIC-LMMSE}$.

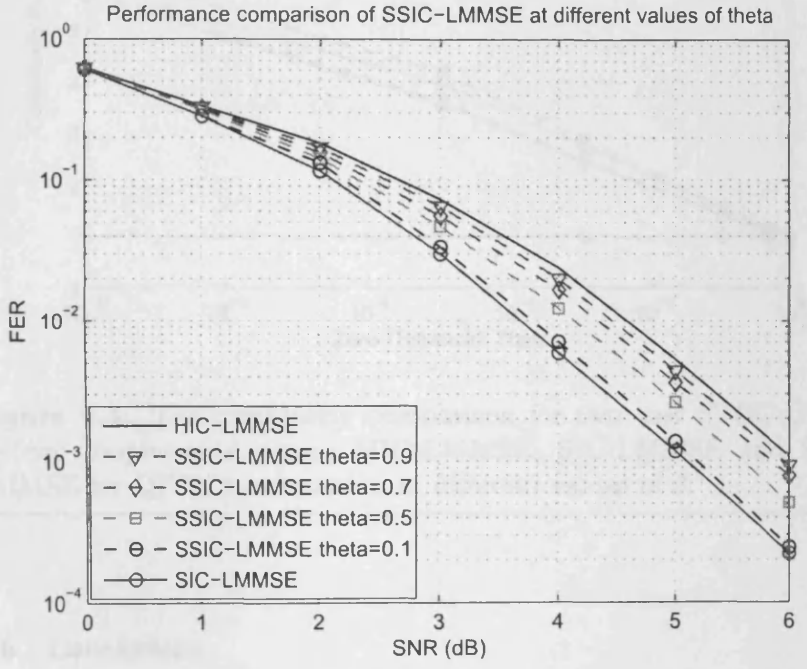

Figure 6.3. The FER vs. SNR performance comparison for two user STBC-OFDM system: implements SSIC-LMMSE MUD-decoding scheme with different values of θ at the 4th iteration.

From Figure 6.4, at the 4dB and 6dB SNR environment respectively, it can be observed that $C_{SSIC-LMMSE}$ is approaching $C_{HIC-LMMSE}$ with θ increases. At $\theta = 0.1$, the SSIC-LMMSE detector approaches the complexity of the HIC-LMMSE detector without deep performance

degradation. At higher level of θ, the proposed scheme also saves computation rather than conventional SIC-LMMSE at the same noise level.

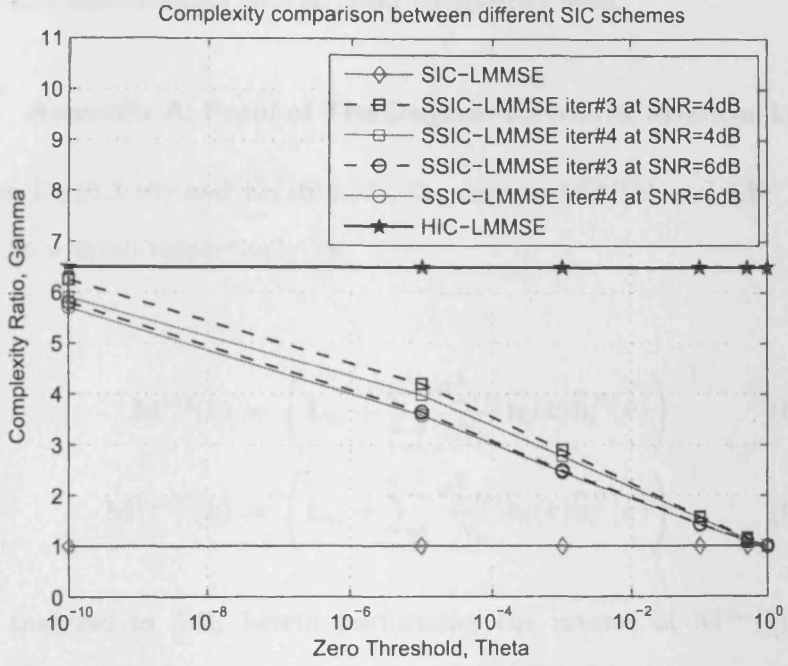

Figure 6.4. The complexity comparison for two user STBC-OFDM system: implements among HIC-LMMSE, SIC-LMMSE and SSIC-LMMSE for QPSK transmission at different values of θ.

6.6 Conclusions

In this chapter, a computational more efficient detection algorithm SSIC-LMMSE is proposed for iterative multiuser detection-decoding STBC MIMO-OFDM system. By reformulating the matrix inversion step and controlling the interference cancellation from the received observations, the scheme achieves complexity reduction without noticeable performance degradation. This allows a more flexible allocation of computational power and an iterative processing receiver more suitable

for practical realization. Moreover, complexity analysis demonstrates that the proposed system can achieve near performance as conventional SIC-LMMSE detector but at lower complexity level.

6.7 Appendix A: Proof of The Degenerate Matrix Inversion Lemma

From Eq.(6.3.16) and Eq.(6.3.17), the matrix $\mathbf{M}^{(n)}(k)$ and $\mathbf{M}^{(n-1)}(k)$ can be written respectively ,as

$$\mathbf{M}^{(n)}(k) = \left(\mathbf{I}_{N_r} + \sum_{i=1}^{n} \frac{\sigma^2_{x_i(k)}}{N_0} \widetilde{\mathbf{h}}_i(k)\widetilde{\mathbf{h}}_i^H(k)\right)^{-1} \tag{6.7.1}$$

$$\mathbf{M}^{(n-1)}(k) = \left(\mathbf{I}_{N_r} + \sum_{i=1}^{n-1} \frac{\sigma^2_{x_i(k)}}{N_0} \widetilde{\mathbf{h}}_i(k)\widetilde{\mathbf{h}}_i^H(k)\right)^{-1} \tag{6.7.2}$$

By analyzed in [93], herein performing the inverse of $\mathbf{M}^{(n)}(k)$ and $\mathbf{M}^{(n-1)}(k)$, it is clear that the matrix $(\mathbf{M}^{(n)}(k))^{-1}$ is a rank-one modification of $(\mathbf{M}^{(n-1)}(k))^{-1}$, as

$$\left(\mathbf{M}^{(n)}(k)\right)^{-1} = \left(\mathbf{M}^{(n-1)}(k)\right)^{-1} + \frac{\sigma^2_{x_n(k)}}{N_0} \widetilde{\mathbf{h}}_n(k)\widetilde{\mathbf{h}}_n^H(k) \tag{6.7.3}$$

Hence, the "degenerate" matrix inversion lemma can be expressed as

$$
\begin{aligned}
\mathbf{M}^{(n)}(k) &= \left[\left(\mathbf{M}^{(n-1)}(k)\right)^{-1} + \frac{\sigma^2_{x_n(k)}}{N_0} \widetilde{\mathbf{h}}_n(k) \widetilde{\mathbf{h}}_n^H(k) \right]^{-1} \\
&= \left[\left(\mathbf{M}^{(n-1)}(k)\right)^{-1} \left(\mathbf{I}_{N_r} + \frac{\sigma^2_{x_n(k)}}{N_0} \mathbf{M}^{(n-1)}(k) \widetilde{\mathbf{h}}_n(k) \widetilde{\mathbf{h}}_n^H(k) \right) \right]^{-1} \\
&= \left(\mathbf{I}_{N_r} + \frac{\sigma^2_{x_n(k)}}{N_0} \mathbf{M}^{(n-1)}(k) \widetilde{\mathbf{h}}_n(k) \widetilde{\mathbf{h}}_n^H(k) \right)^{-1} \mathbf{M}^{(n-1)}(k) \\
&= \left[\mathbf{I}_{N_r} - \frac{\frac{\sigma^2_{x_n(k)}}{N_0} \mathbf{M}^{(n-1)}(k) \widetilde{\mathbf{h}}_n(k) \widetilde{\mathbf{h}}_n^H(k)}{1 + \frac{\sigma^2_{x_n(k)}}{N_0} \widetilde{\mathbf{h}}_n^H(k) \mathbf{M}^{(n-1)}(k) \widetilde{\mathbf{h}}_n(k)} \right] \mathbf{M}^{(n-1)}(k) \\
&= \mathbf{M}^{(n-1)}(k) - \frac{\frac{\sigma^2_{x_n(k)}}{N_0} \left(\mathbf{M}^{(n-1)}(k) \widetilde{\mathbf{h}}_n(k) \right) \left(\mathbf{M}^{(n-1)}(k) \widetilde{\mathbf{h}}_n(k) \right)^H}{1 + \frac{\sigma^2_{x_n(k)}}{N_0} \widetilde{\mathbf{h}}_n^H(k) \left(\mathbf{M}^{(n-1)}(k) \widetilde{\mathbf{h}}_n(k) \right)}
\end{aligned}
$$

Chapter 7

CONCLUSION

In this final chapter of the thesis, the work and results presented in the previous chapters are summarized. Overall conclusions of this study are made and further work is suggested.

7.1 Summary of the thesis

This thesis concerns key technology for the physical layer of next generation wireless communication, including space time codes, MIMO and OFDM techniques, and it also provides a first step to introducing more sophisticated interference cancellation and signal detection techniques into synchronous uplink MIMO-OFDM systems and multiuser applications. In particular, the combination between STBC, MIMO and OFDM are addressed in improving transmission performance of broadband wireless communication systems.

In this thesis, firstly, a STBC MIMO-OFDM transceiver was introduced and the design of a robust receiver was presented based on the MMSE iterative symbol detection algorithm by updating with extrinsic information. The structure of the STBC techniques at the transmitter, concatenated with OFDM operation was exploited to mitigate ISI. The detection process at the receiver was divided into two stages; the first stage estimated frequency domain symbols with an optimum MMSE

equalizer, and then the estimated values were passed to the second stage. In the second stage, the means and variances of the estimated symbols were determined. In order to obtain more accurate estimates, these posteriori means and variances were passed to the first stage to use in the following iteration. The first stage utilizes these values to update the equalizer coefficient values and cancel the interference in order to provide more accurate estimates. Thereby both stages iteratively exchanged their information learnt from each other. The simulation results indicate that the proposed SIE and SDF schemes could obtain substantial performance improvement during iteration processing over both quasi-static channels and a slow fading channel environment. Although SIE outperforms SDF scheme on FER performance, however, SDF saves more computational complexity by sacrificing some performance gain.

The combination of STBC, MIMO and OFDM was also used for utilization of multiuser detection (MUD). In this thesis, a novel and robust MUD technique called parallel interference cancellation was introduced for multiuser STBC-OFDM detections. Firstly, the design of a two-step interference cancellation receiver was addressed to cancel MAI in a multiuser MIMO wideband wireless communication system within both quasi-static and time variant fading channel environment. In this approach, the transmitter serially concatenate STBC with OFDM for each user terminal and the receiver was based on a two-step hard-interference cancellation algorithm. Otherwise, another approach would be to use space-frequency block codes and OFDM modulation to provide further robustness to the time-varying channel. The simulation results indicate that the proposed scheme could obtain substantial

performance improvement without increasing the complexity compared with the L-MMSE scheme for quasi-static and slowly fading rate channels. However, the performance of this scheme will suffer significant degradation from the effect of high fading rate MIMO-ISI channels. This problem could be able to induce error propagation for advanced iterative optimization. By concatenating the transmitter with convolutional channel encoding, the design of a channel coded joint PIC multiuser receiver has been investigated to solve this problem. The MUD receiver was based on a soft PIC algorithm with soft-input-soft-output (SISO) forward error correction (FEC) decoding techniques. The simulation results indicated that by concatenating the transmitter with the half rate outer channel code, the proposed scheme obtained significant performance gain rather than the normal scheme, which obtains benefit for performing more iterations reliably for performance improvement. In addition to the multiple transmit and receive antenna diversities, the frequency selective diversity of order L can also be gained by the effect of coding correction rather than the normal two-step scheme.

The iterative algorithm was also introduced into multiuser STBC MIMO-OFDM system for improving detecting performance. In this thesis, some iterative MUD schemes were implemented over both quasi-static and slow fading rate MIMO-ISI channels. The design of the multiuser receiver was first addressed based on MMSE iterative algorithm by updating with extrinsic information. The structure of STBC techniques at the transmitter was exploited, concatenated with OFDM operation to suppress interference. The simulation results indicated that the proposed scheme could obtain substantial performance improvement over slow fading channel environment (including quasi-static

channels) rather than the MUD based on L-MMSE. Moreover, this structure could be developed by introducing SISO channel decoding technique into the iterative process for performance enhancement. This idea induces a joint iterative MUD and SISO convolutional decoding scheme for K user applications. As shown in simulation results, the developed scheme outperforms conventional iterative MUD in terms of reliability performance, as a result, the ISI and MAI can be cancelled more effectively and efficiently by concatenating the iterative coding correcting processing.

Although the iterative scheme can achieve significant performance improvement, however, the iterative algorithm is impractical due to high computational complexity. In this thesis, a computational more efficient detection algorithm SSIC-LMMSE was proposed for iterative multiuser detection-decoding STBC MIMO-OFDM system. By reformulating the matrix inversion step and controlling when interference was cancelled from received observations, the scheme achieves complexity reduction without noticeable performance degradation. This allowed more flexible allocation of computational power and more suitable for iterative processing receiver. Moreover, complexity analysis demonstrated that the proposed system can achieve near performance as conventional SIC-LMMSE detector but at lower complexity level.

7.2 Future work

All studies in this thesis addressed STBC MIMO-OFDM systems implemented based on perfect synchronization, perfect knowledge of channel state and a small number of users environment. To make the proposed STBC MIMO-OFDM more practical in reality, future research is sug-

gested:

1. The iterative algorithm can also be used for channel estimation and data detection for MIMO-OFDM system over frequency selective channels with multiple frequency offset. In the view of the successful iterative schemes developed in this thesis, the soft estimates of the transmitted signal can be used to estimate the frequency offset and to refine the channel estimates iteratively.

2. More amount of users can be simply introduced into the proposed iterative STBC MIMO-OFDM systems by adding transmit terminals. Moreover this can also be realized by combining the interference cancellation and cooperative base station technique on receiving stage for more coverage and capacity.

3. More transmit antennas can be equipped on each transmit terminal to realize more transmit diversity. This idea can be realized by using novel space time coding techniques such as QO-STBC, which the pre-work has already been done in [141].

4. Beyond the above, application in distributed environments composed of collaborative single antenna nodes could be considered.

BIBLIOGRAPHY

[1] T. S. Rappaport, *Wireless Communications: Principles and Practice.* Upper Saddle River, N.J.: Prentice Hall PTR, 1996.

[2] D. Nob, "The History of Land-Mobile Radio Communications," *IEEE Trans. Vehicular Technology*, pp. 1406–1416, May 1962.

[3] V. H. MacDonald, "The Cellular Concept," *The Bell Systems Technical Journal*, vol. 58, pp. 15–43, Jan. 1979.

[4] J. Palenchar, "CTIA: Net subscriber growth resumes in '03," *This week in Consumer Electronics*, May 2004.

[5] T. Ojanpera and R. Prasad, "An overview of air interface multiple access for IMT-2000/UMTS," *IEEE Commun. Mag.*, vol. 36, pp. 82–86, 1998.

[6] T. Zahariadis and D. Kazakos, "Revolution toward 4G mobile communication systems," *IEEE Trans. Wireless Communications*, vol. 10, pp. 6–7, Aug. 2003.

[7] IEEE802.11a, "Wireless LAN media access control (MAC) and physical layer (PHY) specifications: high-speed physical layer in the 5GHz band," *IEEE Std. 802.11a*, 2001.

[8] IEEE802.11g, "Wireless LAN media access control (MAC) and physical layer (PHY) specifications Amendment 4: further higher data rate extension in the 2.4GHz band," *IEEE Std. 802.11g*, 2003.

[9] A. J. Paulraj, D. A. Gore, R. U. Nabar, and H. Bolcskei, "An Overview of MIMO Communications: A Key to Gigabit Wireless," *Proceedings of the IEEE*, vol. 92, pp. 198–218, Feb. 2004.

[10] R. Prasad, "Wireless broadband communication systems," *IEEE Communications Magazine*, vol. 35, pp. 18–18, Jan. 1997.

[11] R. Prasad, *Universal Wireless Personal Communications.* Norwood, MA: Artech House, 1998.

[12] W. Honcharenko, J. P. Kruys, D. Y. Lee, and N. J. Shah, "Broadband wireless access," *IEEE Communications Magazine*, vol. 35, pp. 20–26, Jan. 1997.

[13] L. M. Correia and R. Prasad, "An overview of wireless broadband communications," *IEEE Communications Magazine*, vol. 35, pp. 28–33, Jan. 1997.

[14] K. H. Teo, Z. Tao, and J. Zhang, "The Mobile Broadband WiMAX Standard [Standards in a Nutshell]," *IEEE Signal Processing Magazine*, vol. 24, pp. 144–148, Sept. 2007.

[15] I. 802.11n Wireless LAN Medium Access Control (MAC) and Physical Layer (PHY) Specifications, 2004. [Online]. Available: *http : //grouper.ieee.org/groups/802/11/Reports/tgn_update.htm.*

[16] IEEEE 802.16, "Air Interface for Fixed Broadband Wireless Access Systems". 2004 Edition.

[17] Broadcom, "The New Mainstream Wireless LAN standards," tech. rep., Broadcom, 2003.

[18] H. Sampath, S. Talwar, J. Tellado, V. Erceg, and A. Paulraj, "A Fourth-Generation MIMO-OFDM Broadband Wireless System: Design, Performance, and Field Trial Results," *IEEE Communications Magazine*, vol. 40, pp. 143–149, Sept. 2002.

[19] G. L. Stüber, J. R. Barry, S. W. McLaughlin, Y. Li, M. A. Ingram, and T. G. Pratt, "Broadband MIMO-OFDM wireless communications," *Proc. of the IEEE*, vol. 92, pp. 271–294, Feb. 2004.

[20] H. Bölcskei and E. Zurich, "MIMO-OFDM wireless systems: basics, perspectives, and challenges," *IEEE Wireless Communications*, vol. 13, pp. 31–37, Aug. 2006.

[21] V. Tarokh, N. Seshadri, and A. R. Calderbank, "Space-time codes for high data rate wireless communication: performance criterion and code construction," *IEEE Transactions on Information Theory*, vol. 42, pp. 744–765, March 1998.

[22] G. J. Foschini and M. J. Gans, "On limits of wireless communications in a fading environment when using multiple antennas," *Wireless Personal Communications*, vol. 6, pp. 311–335, Jan. 1998.

[23] G. J. Foschini, "Layered space-time architecture for wireless communications in a fading environment when using multi-element antennas," *Bell Labs Technical Journal*, vol. 1, pp. 41–59, 1996.

[24] I. E. Telatar, "Capacity of Multi-antenna Gaussian Channels," *AT+T Bell Laboratories, Technical Memorandum*, June 1995.

[25] J. H. Winters, "On the Capacity of Radio Communication Systems with Diversity in a Rayleigh Fading Environment," *IEEE Journal on Selected Areas in Communications*, vol. 5, pp. 871–878, June 1987.

[26] A. Paulraj, R. Nabar, and D. Gore, *Introduction to Space-time Communications*. Cambridge, UK: Cambridge Univ. Press, 2003.

[27] D. Gesbert, M. Shafi, D. S. Shiu, P.J. Smith, and A. Naguib, "From theory to practice: an overview of MIMO space-time coded wireless systems," *IEEE Journal on Selected Areas in Communications*, vol. 21, pp. 281–302, Apr. 2003.

[28] J. Guey, M. P. Fitz, M. R. Bell, and W. Kuo, "Signal Design for Transmitter Diversity Wireless Communication Systems over Rayleigh Fading Channels," in *Proc. IEEE Vehicular Technology Conference (VTC1996)*, pp. 136–140, Jan. 1996.

[29] A. J. Paulraj and T. Kailath, *Increasing capacity in wireless broadcast systems using distributed transmission/directional reception*. U.S. Patent Storm, 1994.

[30] I. E. Telatar, "Capacity of multi-antenna Gaussian channels," *Eur. Trans. Tel.*, vol. 10, pp. 585–595, Nov. 1999.

[31] D. G. H. Bölcskei and A. J. Paulraj, "On the Capacity of OFDM-based Spatial Multiplexing Systems," *IEEE Trans. Commun.*, vol. 50, p. 225C234, Feb. 2002.

[32] G. Caire and S. Shamai, "On the Achievable Throughput of a Multi-antenna Gaussian Broadcast Channel," *IEEE Trans. Information Theory*, vol. 49, pp. 1691–1706, July 2003.

[33] S. Alamouti, "A simple transmit diversity technique for wireless communications," *IEEE Journal on Selected Areas in Communications*, vol. 16, pp. 1451–1458, Oct. 1998.

[34] V. Tarokh, H. Jafarkhani and A. R. Calderbank, "Space-time block codes from orthogonal designs," *IEEE Transactions on Information Theory*, vol. 45, pp. 744–765, July 1999.

[35] L. Zheng and D. N. C. Tse, "Diversity and multiplexing: A fundamental tradeoff in multiple-antenna channels," *IEEE Trans. Information Theory*, vol. 49, pp. 1073–1096, May 2003.

[36] S. Han, J. Wang, V. O. K. Li, S. Zhou and K. Park, "Optimal Diversity Performance of Space Time Block Codes in Correlated Distributed MIMO Channels," *IEEE Transactions on Wireless Communications*, vol. 7, pp. 2106–2118, June 2008.

[37] R. V. Nee and R. Prasad, *OFDM Wireless Multimedia Communications*. Boston: Artech House, 2000.

[38] R. Chang, "Synthesis of band-limited orthogonal signals for multichannel data transmission," *Bell System Technical Journal*, vol. 46, pp. 1775–1796, 1966.

[39] R. Chang and R. Gibby, "A Theoretical Study of Performance of an Orthogonal Multiplexing Data Transmission Scheme," *IEEE Trans. on Communications*, vol. 16, pp. 529–540, Aug. 1968.

[40] B. R. Saltzberg, "Performance of an efficient parallel data transmission system," *IEEE Transactions on Communications Technology*, vol. 15, pp. 805–811, Dec. 1967.

[41] J. Bingham, "Multicarrier modulation for data transmission: an idea whose time has come," *IEEE Communications Magazine*, vol. 28, pp. 5–14, May 1990.

[42] Z. Wang and G. B. Giannakis, "Wireless multicarrier communications," *IEEE Journal on Selected Areas in Communications*, vol. 17, pp. 29–48, May 2000.

[43] N. Yee, J.P.M.G. Linnartz and G. Fettweis, "Multi-Carrier CDMA in indoor wireless Radio Networks," in *Proc. IEEE Reviewers Personal, Indoor and Mobile Radio Communications (PIMRC'93)*, (Yokohama, Japan), pp. 109–113, 1993.

[44] S. Weinstein and P. Ebert, "Data Transmission by Frequency-Division Multiplexing Using the Discrete Fourier Transform," *IEEE Trans. on Communications*, vol. 19, pp. 628–634, Oct. 1971.

[45] H. Sari, G. Karam, and I. Jeanclaude, "Transmission techniques for digital terrestrial TV broadcasting," *IEEE Communications Magazine*, vol. 33, pp. 100–109, Feb. 1995.

[46] M. Ghosh, "Analysis of the effect of impulse noise on multicarrier and single carrier QAM systems," *IEEE Trans. on Communications*, vol. 44, pp. 145–147, Feb. 1996.

[47] ETSI, *Radio broadcasting systems; Digital audio broadcasting (DAB) to mobile, portable and fixed receivers.* ETS 300 744 v 1.1.2: Europ. Telecom. Stand. Inst., 1997.

[48] ETSI, *Digital video broadcasting (DVB); Framing structure, channel coding and modulation for digital terrestrial television.* ETS 300 401 2nd e/d, Valbonne, France: Europ. Telecom. Stand. Inst., 1997.

[49] L. J. Cimini, "Analysis and Simulation of a Digital Mobile Channel Using Orthogonal Frequency Division Multiplexing," *IEEE Trans. on Communications*, vol. 33, pp. 665–675, July 1985.

[50] G. V. Rangaraj, D. Jalihal, and K. Giridhar, "Introducing space sampling for OFDM systems with multipath diversity," in *Proc. IEEE Symposium on Signal Processing and Information Technology-2003*, (Germany), pp. 427–430, Dec. 2003.

[51] G. G. Raleigh and J. M. Cioffi, "Spatio-Temporal Coding for Wireless Communication," *IEEE Transactions on Communications*, vol. 46, no. 3, pp. 357–366, 1998.

[52] K. K. Moon, *Error Correction Coding: Mathematical Methods and Algorithms.* N.J.: Wiley, 2005.

[53] B. Sklar, *Digital Communications: Fundamentals and Applications.* Upper Saddle River, N.J.: Prentice Hall PTR, 2001.

[54] J. G. Proakis, *Digital Communications.* New York: McGraw-Hill, 1995.

[55] G. Caire, G. Taricco, and E. Biglieri, "Bit-Interleaved Coded Modulation," *IEEE Trans. Info. Theory*, vol. 44, pp. 927–946, May 1998.

[56] H. Bölcskei and A. J. Paulraj, "Space-frequency Coded Broadband OFDM Systems," in *Proc. IEEE Wireless Commun. and Networking Conf.*, (Chicago, IL), pp. 1–6, Sept. 2000.

[57] X. Ma and G. B. Giannakis, "Full-Diversity Full-Rate Complex-Field Space-Time Coding," *IEEE Trans. Sig. Processing*, vol. 51, pp. 2917–2930, Nov. 2003.

[58] M. Borgmann and H. Bölcskei, "Noncoherent Space-Frequency Coded MIMO-OFDM," *IEEE JSAC*, vol. 23, pp. 1799–1810, Sept. 2005.

[59] D. N. Liu and M. P. Fitz, "Low complexity affine mmse detector for iterative detection-decoding MIMO OFDM systems," *IEEE Transactions on Communications*, vol. 56, pp. 150–158, Jan. 2008.

[60] D. N. Liu and M. P. Fitz, "Low complexity linear MMSE detector with recursive update algorithm for iterative detection-decoding MIMO OFDM system," in *Proc. IEEE Wireless Communications and Networking Conference, 2006 (WCNC 2006)*, pp. 850–855, 2006.

[61] M. Borgmann and H. Bölcskei, "Interpolation-Based Efficient Matrix Inversion for MIMO-OFDM Receivers," in *Proc. 38th Asilomar Conf. Signals, Syst., and Computers*, (Pacific Grove, CA), pp. 1941–1947, Nov. 2004.

[62] S. Verdu, *Multiuser Detection*. Cambridge, UK: Cambridge University Press, 1998.

[63] A. Duel-Hallen, J. Holtzman, and Z. Zvonar, "Multiuser detection for CDMA systems," *IEEE Personal Communications*, vol. 2, pp. 46–58, Apr. 1997.

[64] S. Moshavi, "Multi-user detection for DS-CDMA communications," *IEEE Communications Magazine*, vol. 12, pp. 124–136, Oct. 1996.

[65] L. Hanzo, M. Münster, B. J. Choi, and T. Keller, *OFDM and MC-CDMA for Broadband Multi-User Communications, WLANs and Broadcasting*. Piscataway, NJ: IEEE Press/Wiley, 2003.

[66] L. Giangaspero, L. Agarossi, G. Paltenghi, S. Okamura, M. Okada, and S. Komaki, "Co-channel interference cancellation based on MIMO OFDM systems," *Wireless Commun.*, vol. 9, pp. 8–17, Dec. 2002.

[67] P. Vandenameele, L. V. D. Perre, and M. Engels, *Space Division Multiple Access for Wireless Local Area Networks. London.* U.K.: Kluwer, 2001.

[68] P. Vandenameele, L. V. D. Perre, M. Engels, B. Gyselinckx, and H. D. Man, "A combined OFDM/SDMA approach," *IEEE Journal on Selected Areas in Communications*, vol. 18, pp. 2312–2321, Nov. 2000.

[69] X. D. Wang and H. V. Poor, "Iterative (turbo) soft interference cancellation and decoding for coded CDMA," *IEEE Trans. on Communications*, vol. 47, pp. 1046–1061, July 1999.

[70] M. E. Austin, "Decision-feedback equalization for digital communication over dispersive channels," tech. rep., M.I.T. Lincoln Laboratory, Lexington, MA, August 1967.

[71] C. A. Belfiore and J. H. Park, "Decision feedback equalization," *Proc. of the IEEE*, vol. 67, pp. 1143–1156, August 1979.

[72] P. Monsen, "Feedback equalization for fading dispersive channels," *IEEE Trans. on Information Theory*, vol. 17, pp. 56–64, Jan. 1971.

[73] P. H. Siegel, D. Divsalar, E. Eleftheriou, J. Hagenauer, D. Rowitch, and W. H. Tranter, "Guest editorial the turbo principle: from theory to practice," *IEEE Journal on Selected Areas in Communications*, vol. 19, pp. 793–799, 2001.

[74] P. H. Siegel, D. Divsalar, E. Eleftheriou, J. Hagenauer, and D. Rowitch, "Guest editorial the turbo principle: from theory to practice II," *IEEE Journal on Selected Areas in Communications*, vol. 19, pp. 1657–1661, Spet. 2001.

[75] M. Moher, "An iterative multiuser decoder for near-capacity communications," *IEEE Trans. on Communications*, vol. 46, pp. 870–880, July 1998.

[76] W. C. Jakes, *Microwave Mobile Communications.* Wiley IEEE Press, May 1994.

[77] A. F. Naguib, N. Seshadri and A. R. Calderbank, "Applications of space-time block codes and interference suppression for high capacity and high data rate wireless systems," in *Proc. 32nd Asilomar Conf. Signals, Systems, and Computers*, vol. 2, (Pacific Grove, CA,), pp. 1803–1810, November 1998.

[78] Website 1G: First Generation wireless technology. [Online]. Available: *http : //www.javvin.com/wireless/1G.html.*

[79] Website 3GPP Homepage, correct as Spetember 2004. [Online]. Available: *http : //www.3gpp.org.*

[80] Website 4G-Beyond 2.5G and 3G Wireless Networks. [Online]. Available: *http : //www.mobileinfo.com.*

[81] J. Ibrahim, "4G Features," *Bechtel Telecommunications Technical Journal*, Dec. 2002.

[82] Y. K. Kim and R. Prasad, *4G Roadmap and Emerging Communication Technologies.* Boston: Artech House, 2006.

[83] W. Mohr, "Mobile Communications Beyond 3G in the Global Context," tech. rep., Siemens mobile, 2002.

[84] E. Biglieri, G. Taricco, and A. Tulino, "Decoding space-time codes with BLAST architectures," *IEEE Transactions on Signal Processing*, vol. 50, pp. 2547–2552, Oct. 2002.

[85] A. L. Lonzano and C. Papadias, "Space-time receiver for wideband BLAST in rich-scattering wireless channels," in *Proc. IEEE Vehicular Technology Conference (VTC2000-spring)*, (Tokyo, Japan), pp. 186–190, May 2000.

[86] H. Claussen, H. R. Karimi, and B. Mulgrew, "High-performance MIMO receivers based on multi-stage partial parallel interference cancellation," in *Proc. IEEE Vehicular Technology Conference (VTC2003-fall)*, pp. 414–418, Oct 2003.

[87] S. Da-Shan, "Iterative decoding for layered space-time codes," in *Proc. IEEE International Conference on Communications (GLOBECOM 2000)*, pp. 297–301, June 2000.

[88] A. Gueguen, "Comparison of Suboptimal Iterative Space-time Receivers," in *Proc. IEEE Vehicular Technology Conference (VTC 2003-Spring)*, pp. 842–846, April 2003.

[89] T. Abe and T. Matsumoto, "Space-time turbo equalization in frequency-selective MIMO channels," *IEEE Transactions on Vehicular Technology*, vol. 52, pp. 469–475, May 2003.

[90] S. R. Saunders, *Antennas and Propagation for Wireless Communication Systems*. J.Wiley & Sons, 1999.

[91] D. Tse and P. Viswanath, *Fundamentals of Wireless Communication.* Cambridge, U.K.: Cambridge University Press, 2005.

[92] C. E. Shannon, "A Mathematical Theory of Communication," *The Bell System Technical Journal*, vol. 27, pp. 379–423 and 623–656, July and October 1948.

[93] R. A. Horn and C. R. Johnson, *Matrix Analysis.* Cambridge, U.K.: Cambridge University Press, 1985.

[94] B. Vucetic and J. Yuan, *Space-Time Coding.* N.J.: Wiley, 2003.

[95] H. Jafarkhani, "A quasi-orthogonal space-time block code," *IEEE Transactions on Communications*, vol. 49, pp. 1–4, Jan. 2001.

[96] V. Tarokh and H. Jafarkhani, "A differential detection scheme for transmit diversity," *IEEE Journal on Selected Areas in Communications*, vol. 18, pp. 1169–1174, July 2000.

[97] H. Jafarkhani and V. Tarokh, "Multiple transmit antenna differential detection from generalized orthogonal designs," *IEEE Transactions on Information Theory*, vol. 47, pp. 2626–2631, Spet. 2001.

[98] B. M. Hochwald and T. L. Marzetta, "Unitary space-time modulation for multiple-antenna communications in Rayleigh flat fading," *IEEE Transactions on Information Theory*, vol. 46, pp. 543–564, March 2000.

[99] V. Tarokh, H. Jafarkhani and A. R. Calderbank, "Space-time block coding for wireless communications: performance results," *IEEE Journal on Selected Areas in Communications*, vol. 17, pp. 451–460, March 1999.

[100] C. Toker, S. Lambotharan, and J. A. Chambers, "Signal design for transmitter diversity wireless communication systems over Rayleigh fading channels," in *Proc. IEEE Information Theory Workshop, 2003*, pp. 195–198, 31st March-4th April 2003.

[101] C. Toker, S. Lambotharan, and J. A. Chambers, "Closed-loop quasi-orthogonal STBCs and their performance in multipath fading environments and when combined with turbo codes," *IEEE Transactions on Wireless Communications*, vol. 3, pp. 1890–1896, Nov. 2004.

[102] T. de Couasnon, R. Monnier, and J. B. Rault, "OFDM for digital TV broadcasting," *Signal processing (ELSEVIER)*, vol. 39, pp. 1–32, 1994.

[103] D. G. Leeper, "WiFi - The Nimble Musician in Your Laptop," *IEEE Computer Magazine-How Things Work*, pp. 108–110, Apr. 2007.

[104] E. H. Moore, "On the reciprocal of the general algebraic matrix," *Bulletin of the American Mathematical Society*, vol. 26, pp. 394–395, 1920.

[105] R. Penrose, "A generalized inverse for matrices," *Proceedings of the Cambridge Philosophical Society*, vol. 51, pp. 406–413, 1955.

[106] S. Haykin, *Communication Systems.* John Wiley and Sons, Inc, 2000.

[107] Y. S. Choi, P. J. Voltz, and F. A. Cassara, "On Channel Estimation and Detection for Multi-carrier Signals in Fast and Selective Rayleigh Fading Channels," *IEEE Transactions on Communications*, vol. 49, pp. 1375–1387, Aug. 2001.

[108] P. Schniter, "Low-complexity equalization of OFDM in doubly selective channels," *IEEE Transactions on Signal Processing*, vol. 52, pp. 1002–1011, April 2004.

[109] J. T. Chen, A. Paulraj, and U. Reddy, "Multichannel maximum-likelihood sequence estimation (MLSE) equalizer for GSM using a parametric channel model," *IEEE Transactions on Communications*, vol. 47, pp. 53–63, Jan. 1999.

[110] H. Chen, R. Perry, and K. Buckley, "On MLSE algorithms for unknown fast time-varying channels," *IEEE Transactions on Communications*, vol. 51, pp. 730–734, May 2003.

[111] S. Qureshi, "Adaptive equalization," *IEEE Transaction on Signal Processing*, vol. 20, pp. 9–16, 1982.

[112] J. G. Proakis, "Adaptive equalization for TDMA digital mobile radio," *IEEE Trans. on Vehicular Technology*, vol. 40, pp. 333–341, May 1991.

[113] Engadget Dell offering draft-802.11n card for notebooks, posted July 17th 2006. [Online]. Available: $http : //www.engadget.com/2006/07/17/dell - offering - draft - 802 - 11n - card - for - notebooks.$

[114] Broadcom Broadcom Intensi-fi Draft-802.11n Technology Equips New Acer Notebooks with High-Performance Wi-Fi Connectivity. [Online]. Available: $http : //www.broadcom.com/press/release.php?id = 892726.$

[115] Z. Liu, Y. Xin and G. B. Giannakis, "Space-time-frequency coded

OFDM over frequency-selective fading channels," *IEEE Transactions on Signal Processing*, vol. 50, pp. 2465–2476, Oct. 2002.

[116] S. Suthaharan, A. Nallanathan and B. Kannan, "Space-Time coded MIMO-OFDM for high capacity and high data-rate wireless communication over frequency selective fading channels," in *Proc. Mobile and Wireless Communications Network 2002, 4th International Workshop*, pp. 424–428, Sept. 2002.

[117] P. L. Kafle, A. B. Sesay and J. McRory, "An Iterative MMSE-decision Feedback Multiuser Detector for Space-time Coded Multicarrier CDMA System," in *Proc. Electrical and Computer Engineering, 2004. Canadian Conference*, no. 4, pp. 2281–2286, May 2004.

[118] G. D. Forney, "The Viterbi algorithm," *IEEE Proceedings*, vol. 61, pp. 268–278, Mar. 1978.

[119] M. Tüchler, R. Koetter, and A. C. Singer, "Turbo equalization: Principles and new results," *IEEE Transactions on Communications*, vol. 50, pp. 754–766, May 2002.

[120] P. Schniter and S. H. D'Silva, "Low-complexity detection of OFDM in doubly-dispersive channels," in *Proc. Asilomar Conf. Signals, Syst., Comput.*, Nov. 2002.

[121] L. Zhang, M. Sellathurai, and J. A. Chambers, "A two-step multiuser detection scheme for space-time coded mimo ofdm systems," in *Proc. 10th IEEE Singapore International Conference on Communication systems, 2006 (ICCS 2006)*, (Singapore), pp. 1–5, Oct. 2006.

[122] L. Zhang, M. Sellathurai, and J. A. Chambers, "A joint coded two-step multiuser detection scheme for mimo ofdm system," in *Proc. IEEE*

International Conference on Acoustics, Speech and Signal Processing, 2007 (ICASSP 2007), vol. 3, (HI, USA), pp. III–85 – III–88, 15-20 April. 2007.

[123] B. Hagerman, *Single-User Receivers for Partly Known Interference in Multi-User Environments.* PhD thesis, Royal Institute of Technology, Sweden, Sept. 1995.

[124] F. Nordstorm, *Interferer Detection and Cancellation in TDMA-Systems.* PhD thesis, Centre for Mathematical Sciences, Lund University, Sweden, 2002.

[125] M. Jiang and L. Hanzo, "Multiuser MIMO-OFDM for Next-Generation Wireless Systems," *Proceedings of the IEEE*, vol. 95, pp. 1430–1469, July 2007.

[126] P. Patel and J. Holtzman, "Analysis of a simple successive interference cancellation scheme in a DS/CDMA system," *IEEE Journal on Selected Areas on Communications*, pp. 976–807, June 1994.

[127] M. K. Varanasi and B. Aazhang, "Multistage detection in asynchronous code division multiple access communications," *IEEE Transactions on Communications*, vol. 38, pp. 509–519, April 1990.

[128] R. K. Y. C. Yoon and H. Imai, "A spread-spectrum multiaccess system with cochannel interference cancellation for multipath fading channels," *IEEE Journal on Selected Areas in Communications*, vol. 11, pp. 1067–1075, Sept 1993.

[129] D. Guo, L. K. Rasmussen, and T. J. Lim, "Linear parallel interference cancellation in long-code CDMA multiuser detection," *IEEE*

Journal on Selected Areas in Communications, vol. 17, pp. 2074–2081, Dec. 1999.

[130] A. Nahler, R. Irmer, and G. Fettweis, "Reduced and differential parallel interference cancellation for CDMA systems," *IEEE Journal on Selected Areas in Communications*, vol. 20, no. 2, 2002.

[131] R. M. Buehrer, N. S. Correal-Mendoza, and B. D.Woerner, "A simulation comparison of multiuser receivers for cellular CDMA," *IEEE Transactions on Vehicular Technology*, vol. 49, pp. 1065–1085, July 2000.

[132] E. A. Fain and M. K. Varanasi, "Diversity order gain for narrowband multiuser communications with precombining group detection," *IEEE Transactions on Communications*, vol. 48, pp. 533–536, April 2000.

[133] D. Divsalar, M. K. Simon, and D. Raphaeli, "Improved parallel interference cancellation for CDMA," *IEEE Transactions on Communications*, vol. 46, no. 2, 1998.

[134] R. M. Buehrer and S. P. Nicoloso, "Comments on partial parallel interference cancellation for CDMA," *IEEE Transactions on Communications*, vol. 47, pp. 658–661, May 1999.

[135] L. Zhang, M. Sellathurai, and J. A. Chambers, "A space-time coded mimo-ofdm multiuser application with iterative mmse-decision feedback algorithm," in *Proc. 8th IEEE International Conference on Signal Processing (ICSP2006)*, vol. 3, (Guilin, P.R.China), Nov. 2006.

[136] M. Nasiri-Kenari, R. R. Sylvester, and C. K. Rushforth, "An efficient soft-in softout multiuser detector for synchronous CDMA with

error-control coding," *IEEE Transactions on Vehicular Technology*, vol. 47, no. 2, 1998.

[137] L. Zhang, M. Sellathurai, and J. A. Chambers, "An iterative multi-user receiver for space-time coded mimo ofdm systems," in *Proc. 7th International Conference on Mathematics in Signal Processing*, (Cirencester, UK), Dec. 2006.

[138] C. Berrou and A Glavieux, "Near optimum error correcting coding and decoding: Turbo Codes," *IEEE Trans. on Communications*, vol. 44, no. 10, pp. 1261–1271, 1996.

[139] H. V. Poor and S. Verdu, "Probablity of error in MMSE mutiluser detection," *IEEE Transactions on Information Theory*, 1997.

[140] A. Matache, C. Jones and R. Wesel, "Reduced complexity MIMO detectors for LDPC coded systems," in *Proc. IEEE Military Communications Conference 2004 (MILCOM 2004)*, vol. 2, (CA, USA), pp. 1073–1079, Nov 2004.

[141] C. Shen, L. Zhang, and J. A. Chambers, "A two-step interference cancellation technique for a mimo-ofdm system with four transmit antennas," in *Proc. 2007 15th International Conference on Digital Signal Processing*, (Cardiff, UK), 1-4 July 2007.